

BIS(BIPYRIDYL)SILICON(IV) COMPLEXES – SYNTHESIS,  
CHARACTERIZATION, AND CATALYTIC PROPERTIES

by

Christina Maguylo

A thesis submitted to the faculty of  
The University of North Carolina at Charlotte  
in partial fulfillment of the requirements  
for the degree of Master of Science in  
Chemistry

Charlotte

2015

Approved by:

---

Dr. Thomas A. Schmedake

---

Dr. Bernadette T. Donovan-Merkert

---

Dr. Craig A. Ogle

---

Dr. Irina V. Nesmelova



## ABSTRACT

CHRISTINA MAGUYLO. Bis(bipyridyl)silicon(IV) compounds – synthesis, characterization, and catalytic properties. (Under the direction of DR. THOMAS A. SCHMEDAKE.)

A series of novel hexacoordinate bis-bipyridylsilicon(IV) complexes have been synthesized by reacting  $[\text{Si}(\text{bpy})_2\text{I}_2]\text{I}_2$  with the appropriate alcohol or diol. Characterization was done and crystal structures have been obtained for the complexes:  $[\text{Si}(\text{bpy})_2(\text{OMe})_2]\text{I}_2$ ,  $[\text{Si}(\text{bpy})_2(-\text{OCH}_2\text{CH}_2\text{O}-)](\text{I})(\text{I}_3)$ ,  $[\text{Si}(\text{bpy})_2(\text{OPh})_2](\text{I}_3)_2$ ,  $[\text{Si}(\text{bpy})_2(\text{cat})](\text{PF}_6)_2$ ,  $[\text{Si}(\text{bpy})_2(\text{bph})](\text{PF}_6)_2$ , and  $[\text{Si}(\text{dmbpy})_2(\text{OH})_2]\text{I}_2$  (bpy = 2,2'-bipyridine, dmbpy = 4,4'-dimethyl-2,2'-bipyridine, bbbpy = 4,4'-di-tert-butyl-2,2'-dipyridyl cat = 1,2-benzenediolato, bph = 2,2'-biphenolato ligand). Two of these new hexacoordinate silicon diol complexes has been synthesized and tested for catalytic activity. Dihydroxy-bis-(4,4'-di-tert-butyl-2,2'-dipyridyl)silicon(IV) and dihydroxy-bis-(4,4'-dimethyl-2,2'-bipyridine)silicon(IV) were synthesized and found to be quite soluble in organic solvents due to the t-butyl or methyl groups on the bipyridine. Catalytic studies, such as the addition of indole to trans- $\beta$ -nitrostyrene, show that these complexes can act similar to other silicon diol catalysts.

## DEDICATION

*For my mother.*

## ACKNOWLEDGMENTS

I would foremost like to acknowledge and thank Dr. Thomas Schmedake for his guidance, supervision, and support in both my undergraduate and graduate studies at UNC-Charlotte.

I would like to thank my thesis committee, Dr. Bernadette Donovan-Merkert, Dr. Craig Ogle, and Dr. Irina Nesmelova, for their guidance and support, especially your efforts in helping me to graduate.

I would also like to thank Dr. Marcus Etzkorn, diligent graduate coordinator, for sticking through the ups and downs of graduate life and always keeping extra copies of all forms, should they be lost.

Additionally, the Chemistry Department at UNC-Charlotte has been full of helpful, intelligent, and creative individuals. I would not be graduating without the help of so many people within this department, especially: Dr. Cooper for his help in getting me into the graduate program and for teaching me so much about analytical chemistry with notes to which I still refer; Dr. Merkert for his help in making me able to speak in public and for the endless hours of help with electrochemistry; Dr. Murphy for instructing me in all things in physical and instrumental chemistry; Dr. Carlin for his help with all instruments; Caroline and Robin for their help and assistance throughout the years; and everyone else not mentioned by name, but without whom I would not be graduating today.

Additionally, I thank the many members of the Schmedake group, both past and present, which have helped me within the lab. My research began through the efforts of Binita Suthar and Chika Chukwu, has continued through with the help of many

undergraduates, and will continue through the efforts of Crystal Waters. I am grateful for all the help and support. I would especially like to thank Derek Peloquin, who, with the desk beside mine, has been around for my entire graduate career always supporting and helping me.

Finally, I would not be able to accomplish anything in life without the support and love of my family. My parents, Joe, Cecilia, and Jim, have been there to support and encourage me through my life. My grandmothers have nurtured and shown me what strong women can accomplish. My god-daughter, Lily, who is beyond amazing and through her baking might be the only reason I am graduating, has been there to keep me going. My nieces, Journey and Aria, have always been able to make me smile and, although grateful that I am finished with school and graduating, have always kept me motivated and learning about science. I hope that their love of science and learning will not end. And even my little nephew Petros, who never stops smiling, has continued to keep me smiling.

I also come from a close (and large) family that has always been there through thick and thin, stepping up to help when things got hectic or tough for me. It is truly a blessing to know that someone is always there to have my back and help me to keep going. There is nothing that I can accomplish without their love and support.

## TABLE OF CONTENTS

	viii
LIST OF TABLES	
	ix
LIST OF FIGURES	
	x
LIST OF ABBREVIATIONS	
	1
CHAPTER 1: INTRODUCTION	
	1
1.1    Hexacoordinate Silicon Chemistry	2
1.2    Homoleptic Polypyridyl Silicon(IV) Chemistry	6
1.3    Bisbipyridyl Silicon(IV) Chemistry	8
1.4    Research Goals	
CHAPTER 2: EXPLORING THE STRUCTURE AND REDOX ACTIVITY OF HEXACOORDINATE BIS(BIPYRIDYL)SILICON(IV) COMPLEXES <sup>1</sup>	10
2.1    Introduction	10
2.2    Results and Discussion	12
2.3    Experimental	17
CHAPTER 3: DIOL CATALYSIS	26
3.1    Dual Hydrogen Bond Catalysis	27
3.2    Silicon Diol Chemistry	30
3.3    Results and Discussion	31
3.4    Experimental	35
CHAPTER 4: DISCUSSION	39
REFERENCES	41
APPENDIX A: SUPPLEMENTAL DATA FOR CHAPTER 2	45
APPENDIX B: SUPPLEMENTAL DATA FOR CHAPTER 3	75

## LIST OF TABLES

TABLE 1:	Reactions of ligands with diiodosilanes reported by Kummer, et. al.	8
TABLE 2:	$E_{1/2}$ values, $\Delta E_p$ and calculated $E_{LUMO}$ for compounds 1–5. Electrochemistry studies conducted in $CH_3CN/TBAPF_6$ solution at scan rate = 0.200 V/s using a platinum disk working electrode. $E_{LUMO}$ calculated using DFT (B3LYP/6-31G(d), Spartan 2010).	15
TABLE 3:	Crystallographic data for Compounds 1-5.	20



## LIST OF FIGURES

FIGURE 1:	First reported silicon hexacoordinated complex, $\text{SiF}_6^{-2}$	1
FIGURE 2:	Method used by Herzog and Krebs	3
FIGURE 3:	Kummer's synthesis of $[\text{Si}(\text{bpy})_3]^0$ from $\text{SiI}_4$ in a melt	4
FIGURE 4:	Suthar's synthesis of $[\text{Si}(\text{bpy})_3]\text{I}_4$	5
FIGURE 5:	CV scans of $\text{Si}(\text{bpy})_3(\text{PF}_6)_4$	6
FIGURE 6:	Kummer's synthesis	7
FIGURE 7:	Structures and yields of the five complexes	12
FIGURE 8:	Crystal structures have been obtained for the complexes	13
FIGURE 9:	CV of $5(\text{PF}_6)_2$	14
FIGURE 10:	Calculated HOMO (bottom) and LUMO (top) of compounds 1–5	16
FIGURE 11:	Images of several types of hydrogen bonding catalysts	27
FIGURE 12:	Schreiner's catalyst	28
FIGURE 13:	Kozlowski's catalysts examined as HBD catalysts	29
FIGURE 14:	Data of catalytic tests done by Kozlowski	30
FIGURE 15:	Image of BINOL and Kondo's di(1-naphthyl)silanediol	30
FIGURE 16:	Franz's figure showing self-recognition	32
FIGURE 17:	Preliminary crystal structure of $[\text{Si}(\text{dmbpy})_2(\text{OH})_2](\text{PF}_6)_2$	32
FIGURE 18:	Catalytic reaction of indole with trans- $\beta$ -nitrostyrene	33
FIGURE 19:	GCMS spectra of qualitative evidence of catalysis	34
FIGURE 20:	Reaction of n-methylindole with trans- $\beta$ -nitrostyrene	34
FIGURE 21:	Initial Results showing a 3 fold increase of reaction using 5% mol catalyst	35

## LIST OF ABBREVIATIONS

BBBPY	4,4'-di-tert-butyl-2,2'-dipyridyl ligand
BPH	2,2'-biphenolato ligand
BPY	2,2'-bipyridine
CAT	1,2-benzenediolato ligand
COSY	correlation spectroscopy
CV	cyclic voltammetry
DFT	density functional theory
DMBPY	4,4'-dimethyl-2,2'-bipyridine ligand
DPCAT	dipyidocatecholate
DPY	2,2'-bipyridine
EA	elemental analysis
ESI-MS	electrospray ionization spectroscopy
FTIR	fourier transform infrared spectroscopy
GC-MS	gas chromatography mass spectrometry
HMBC	heteronuclear multiple-bond correlation spectroscopy
HOMO	highest occupied molecular orbital
HSQC	heteronuclear single-quantum correlation spectroscopy
IR	infrared spectroscopy
LUMO	lowest unoccupied molecular orbital
MLCT	metal to ligand charge transfer
NMR	nuclear
OME	methanolato ligand

OPH	phenolato ligand
THF	tetrahydrofuran
TOF	time of flight
UV-Vis	ultraviolet-visible spectroscopy

## CHAPTER 1: INTRODUCTION

Hexacoordinate silicon(IV) chemistry has been recently explored by the Schmedake group for electrochemical, photochemical, and spectroelectrochemical characteristics and applications. Starting in 2010 with Suthar's contribution to the research of silicon hexacoordinated silicon(IV) complexes, the Schmedake group has revealed a greater understanding of these complexes and their relationship to their transition metal analogues.<sup>1,2,3</sup>

### 1.1 Hexacoordinate silicon chemistry

Although hexacoordinated silicon chemistry has not been extensively studied over the past several decades, the first reported silicon hexacoordinated complex,  $\text{SiF}_6^{2-}$ , was published in 1935 (Figure 1).<sup>4</sup> The structure of this dianion was established through X-ray diffraction.<sup>4</sup>

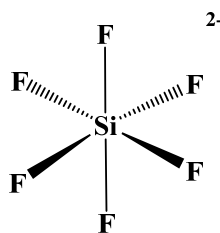


Figure 1: First reported silicon hexacoordinated complex,  $\text{SiF}_6^{2-}$

The chemistry of hexacoordinated silicon complexes involves the utilization of the empty d-orbitals of silicon.<sup>4</sup> The ability of multiple ligands to coordinate to silicon in an octahedral geometry contributes to the reactivity of these complexes.<sup>4</sup> The reactivity

of cationic hexacoordinated silicon(IV) complexes was noted to depend on the ligands and varies greatly.<sup>4</sup> In addition, their solubility is also affected with the counter anions contributing to this effect. Therefore, no universal claims can be made about the reactivity of hexacoordinated silicon(IV) complexes.

Chuit notes that the synthesis of these complexes is analogous to penta-coordinated silicon complexes.<sup>4</sup> The two noted synthetic routes include the formation of an anionic or neutral complex through the reaction of an anionic or neutral nucleophilic reagent with tetravalent silicon or the nucleophilic substitution of an organosilane with bidentate ligands.<sup>4</sup> The approach of nucleophilic substitution of  $\text{SiI}_4$  with 2,2'-bipyridine was utilized for the synthesis of homoleptic and heteroleptic complexes studied by the Schmedake group.

## 1.2 Synthesis and characterization of homoleptic polypyridine silicon chemistry

After Wannagat published his paper about the synthesis of  $\text{SiCl}_4\text{Dpy}$ , the first reported synthesis of a trisbipyridylsilicon(IV) complex was  $[\text{Si}(\text{bpy})_3]^0$  by Herzog and Krebs in 1963.<sup>5</sup> This followed their earlier synthesis of similar complexes with tin, zinc, and aluminum.<sup>5</sup> The synthesis of Herzog and Krebs was a multistep process starting with  $\text{SiCl}_4$  and with the reaction proceeding entirely in THF at room temperature (Figure 2).<sup>5</sup> The final reaction done was reacting elemental iodine with  $[\text{Si}(\text{bpy})_3]^0$ , oxidizing the compound to form the  $[\text{Si}(\text{bpy})_3]\text{I}_4$  complex.<sup>5</sup> They noted that this complex was soluble in water; however, they also noted that the complex decomposes in air, water, and methanol.<sup>5</sup>

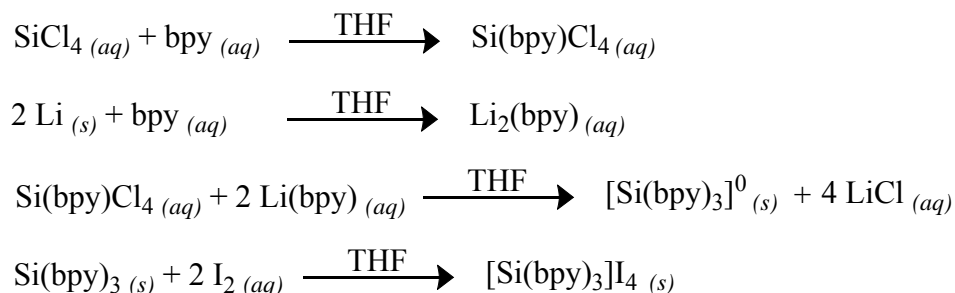


Figure 2: Method used by Herzog and Krebs for the synthesis of  $[\text{Si}(\text{bpy})_3]^{+4}$  oxidizing the  $[\text{Si}(\text{bpy})_3]^0$  by elemental iodine.<sup>5</sup>

In 1967, Herzog and Zimmer (Franz) synthesized  $\text{NaSi}(\text{bpy})_3$  from  $\text{Si}(\text{bpy})_3$  with  $\text{Na}(\text{bpy})$  in THF.<sup>5</sup> They noted that this complex also decomposed with exposure to air, methanol, and water.<sup>5</sup> They also went on to state that  $\text{Na}_2\text{Si}(\text{bpy})_3$  was formed in the presence of excess metallic sodium.<sup>5</sup>

Kummer *et. al.* reported in 1973 the synthesis of  $[\text{Si}(\text{bpy})_3]\text{Br}_4$  by reaction of  $\text{Si}_2\text{Br}_6$  with bpy in benzene.<sup>7,8</sup> This reaction was done at room temperature over a period of five days and had only a 2.1% yield with respect to  $\text{Si}_2\text{Br}_6$ . Characterization of this complex was reported and involved elemental analysis, conductivity measurements,  $^1\text{H}$  NMR, IR, mass spectroscopy, and UV-Vis.<sup>7,8</sup> Kummer *et. al.* also noted that unlike previous polypyridyl hexacoordinate silicon complexes,  $[\text{Si}(\text{bpy})_3]\text{Br}_4$  was both soluble and stable in an aqueous solution, which could be monitored through NMR and UV-Vis.<sup>7,8</sup> Additionally, they noted that the silicon was coordinated octahedrally, which was analogous to other complexes that have three bipyridines bound to a central atom.<sup>7,8</sup>

In 1979, Kummer and coworkers published the synthesis of  $[\text{Si}(\text{bpy})_3]^0$  from  $\text{SiI}_4$  in a melt with  $\text{CHCl}_3$  (Figure 3).<sup>9</sup> They had previously attempted a similar synthesis of  $[\text{Si}(\text{bpy})_3]\text{Br}_4$  from  $\text{SiBr}_4$ ; however, this led to the formation of only  $\text{Si}(\text{bpy})\text{Br}_4$ .<sup>9</sup> They noted, that even when an excess of bpy was used, the second or third bpy ligand did not

react with the monobipyridine complex.<sup>9</sup> Therefore, they concluded that SiBr<sub>4</sub> and SiCl<sub>4</sub> could not be used to form a Si(bpy)<sub>3</sub> complex.<sup>9</sup>

Their synthesis of [Si(bpy)<sub>3</sub>]<sup>0</sup> required 20 equivalents of bipyridine ligand to achieve the required viscous melt and sublimation of ligand, which was a time consuming slow process.<sup>9</sup> Upon completion of the reaction and purification, where the formation of some [Si(bpy)<sub>2</sub>I<sub>2</sub>]<sub>2</sub> was observed, the reaction only gave a 57% yield.<sup>9</sup>

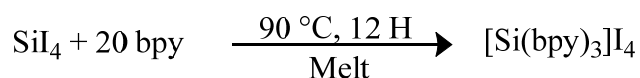


Figure 3: Kummer's synthesis of [Si(bpy)<sub>3</sub>]<sup>0</sup> from SiI<sub>4</sub> in a melt

Characterization reported by Kummer included <sup>1</sup>H NMR, IR, and UV-Vis, which confirmed the octahedral structure of the complex with a +4 charge, which furthered the understanding of these complexes, especially their structure and characteristics.<sup>9</sup>

In 1992, Ohmori reported the optical resolution of the [Si(bpy)<sub>3</sub>]<sup>4+</sup> cation and reported the stability of this complex in water.<sup>11</sup> After confirming both the Λ and Δ enantiomers were confirmed by circular dichroism spectra and their successful separation of optical isomers, it was noted that the enantiomers were also stable in an aqueous solution for a month.<sup>11</sup> Ohmori also stated that the chemistry of hexacoordinated silicon(IV) complexes is similar to that of other similar transition metal complexes, where the coordination number and valence state determine the chemistry of silicon.<sup>11</sup> The separation of isomers provided additional understanding of the hexacoordinated silicon(IV) complexes.

In 2010, Suthar further optimized the synthesis of the [Si(bpy)<sub>3</sub>]<sup>4+</sup> cation (Figure 4).<sup>2,12</sup> This was done through a one pot synthesis with equivalent amounts of bipyridine ligand.<sup>2,12</sup> Compared to previous attempts, the one step reaction was an improvement

over the four step synthesis of Herzog and Krebs, which also required fewer reactants to achieve the target complex. This synthesis also improved upon the synthesis by Kummer, which required 20 equivalents of ligand.

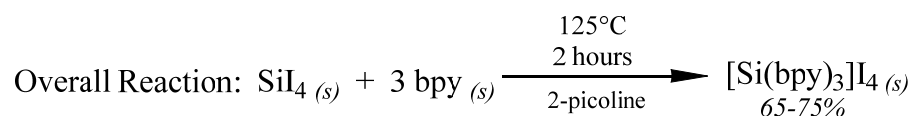


Figure 4: Suthar's synthesis of  $[\text{Si}(\text{bpy})_3]\text{I}_4$ <sup>2,12</sup>

Suthar also noted color changes that were produced by metathesis reactions with additional counterions including chloride, bromide, iodide, and hexafluorophosphate.<sup>2,12</sup> Characterization of  $[\text{Si}(\text{bpy})_3](\text{PF}_6)_4$  by Suthar included EA, ESI-MS,  $^1\text{H}$  NMR,  $^{13}\text{C}$  NMR,  $^{29}\text{Si}$  NMR, fluorescence, UV-vis, and CV.<sup>2,12</sup> Adding to previously published work, Suthar focused primarily on the electrochemistry, spectrochemistry, and the comparison of these silicon(IV) complexes and their transition metal analogues.<sup>2,12</sup> She went on to conclude the various salts of these complexes, mentioned above, have several stable oxidation states, which were shown through the cyclic voltammograms of  $[\text{Si}(\text{bpy})_3]^{+4}$  (Figure 5).<sup>2,12</sup>



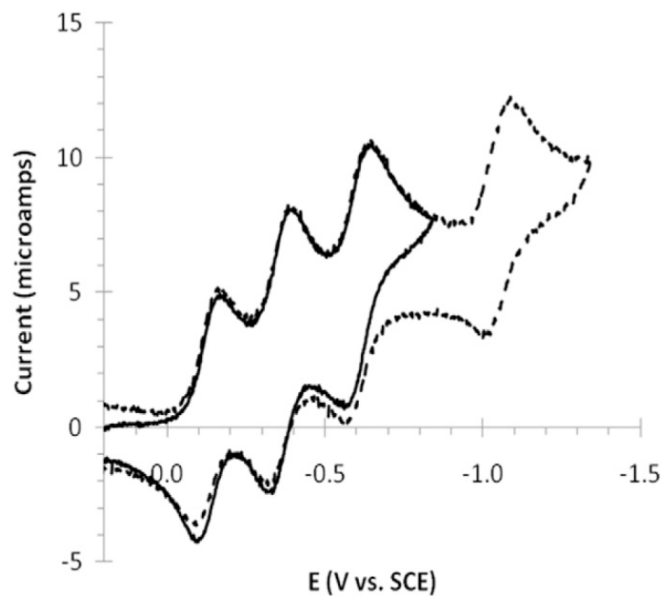


Figure 5: CV scans of  $\text{Si}(\text{bpy})_3(\text{PF}_6)_4$  in acetonitrile/0.1M  $\text{TBAPF}_6$  solution using a platinum disk working electrode scan rate = 200 mV/s; iR compensation employed.

Additional conclusions made about the structure of  $[\text{Si}(\text{bpy})_3]^{+4}$  from its characterization showed that this homoleptic polypyridyl complex was a stable, covalently bonded structure with multiple oxidation states and absorption in the visible spectrum.<sup>2,12</sup> These observations are being further studied by the Schmedake group for possible devices.

### 1.3 Synthesis and characterization of heteroleptic bipyridyl silicon chemistry

Adapting the synthesis of Herzog and Kreb, Kummer in 1973 published the synthesis of  $[\text{Si}(\text{OH})_2(\text{bpy})_2]\text{Cl}_2$  and  $[\text{Si}(\text{OCH}_3)_2(\text{bpy})_2]\text{Cl}_2$ .<sup>7,8</sup> However, soon after that, in 1977 Kummer published the results of a more facile synthesis by reacting starting material with polyiodosilanes (Figure 6).<sup>13</sup>

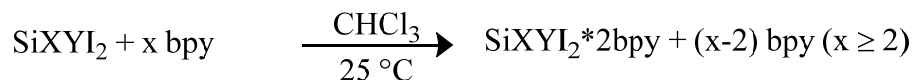


Figure 6: Kummer's synthesis of hexacoordinated heteroleptic bisbipyridylsilicon(IV) complexes

Kummer noted that the slow decomposition of these complexes, allowed for complete characterization of these heteroleptic complexes as cis-octahedral cations with iodide anions.<sup>7,8,13</sup> However, he noted that the anions could be easily exchanged, only limited by their solubility.<sup>8,13</sup>

Kummer, et. al. went on to synthesize thirteen bis-bpy complexes with direct reactions of ligands with diiodosilanes in  $\text{CHCl}_3$  (Table 1).<sup>13</sup> All of these 1:2 complexes expanded their library of cis-octahedral  $[\text{SiXYbpy}_2]^{2+}$  cations.<sup>13</sup> It was also noted that for the reaction to be successful there had to be two Si-I bonds present, since  $\text{SiBr}_4$ ,  $\text{SiCl}_4$ , and dichlorosilanes form only a 1:1 complex.<sup>13</sup> Additionally, Kummer stated that a reaction in benzene lead to only the 1:1 complex.<sup>13</sup> This gave possibility for the synthesis of additional heteroleptic polypyridyl silicon(IV) complexes and some insight into their synthesis and solubility.<sup>13</sup>

Table 1: Reactions of ligands with diiodosilanes reported by Kummer, et. al.

Compound	X	Y
1	Cl	Cl
2	Cl	CH <sub>3</sub>
3	Cl	H
4	H	H
5	H	CH <sub>3</sub>
6	CH <sub>3</sub>	CH <sub>3</sub>
7	I	I
8	I	CH <sub>3</sub>
9	I	H
10	C <sub>6</sub> H <sub>5</sub>	CH <sub>3</sub>
11	C <sub>6</sub> H <sub>5</sub>	C <sub>6</sub> H <sub>5</sub>
12	OCH <sub>3</sub>	CH <sub>3</sub>
13	OCH <sub>3</sub>	H
14	bpy	

In 2011 Chukwu synthesized a series of bis-bipyridylsilicon(IV) complexes by reacting the isolated intermediate,  $[\text{Si}(\text{bpy})_2\text{I}_2]\text{I}_2$  with a series of alcohols and phenols.<sup>14</sup> The initial complexes of  $[\text{Si}(\text{bpy})_2(\text{cat})]\text{I}_2$  was synthesized by reacting the  $[\text{Si}(\text{bpy})_2\text{I}_2]\text{I}_2$  intermediate with catechol in a variety of polar solvents, since Suthar demonstrated that the  $[\text{Si}(\text{bpy})_2\text{I}_2]\text{I}_2$  intermediate was soluble in polar solvents.<sup>14</sup> Solvents attempted included  $\text{CHCl}_3$  (which was utilized by Suthar), 2-picoline, pyridine, 2,6-lutidine, and acetonitrile.<sup>14</sup> Acetonitrile resulted in the most facile synthesis, which was done at room temperature for 24 hours.<sup>14</sup>

The synthesis initiated precedence for synthetic routes for a series of bipyridyl silicon(IV) complexes, by reacting the isolated  $[\text{Si}(\text{bpy})_2\text{I}_2]\text{I}_2$  intermediate directly with alcohols or with phenols in ACN.<sup>14</sup> The complexes were synthesized and characterized with EA,  $^1\text{H}$  NMR,  $^{13}\text{C}$  NMR,  $^{29}\text{Si}$  NMR, IR, and UV-vis. Additionally, Chukwu obtained the crystal structures of  $[\text{Si}(\text{bpy})_2(\text{cat})](\text{PF}_6)_2$  and  $[\text{Si}(\text{bpy})_2(-\text{OCH}_2\text{CH}_2\text{O}-)]\text{I}_2$ .<sup>14</sup>

Recently, Meggers reported high affinity of hexacoordinate silicon complexes for DNA binding.<sup>15</sup> His group's is interested in the octahedral coordination geometry and

their application for DNA binding due to their rigid structure with stereochemistry suitable for biochemical applications.<sup>15</sup> Additionally, they reported data of the structure of the  $[\text{Si}(\text{bpy})_2(\text{cat})]^{+2}$  crystal structure, further indicating their confirmation of this structure and its possible applications.<sup>15</sup>

#### 1.4 Research Goals

The focus of this thesis was to elaborate the structural and electrochemical properties of a series of heterolepic bis-bipyridylsilicon(IV) complexes. These complexes would be synthesized by reacting the  $[\text{Si}(\text{bpy})_2\text{I}_2]\text{I}_2$  precursor with an appropriate alcohol or phenol. The following complexes were successfully synthesized and completely characterized:  $[\text{Si}(\text{bpy})_2(\text{OMe})_2](\text{I})(\text{I}_3)$ ,  $[\text{Si}(\text{bpy})_2(-\text{OCH}_2\text{CH}_2\text{O}-)]\text{I}_2$ ,  $[\text{Si}(\text{bpy})_2(\text{OPh})_2](\text{I}_3)_2$ ,  $[\text{Si}(\text{bpy})_2(\text{bph})](\text{PF}_6)_2$ , and  $[\text{Si}(\text{bpy})_2(\text{cat})](\text{PF}_6)_2$ .

Additionally, new research into the possible dual hydrogen bond catalytic potential for  $[\text{Si}(\text{bpy}^*)_2(\text{OH})_2](\text{PF}_6)_2$  ( $\text{bpy}^*$  = bipyridine, bis-dimethylbipyridine, or 4,4'-bis-t-butylbipyridine) was explored and reported for the Michael Addition or Friedel-Crafts alkylation reaction of indole and methylindole with trans-b-nitrostyrene. This new catalytic system should add to the recent demonstration of silicon based diols as DHB catalysts.<sup>16,17,18,19,20</sup>

## CHAPTER 2: EXPLORING THE STRUCTURE AND REDOX ACTIVITY OF HEXACOORDINATE BIS(BIPYRIDYL)SILICON(IV) COMPLEXES<sup>1</sup>

### 2.1 Introduction

In recent years, there has been a significant increase in the structural diversity of stable hexacoordinate silicon complexes, especially ones containing N or O chelating ligands, and the bipyridine ligand is an especially well-known and important ligand for stabilizing hexacoordinate silicon complexes.<sup>21</sup> Our lab has been exploring redox active polypyridylsilicon complexes for electronic and electrochromic applications, demonstrating for example that salts of  $\text{Si}(\text{bpy})_3^{+4}$  and  $\text{Si}(\text{terpy})_2^{+4}$  are well behaved electrochemically, undergoing multiple, reversible one-electron reductions at low reduction potentials.<sup>2</sup> Wieghardt employed DFT calculations and X-ray crystallography to explore the non-innocence of bipyridine ligands in group 14 complexes, and concluded that both of the neutral species  $\text{Si}(\text{bpy})_3$  and  $\text{Si}(\text{bpy})_2$  possess tetravalent silicon centers with ligand localized reductions.<sup>22</sup> These species are therefore best described as  $\text{Si}^{\text{IV}}(\text{bpy}^*)_2(\text{bpy}^{2-})$  and  $\text{Si}^{\text{IV}}(\text{bpy}^{2-})_2$  respectively.<sup>22</sup> Likewise, MacDiarmid also concluded that neutral  $\text{Si}(\text{bpy})_2\text{Cl}_2$  should be described as a tetravalent silicon with ligand localized reductions based on EPR data.<sup>23</sup> The ability of the bipyridine ligand, aided by the tetravalent silicon center, to store multiple electrons is attractive for redox applications. As part of our ongoing investigation into redox active hexacoordinate silicon complexes, we decided to synthesize and measure the electrochemical properties of bis(bipyridyl)silicon(IV) complexes with various alkoxide or phenoxide ligands to

determine the effect of the ligand on the reduction potential and on the stability of the reduced species. Alkoxide and phenoxide ligands are of particular interest because of the stability and variety these ligands provide for hexacoordinate silicon complexes, and ultimately they might provide a means of tuning the electrochromic properties.

A recent report by Meggers, which demonstrated the high affinity of hexacoordinate bis(phenanthroline)silicon(IV) compounds for DNA binding, could usher in a new renaissance in hexacoordinate silicon chemistry.<sup>24</sup> These complexes act as substitutionally inert octahedral scaffolds without the MLCT transitions typical of their transition metal analogs. In a subsequent study Meggers demonstrated DNA mismatch recognition using a hexacoordinate bis(phenanthroline)silicon(IV) sandwich complex with a ruthenium center.<sup>15</sup> Hexacoordinate bis(bipyridyl)silicon(IV) complexes have also been investigated recently, and it is likely that these complexes will demonstrate similar biological activity.<sup>25</sup> Currently, only five hexacoordinate bis(bipyridyl)silicon(IV) complexes appear in the Cambridge Structural Database: [Si(bpy)<sub>2</sub>(catecholato)] (PF<sub>6</sub>)<sub>2</sub> [25], [Si(bpy)<sub>2</sub>(binolato)] (PF<sub>6</sub>)<sub>2</sub> [25], [Si(bpy)<sub>2</sub>Cl<sub>2</sub>]I<sub>2</sub> [26], [Si(bpy)<sub>2</sub>(OH)<sub>2</sub>]I<sub>2</sub> [27], and Na[Si(bpy)<sub>2</sub>(dpcat-H)](ClO<sub>4</sub>)<sub>4</sub> (dpcat-H = protonated dipyridocatecholate) [3].<sup>3,25,26,27</sup> In this paper we explore the electrochemical and structural properties of five bis(bipyridyl)silicon(IV) complexes: [Si(bpy)<sub>2</sub>(OMe)<sub>2</sub>]<sup>2+</sup> (1), [Si(bpy)<sub>2</sub>(-OCH<sub>2</sub>CH<sub>2</sub>O-)]<sup>2+</sup> (2), [Si(bpy)<sub>2</sub>(OPh)<sub>2</sub>]<sup>2+</sup> (3), [Si(bpy)<sub>2</sub>(bph)]<sup>2+</sup> (4), and [Si(bpy)<sub>2</sub>(cat)]<sup>2+</sup> (5), (bpy = 2,20-bipyridine, cat = 1,2-benzenediolato, bph = 2,20-biphenolato ligand). (Figure 7).

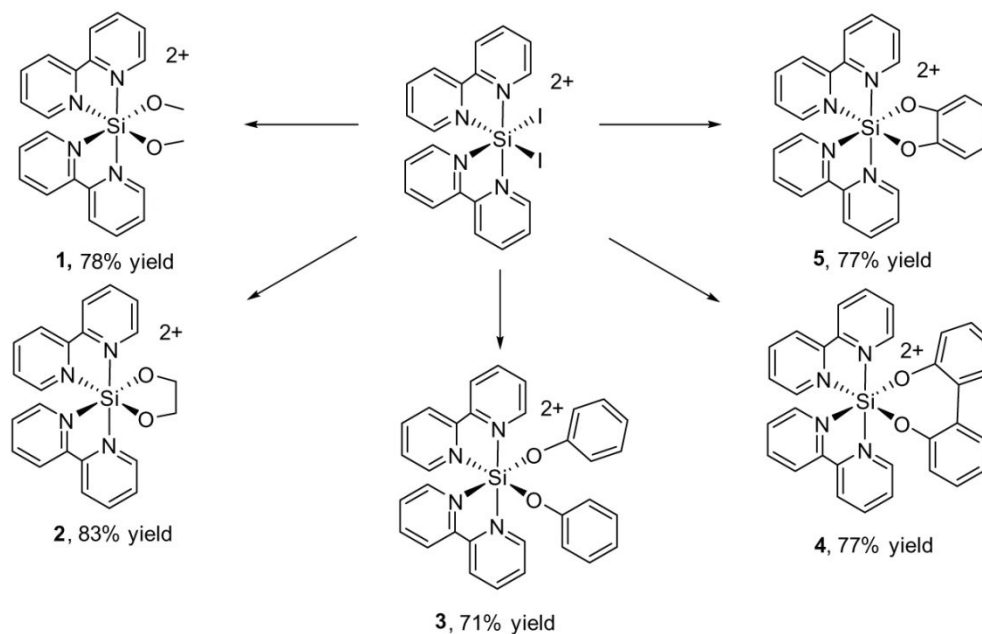


Figure 7: Structures and yields of the five complexes:  $[\text{Si}(\text{bpy})_2(\text{OMe})_2]^{2+}$  (1),  $[\text{Si}(\text{bpy})_2(-\text{OCH}_2\text{CH}_2\text{O}-)]^{2+}$  (2),  $[\text{Si}(\text{bpy})_2(\text{OPh})_2]^{2+}$  (3),  $[\text{Si}(\text{bpy})_2(\text{bph})]^{2+}$  (4), and  $[\text{Si}(\text{bpy})_2(\text{cat})]^{2+}$  (5), ( $\text{bpy}$  = 2,2'-bipyridine,  $\text{cat}$  = 1,2-benzenediolato,  $\text{bph}$  = 2,20-biphenolato ligand).

## 2.2 Results and Discussion

### 2.2.1 Crystal Structures

Crystal structures of the five complexes are shown in (Figure 8). The anions have been removed for clarity. Crystals of salts containing cations 1–3 were obtained by recrystallization of the crude reaction products. Surprisingly, complex 1 crystallized as a mixed triiodide/iodide salt,  $[\text{Si}(\text{bpy})_2(\text{OMe})_2](\text{I})(\text{I}_3)$ . Complexes 2 and 3 crystallized as the iodide and triiodide salts respectively. Complexes 4 and 5 were crystallized as the hexafluorophosphate salts following a metathesis reaction. A crystal structure was previously reported for  $[\text{Si}(\text{bpy})_2(\text{cat})](\text{PF}_6)_2$  containing disordered  $\text{CH}_3\text{CN}$  solvent molecules in the unit cell as triclinic with a  $P\bar{1}$  space group, but we find that the non-solvated  $[\text{Si}(\text{bpy})_2(\text{cat})](\text{PF}_6)_2$  complex crystallizes in an orthorhombic unit cell with

space group *Pbca*. All five complexes exhibit a distorted octahedral geometry.<sup>25</sup> The O–Si–O bond angle is significantly shorter in complexes 2 and 5 presumably due to steric constraints imposed by the five-membered ring. The alkoxide ligands exhibit a subtle trans influence on the Si–N bond length in the order: catecholate < ethylene glycolate < biphenolate < phenolate < methoxide. The trend suggests a combination of steric and electronic factors, with monodentate ligands exhibiting a stronger trans influence than the bidentate ligands (especially the five membered rings), and alkoxides exhibiting a stronger trans influence than phenolates.

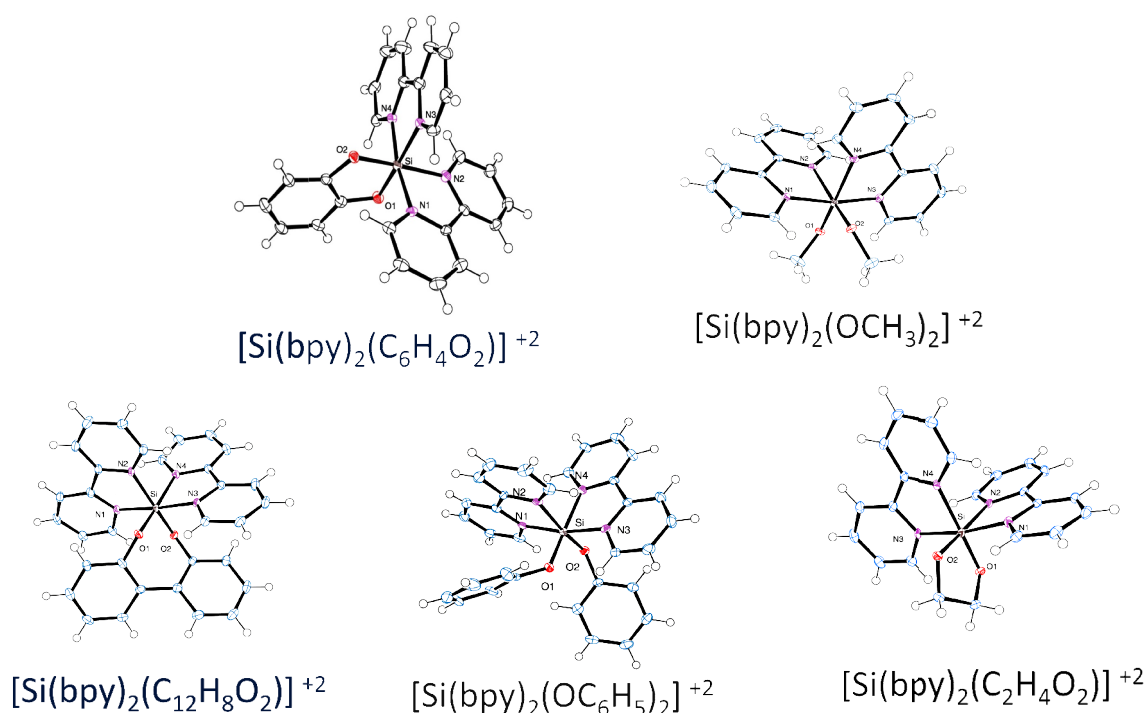


Figure 8: Crystal structures have been obtained for the complexes: (a)  $[\text{Si}(\text{bpy})_2(\text{OMe})_2]\text{I}_2$ , (b)  $[\text{Si}(\text{bpy})_2(-\text{OCH}_2\text{CH}_2\text{O}-)](\text{I})(\text{I}_3)$ , (c)  $[\text{Si}(\text{bpy})_2(\text{OPh})_2](\text{I}_3)_2$ , (d)  $[\text{Si}(\text{bpy})_2(\text{bph})](\text{PF}_6)_2$ , and (e)  $[\text{Si}(\text{bpy})_2(\text{cat})](\text{PF}_6)_2$ , and, (bpy= 2,2'-bipyridine, cat= 1,2-benzenediolate, bph=2,2'-biphenolato ligand). Anions have been removed for clarity.

2.2.2 CV



Table 2 contains the results of cyclic voltammetry experiments on the hexafluorophosphate salts of complexes 1–5 (V versus Fc/ Fc<sup>+</sup>) in acetonitrile/tetra-*n*-butylammonium hexafluorophosphate solution using a platinum disk working electrode. The potential of the first wave,  $E_{1/2} (+2/+1)$ , is only slightly influenced by the nature of the alkoxide ligand and involves a chemically reversible, single electron process. Each of the five species also underwent a second reduction process at a potential,  $E_{1/2} (+1/0)$ , ranging from -1.297 V to -1.404 V versus Fc. Only the bidentate biphenolate (4) and catecholate (5) complexes showed complete chemical reversibility at 200 mV/s for the second reduction wave (Figure 9).

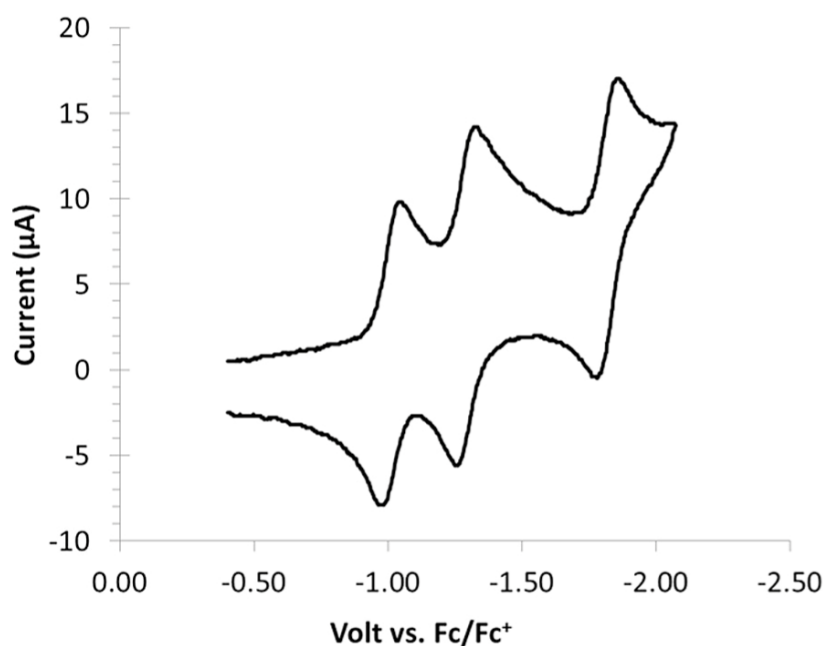


Figure 9: CV of  $5(\text{PF}_6)_2$  at 200 mV/s scan rate with a platinum working electrode in acetonitrile with  $\text{TBAPF}_6$  (0.1 M) and  $iR$  compensation.

Table 2:  $E_{1/2}$  values,  $\Delta E_p$  and calculated  $E_{LUMO}$  for compounds 1–5. Electrochemistry studies conducted in  $CH_3CN/TBAPF_6$  solution at scan rate = 0.200 V/s using a platinum disk working electrode.  $E_{LUMO}$  calculated using DFT (B3LYP/6-31G(d), Spartan 2010).

Compound	$E_{1/2}$ (V vs. Fc/Fc <sup>+</sup> )	$0 -1$ ( $\Delta E_p$ (mV))		$E_{LUMO}$ (eV)
	+2/+1 ( $\Delta E_p$ (mV))	+1/0 ( $\Delta E_p$ (mV))		
<b>1</b>	-1.147 (87) chemically reversible	-1.382 (80) limited chemical reversibility		-2.7
<b>2</b>	-1.128 (86) chemically reversible	-1.404 (102) limited chemical reversibility		-2.8
<b>3</b>	-1.074 (64) chemically reversible	-1.359 (95) limited chemical reversibility	-1.911 (112) limited chemical reversibility	-2.7
<b>4</b>	-1.080 (84) chemically reversible	-1.366 (77) chemically reversible	-1.914 (71) limited chemical reversibility	-2.7
<b>5</b>	-1.014 (75) chemically reversible	-1.297 (73) chemically reversible	limited chemical reversibility -1.835 (93) limited chemical reversibility	-2.8

$E_{1/2} = (E_{pc} + E_{pa})/2$ ;  $\Delta E_p = E_{pc} - E_{pa}$ .

$$E_{1/2} = (E_{pc} + E_{pa})/2; \Delta E_p = E_{pc} - E_{pa}$$

The small variation in potentials for the first reduction waves is consistent with DFT calculations, which predict that the LUMO is localized on the bipyridine ligands and that the LUMO varies by less than 0.1 eV for all five species (Figure 10).

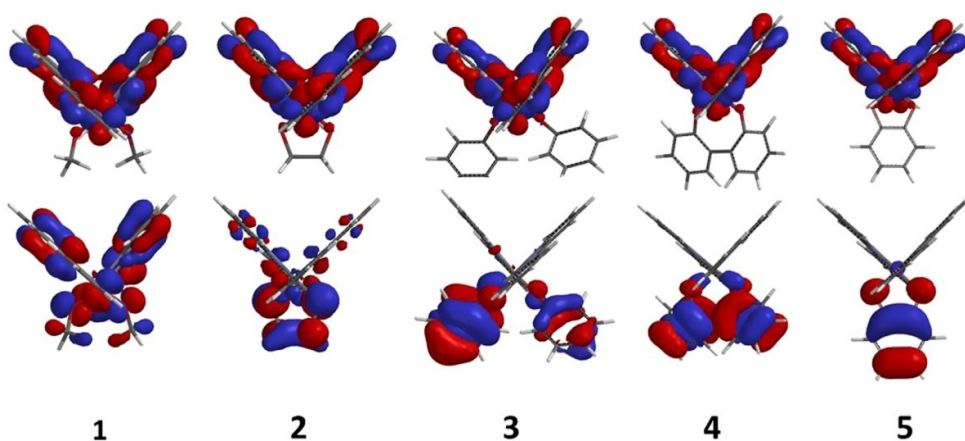


Figure 10: Calculated HOMO (bottom) and LUMO (top) of compounds 1–5 using DFT (B3LYP/6-31G\*, Spartan 2010).

The bipyridine based reduction occurs at much less negative potentials than for the transition metal analogs due to the effect of the tetravalent silicon center. For example, the potential for the first reduction of 5 is approximately 1.1 V less negative than that of  $\text{Ru}(\text{bpy})_2(\text{cat})$  ( $E_{1/2} (0/-1) = -2.16 \text{ V}$  versus  $\text{Fc}/\text{Fc}^+$ ) or  $\text{Os}(\text{bpy})_2(\text{cat})$  ( $E_{1/2} (0/-1) = -2.09 \text{ V}$ ).<sup>29</sup> A similar anodic shift (approximately 1.2 V) was observed for the first bipyridine based reduction of  $\text{Si}(\text{bpy})_3^{+4}$  compared to  $\text{Ru}(\text{bpy})_3^{+2}$ .<sup>2</sup> The lack of reversible oxidation waves was surprising, especially for the catecholate complex since the catecholate is well known for its ability to be oxidized to a semiquinolate and ultimately a quinone. Species 5 had a poorly defined  $E_{\text{pa}}$  wave at +1.2 V (versus  $\text{Fc}^+/\text{Fc}$ ) with no clear  $E_{\text{pc}}$ . This very positive oxidation potential is consistent with a previously reported unsuccessful attempt to oxidize  $\text{Si}(\text{bpy})_2(\text{cat})^{+2}$  with lead(IV) oxide, in which

only starting material was recovered.<sup>25</sup> The difficulty in oxidizing the catechol ligand in this silicon complex contrasts with the ruthenium analog, Ru(bpy)<sub>2</sub>(cat), which exhibits a reversible semiquinolate/catecholate wave at -0.73 V (versus Fc<sup>+</sup>/Fc, converted from published SCE referenced data assuming Fc<sup>+</sup>/Fc is at +0.400 V versus SCE).<sup>30,31</sup>

The emergence of hexacoordinate polypyridylsilicon complexes as substitutionally inert, structurally rigid scaffolds is a promising new direction for 3-dimensional molecular design, and has already proven successful in biological applications. The current study demonstrates that these complexes, particularly the (arenedialato) bis(bipyridyl)silicon(IV) complexes (4 and 5), also exhibit reversible redox activity and could potentially serve as electron transfer or multi-electron transfer reagents. While the first reduction potential of the compounds does not appear to vary much, the stability of the reduced species depends on the nature of the ligand, with catecholates > biphenolate > phenolate > ethylene glycolate > methoxy.

## 2.3 Experimental

### General Procedures

Silicon(IV) iodide (99% metals base) was used as provided from Alfa Aesar and handled under nitrogen in a glove box. Phenol, biphenol, and 1,2-benzenediol were dried prior to use by azeotropic distillation of toluene. Methanol and ethylene glycol were stored over molecular sieves prior to use. NMR spectra were acquired using a JEOL 500 MHz NMR spectrometer. For the <sup>29</sup>Si spectra, a 60° pulse width was used with a relaxation delay of 10s, and a pre-transform blip routine was used to suppress the signal from the quartz NMR tube. Two-dimensional COSY, HSQC, and HMBC spectra were used to assign all of the hydrogen and carbon peaks. IR spectra were obtained on a Perkin Elmer Spectrum

One FTIR with a Universal ATR sample accessory (diamond). A Mariner Perceptive Biosystems ESI-TOF mass spectrometer was used to obtain all ESI-MS data.

Combustion analysis (C, H, and N) was conducted by Atlantic Microlab, Inc.

Cyclic voltammetry studies were performed using a Princeton Applied Research Model 273A Potentiostat / Galvanostat employing a conventional three-electrode setup consisting of a platinum disk or glassy carbon working electrode, a silver/silver chloride reference electrode, and a platinum wire auxiliary electrode. Positive feedback iR compensation was routinely used. Voltammograms were obtained in 0.1 M tetrabutylammonium hexafluorophosphate (TBAPF<sub>6</sub>)/acetonitrile solution using solvent that had previously been purified and dried using a solvent purification system (SPS-400, Innovative Technologies) and subsequently purged with nitrogen. The supporting electrolyte (TBAPF<sub>6</sub>) was recrystallized from ethanol and dried under vacuum prior to use. Ferrocene was used as an internal standard without further purification.

Crystals of suitable size of compounds 1-5 were removed from the mother liquor, coated with a thin layer of paratone-N oil, mounted on the Agilent Gemini R Ultra diffractometer, and flash-cooled to 100° K in the cold stream of the Cryojet XL liquid nitrogen cooling device (Oxford Instruments) attached to the diffractometer. The Gemini R Ultra diffractometer was equipped with a sealed-tube long fine focus X-ray source with Mo target ( $\lambda = 0.71073 \text{ \AA}$ ) and Cu target ( $\lambda = 1.5418 \text{ \AA}$ ), four-circle kappa goniometer, and Ruby CCD detector. CrysAlis Pro software was used to control the diffractometer and perform data reduction and analysis.<sup>62</sup> The crystal structure was solved with ShelXS.<sup>63</sup> All non-hydrogen atoms appeared in the E-map of the correct solution. Alternate cycles of model-building in Olex2 and refinement in ShelXL followed.<sup>63,64</sup> All

non-hydrogen atoms were refined anisotropically. All hydrogen atom positions were calculated based on idealized geometry, and recalculated after each cycle of least squares. During refinement, hydrogen atom – parent atom vectors were held fixed (riding motion constraint). Crystallographic data are provided in Table 3.

TABLE 3: Crystallographic data for Compounds 1-5.

Compound	1	2	3	4	5
CCDC Number	1040073	1040074	1040075	1040076	1040077
Formula	$C_{22}H_{22}N_4O_2Si(1)(I_3)$	$C_{22}H_{20}N_4O_2Si_2(1)$	$C_{32}H_{26}N_4O_2Si_2(I_3)$	$C_{32}H_{24}N_4O_2Si_2(PF_6)$	$C_{26}H_{20}N_4O_2Si_2(PF_6)$
Formula weight	910.13	654.31	1288.06	814.58	738.49
T (K)	100.05(10)	100(2)	100(2)	100(2)	100(2)
Crystal system	orthorhombic	monoclinic	triclinic	triclinic	orthorhombic
Space group	$P2_12_12_1$	$C2/c$	$P\bar{1}$	$P\bar{1}$	$Pbca$
a (Å)	10.71625(16)	21.6751(15)	11.4700(3)	10.7920(4)	18.1742(4)
b (Å)	14.6868(3)	8.8715(3)	13.0962(4)	12.0504(6)	11.9283(3)
c (Å)	17.5844(3)	14.6212(9)	13.7432(3)	14.3570(5)	26.3018(6)
$\alpha$ (°)	90.00	90	101.942(2)	82.585(4)	90
$\beta$ (°)	90.00	127.359(10)	101.730(2)	71.896(3)	90
$\gamma$ (°)	90.00		105.076(2)	66.056(4)	90
V (Å <sup>3</sup> )	2767.57(8)	2234.7(4)	1876.59(9)	1621.94(12)	5701.9(2)
Z	4	4	2	2	8
$D_{calc}$ (g/cm <sup>3</sup> )	2.184	1.945	2.28	1.668	1.721
$\mu$ (mm <sup>-1</sup> )	4.573	2.896	5.032	0.28	2.855
F(000)	1696.0	1264.0	1188.0	824.0	2976.0
Crystal size (mm <sup>3</sup> )	$0.4446 \times 0.2746 \times 0.0526$	$0.47 \times 0.28 \times 0.12$	$0.19 \times 0.05 \times 0.05$	$0.28 \times 0.09 \times 0.06$	$0.22 \times 0.08 \times 0.05$
$\theta$ range for data collection	3.3 to 26.4°	3.5 to 29.3°	3.3 to 29.4°	3.4 to 29.4°	3.4 to 67.1°
Reflections collected	21332	8807	31794	22367	51346
Independent reflections	5662 [ $R_{int} = 0.0312$ ]	2714 [ $R_{int} = 0.034$ ]	9195 [ $R_{int} = 0.0506$ ]	6764 [ $R_{int} = 0.0811$ ]	5078 [ $R_{int} = 0.1019$ ]
Data/restraints/parameters	5662/0/300	2714/0/141	9195/0/410	6764/0/478	5078/0/424
Goodness-of-fit on $F^2$	1.026	1.083	1.032	0.968	1.029
Final R indexes [ $I > 2\sigma(I)$ ]	$R_1 = 0.0173$ , $wR_2 = 0.0329$	$R_1 = 0.0261$ , $wR_2 = 0.0500$	$R_1 = 0.0399$ , $wR_2 = 0.0660$	$R_1 = 0.0522$ , $wR_2 = 0.1057$	$R_1 = 0.0504$ , $wR_2 = 0.1320$
Final R indexes [all data]	$R_1 = 0.0193$ , $wR_2 = 0.0335$	$R_1 = 0.0369$ , $wR_2 = 0.0559$	$R_1 = 0.0687$ , $wR_2 = 0.0749$	$R_1 = 0.1100$ , $wR_2 = 0.1211$	$R_1 = 0.0582$ , $wR_2 = 0.1398$

## Syntheses

Method A:  $[\text{Si}(\text{bpy})_2\text{I}_2]\text{I}_2$  was synthesized and isolated according to the procedure of Kummer and coworkers [11]. Silicon(IV) iodide (1.00 g, 1.87 mmol), bipyridine (0.80 g, 5.12 mmol), and chloroform, were added to an ampoule inside a glove box, along with a stir bar. The sealed ampoule was then heated in an oil bath at 75° C for 12 hours. The resulting suspension was then filtered inside the glove box and rinsed with chloroform. The resulting deep burgundy powder was used in the following procedures without further purification. In a typical reaction, methanol (5.00 mL, 3.96 g, 0.12 mol) or ethylene glycol (5.00 mL, 5.57g, 89.67 mmol) was injected into an oxygen-free flask with  $[\text{Si}(\text{bpy})_2\text{I}_2]\text{I}_2$  (1.00g, 2.94 mmol). The reaction mixture stirred for 24 hours at room temperature. The reaction mixture was centrifuged, and the precipitate was retained and rinsed with dichloromethane and diethyl ether. The precipitate was dried under vacuum. The crude product was converted to the hexafluorophosphate salt by dissolving in minimal amounts of water followed by addition of  $\text{NH}_4\text{PF}_6$ . The precipitate was rinsed with water, ethanol, and ether before drying in a vacuum.

Method B: Silicon(IV) iodide (1.00 g, 1.87 mmol), bipyridine (0.80 g, 5.12 mmol), and chloroform, were added to an ampoule inside a glove box, along with a stir bar. The sealed ampoule was then heated in an oil bath at 75° C for 12 hours. The resulting deep burgundy suspension in chloroform was taken back into the glove box and phenol (0.40 g, 4.25 mmol), biphenol (0.40 g, 2.15 mmol), or ortho-catechol (0.25 g, 2.27 mmol) was added. The reaction mixture was placed back in the 75 °C oil bath sealed in the same ampoule for 24 hours. The suspension was removed and cooled to room temperature.



The contents of the ampoule were centrifuged and the precipitate was collected and rinsed with chloroform and ether. The resulting red precipitate was dried under vacuum. The crude product was converted to the hexafluorophosphate salt by dissolving in minimal amounts of water followed by addition of  $\text{NH}_4\text{PF}_6$ . The precipitate was rinsed with water, ethanol, and ether before drying in a vacuum.

## Experimental

$[\text{Si}(\text{bpy})_2(\text{OMe})_2](\text{PF}_6)_2$  Synthesized according to method A. The yield of  $[1](\text{PF}_6)_2$  was 78% (1.01 g, 1.46 mmol) based on  $\text{SiI}_4$ .  $^1\text{H}$  NMR ( $\text{CD}_3\text{CN}$ , 500 MHz) :  $\delta$  3.03 (3H, s,), 7.19 (1H, d,  $J = 5.5$  Hz), 7.62 (1H, dd,  $J = 7.3$  Hz), 8.33 (1H, dd,  $J = 6.4$  Hz), 8.40 (1H, dd,  $J = 7.7$  Hz), 8.67 (1H, d,  $J = 8.3$  Hz), 8.88 (2H, m), 9.53 (1H, d,  $J = 6.0$  Hz).  $^{13}\text{C}\{^1\text{H}\}$  NMR( $\text{CD}_3\text{CN}$ , 500 MHz) :  $\delta$  149.82, 148.07, 145.69, 145.11, 143.91, 131.15, 131.01, 125.54, 125.40, 51.65 ppm.  $^{29}\text{Si}$  NMR( $\text{CD}_3\text{CN}$ , 500 MHz) : -156.7 ppm. ESI-MS:  $[\text{Si}(\text{bpy})_2(\text{OMe})_2](\text{PF}_6)^{+1}$ :  $\{\text{C}_{22}\text{H}_{22}\text{N}_4\text{O}_2\text{SiPF}_6\}^{+1}$ , 547.10 m/z,  $[\text{Si}(\text{bpy})_2(\text{OMe})_2]^{+2}$ :  $\{\text{C}_{22}\text{H}_{22}\text{N}_4\text{O}_2\text{Si}\}^{+2}$ , 201.10 m/z. Anal. Calc. For  $\text{C}_{22}\text{H}_{22}\text{N}_4\text{O}_2\text{SiP}_2\text{F}_{12}$  (692.46 g  $\text{mol}^{-1}$ ): C, 38.16; H, 3.20; N, 8.09%. Found: C, 37.98; H, 3.23; N, 7.97%. Crystals of  $[1](\text{I})(\text{I}_3)$  suitable for x-ray analysis were obtained by recrystallization of the crude reaction product from a filtered acetone solution by slow evaporation at room temperature.

$[\text{Si}(\text{bpy})_2(-\text{OCH}_2\text{CH}_2\text{O}-)](\text{PF}_6)_2$  Synthesized according to method A. The yield of  $[2](\text{PF}_6)_2$  was 83% (1.07 g, 1.55 mmol) based on  $\text{SiI}_4$ .  $^1\text{H}$  NMR( $\text{CD}_3\text{CN}$ , 500 MHz) :  $\delta$  3.47 (2H, dd,  $J = 6$  Hz), 4.00 (2H, dd,  $J = 6$  Hz), 7.43 (2H, d,  $J = 6$  Hz), 7.69 (2H, dd,  $J = 6$  Hz), 8.30 (2H, dd,  $J = 6$  Hz), 8.49 (2H, dd,  $J = 8$  Hz), 8.73 (2H, d,  $J = 8$  Hz), 8.83 (2H,

dd,  $J = 6$  Hz), 8.87 (4H, m,  $J = 8$  Hz), 9.40 (2H, d,  $J = 6$  Hz).  $^{13}\text{C}\{^1\text{H}\}$  NMR( $\text{CD}_3\text{CN}$ , 500 MHz):  $\delta$  148.64, 147.91, 146.98, 145.58, 144.91, 144.84, 131.21, 130.88, 125.59, 125.53, 61.94 ppm.  $^{29}\text{Si}$  NMR( $\text{CD}_3\text{CN}$ , 500 MHz): -144.1 ppm. ESI-MS:  $[\text{Si}(\text{bpy})_2(-\text{OCH}_2\text{CH}_2\text{O}-)](\text{PF}_6)^{+1}$ :  $\{\text{C}_{22}\text{H}_{20}\text{N}_4\text{O}_2\text{SiPF}_6\}^{+1}$  545.10 m/z,  $[\text{Si}(\text{bpy})_2(-\text{OCH}_2\text{CH}_2\text{O}-)]^{+2}$ :  $\{\text{C}_{22}\text{H}_{20}\text{N}_4\text{O}_2\text{Si}\}^{+2}$ , 200.07 m/z. Anal. Calc. for  $\text{C}_{22}\text{H}_{20}\text{N}_4\text{O}_2\text{SiP}_2\text{F}_{12}$  (690.44 g mol $^{-1}$ ): C, 38.27; H, 2.92; N, 8.11%. Found: C, 38.23; H, 2.96; N, 8.02%. Crystals of  $[2](\text{I})_2$  suitable for x-ray analysis were obtained by recrystallization of the crude reaction product from a filtered acetone solution by slow evaporation at room temperature.

$[\text{Si}(\text{bpy})_2(\text{OPh})_2](\text{PF}_6)_2$  Synthesized according to Method B.  $[\text{Si}(\text{bpy})_2(\text{OPh})_2](\text{PF}_6)_2$  was obtained by metathesis as described above, 71% yield (1.08 g, 1.33 mmol) based on  $\text{SiI}_4$ .  $^1\text{H}$  NMR( $\text{CD}_3\text{CN}$ , 500 MHz):  $\delta$  6.21 (4H, d,  $J = 6$  Hz), 6.86 (2H, td,  $J = 6$  Hz), 6.95 (4H, td,  $J = 7$  Hz), 7.51 (2H, d,  $J = 6$  Hz), 7.73 (2H, td,  $J = 4$  Hz), 8.26 (2H, td,  $J = 5$  Hz), 8.41 (2H, td,  $J = 7$  Hz), 8.53 (2H, d,  $J = 8$  Hz), 8.69 (2H, d,  $J = 8$  Hz), 8.78 (2H, td,  $J = 6$  Hz), 9.68 (2H, d,  $J = 6$  Hz).  $^{13}\text{C}\{^1\text{H}\}$  NMR( $\text{CD}_3\text{CN}$ , 500 MHz):  $\delta$  154.59, 150.15, 148.68, 146.41, 145.03, 144.52, 143.07, 131.58, 131.47, 130.58(2C), 125.15, 125.09, 123.59, 120.72(2C) ppm.  $^{29}\text{Si}$  NMR( $\text{CD}_3\text{CN}$ , 500 MHz): -167.4 ppm. ESI-MS:  $[\text{Si}(\text{bpy})_2(\text{OPh})_2](\text{PF}_6)^{+1}$ :  $\{\text{C}_{32}\text{H}_{26}\text{N}_4\text{O}_2\text{SiPF}_6\}^{+1}$  671.10 m/z,  $[\text{Si}(\text{bpy})_2(\text{OPh})_2]^{+2}$ :  $\{\text{C}_{32}\text{H}_{26}\text{N}_4\text{O}_2\text{Si}\}^{+2}$ , 263.10 m/z. Anal. Calc. for  $\text{C}_{32}\text{H}_{26}\text{N}_4\text{O}_2\text{SiP}_2\text{F}_{12}$  (816.60 g mol $^{-1}$ ): C, 47.07; H, 3.21; N, 6.86%. Found: C, 45.82; H, 3.24; N, 6.71%. Crystals of  $[3](\text{I}_3)_2$  suitable for x-ray analysis were obtained by vapor diffusion of diethyl ether into a filtered, saturated acetone solution of the crude reaction product.

[Si(bpy)<sub>2</sub>(bph)](PF<sub>6</sub>)<sub>2</sub> Synthesized according to Method B. [Si(bpy)<sub>2</sub>(bph)](PF<sub>6</sub>)<sub>2</sub> was isolated in a 77% yield (1.17 g, 1.44 mmol) based on SiI<sub>4</sub>. <sup>1</sup>H NMR (CD<sub>3</sub>CN, 500 MHz): δ 5.97 (2H, d, J = 7 Hz), 6.90 (2H, td, J = 6 Hz), 7.05 (2H, td, J = 6 Hz), 7.45 (2H, dd, J = 6 Hz), 7.58 (2H, d, J = 6 Hz), 7.74 (4H, m), 8.55 (2H, td, J = 7 Hz), 8.69 (2H, td, J = 6 Hz), 8.86 (2H, d, J = 8 Hz), 8.87 (2H, dd, J = 8 Hz), 8.98 (4H, dd, J = 5 Hz). <sup>13</sup>C{<sup>1</sup>H} NMR (CD<sub>3</sub>CN, 500 MHz): δ 153.20, 149.08, 148.36, 146.59, 145.04, 144.53, 143.33, 131.38, 131.26, 131.08, 130.25, 130.10, 126.27, 125.83, 124.19, 120.74 ppm. <sup>29</sup>Si NMR (CD<sub>3</sub>CN, 500 MHz): -155.7 ppm. ESI-MS: [Si(bpy)<sub>2</sub>(bph)](PF<sub>6</sub>)<sub>6</sub><sup>+</sup>: {C<sub>32</sub>H<sub>24</sub>N<sub>4</sub>O<sub>2</sub>SiPF<sub>6</sub>}<sup>+</sup> 669.10 m/z, [Si(bpy)<sub>2</sub>(bph)]<sup>+</sup>: {C<sub>32</sub>H<sub>24</sub>N<sub>4</sub>O<sub>2</sub>Si}<sup>+</sup> 262.10 m/z. Anal. Calc. for C<sub>32</sub>H<sub>24</sub>N<sub>4</sub>O<sub>2</sub>SiP<sub>2</sub>F<sub>12</sub> (814.58 g mol<sup>-1</sup>): C, 47.18; H, 2.97; N, 6.88%. Found: C, 46.90; H, 3.04; N, 6.74%. Crystals of [4](PF<sub>6</sub>)<sub>2</sub> suitable for x-ray analysis were obtained by vapor diffusion of diethyl ether into a filtered, saturated acetone solution of the hexafluorophosphate salt.

[Si(bpy)<sub>2</sub>(-OC<sub>6</sub>H<sub>4</sub>O-)](PF<sub>6</sub>)<sub>2</sub> Synthesized according to Method B. [5](PF<sub>6</sub>)<sub>2</sub> was obtained in a 77% yield (1.06 g, 1.44 mmol) based on SiI<sub>4</sub>. <sup>1</sup>H NMR (CD<sub>3</sub>CN, 500 MHz): δ 6.76 (2H, m), 6.83 (2H, m), 7.59 (2H, d, J = 6 Hz), 7.81 (2H, td, J = 5 Hz), 8.18 (2H, td, J = 6 Hz), 8.62 (2H, td, J = 6 Hz), 8.80 (2H, td, J = 6 Hz), 8.83 (2H, d, J = 8 Hz), 8.92 (2H, d, J = 8 Hz), 9.08 (2H, d, J = 5 Hz). <sup>13</sup>C{<sup>1</sup>H} NMR (CD<sub>3</sub>CN, 500 MHz): δ 148.66, 148.37, 148.05, 146.92, 146.17, 144.86, 144.13, 131.92, 131.39, 126.17, 125.93, 123.04, 114.69 ppm. <sup>29</sup>Si NMR (CD<sub>3</sub>CN, 500 MHz): -148.9 ppm. ESI-MS: [Si(bpy)<sub>2</sub>(-OC<sub>6</sub>H<sub>4</sub>O-)](PF<sub>6</sub>)<sub>6</sub><sup>+</sup>: {C<sub>26</sub>H<sub>20</sub>N<sub>4</sub>O<sub>2</sub>SiPF<sub>6</sub>}<sup>+</sup> 593.11 m/z, [Si(bpy)<sub>2</sub>(-OC<sub>6</sub>H<sub>4</sub>O-)]<sup>+</sup>: {C<sub>26</sub>H<sub>20</sub>N<sub>4</sub>O<sub>2</sub>Si}<sup>+</sup> 224.07 m/z. Anal. Calc. for C<sub>26</sub>H<sub>20</sub>N<sub>4</sub>O<sub>2</sub>Si(PF<sub>6</sub>)<sub>2</sub> (738.48 g mol<sup>-1</sup>): C, 42.29; H, 2.73; N,

7.59%. Found: C, 42.22; H, 2.67; N, 7.51%. Crystals of  $[5](PF_6)_2$  suitable for x-ray analysis were obtained by vapor diffusion of diethyl ether into a saturated acetone solution of the hexafluorophosphate salt.

## CHAPTER 3: DIOL CATALYSIS

“Hydrogen bonding is a ubiquitous force in nature.”<sup>49</sup> Research interest in the exploration of hydrogen bond donor catalysis (HBD) has greatly increased in the last two decades.<sup>19,39,40</sup> Catalytic design incorporating HBD, which act as Bronsted Acids, can provide many opportunities in catalytic design.<sup>39,40</sup> Conversely Lewis Acid (LA) metal centered catalysts, such as  $\text{Al}_2\text{Cl}_6$ , have been more widely used in many catalytic reactions. Starting in 1960, with a report by Yates and Eaton, an interest in this type of Lewis Acid catalysis has not diminished and continues to this day.<sup>39,40</sup> Jacobsen’s review discusses this interest in comparison to Bronsted Acid catalysis, which is noted to feature predominately in biocatalysis and in nature.<sup>39,40,41,42</sup> Looking at the two types of catalysts, their differences outweigh their similarities, which many reviews and articles have discussed.<sup>39,40,41,42,43,44,45,46</sup> However, the most interesting is the comparison of their toxicity and tunability. Metal-centered LA catalysts are usually highly toxic but are usually highly tunable. In contrast HBD BA catalysts are only somewhat tunable but usually environmentally benign. With the increased interest in green chemistry and the expanding library of HBD catalysis, the Schmedake group is exploring the use of hexacoordinate silicon(IV) complexes as HBD catalysts.

Several groups of single and dual donating HBD catalysts (protonated catalysts), have been published, including amidine, guanidine, phosphoric acid, urea, thiourea, squaramide, TADDOL, BINOL, and more recently silanediols.<sup>19,39,41,44,46,47,48,49,50,60</sup>

These types of catalysts have been particularly used for stereoselective nucleophile-electrophile transformations.<sup>39,40,41,44</sup>

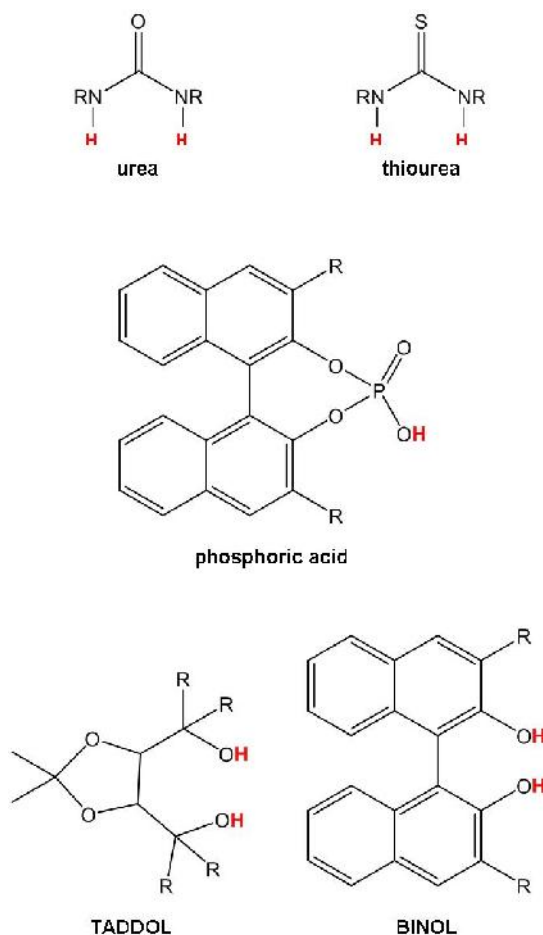


Figure 11: Images of several types of hydrogen bonding catalysts

### 3.1 Dual hydrogen bond catalysis

Enantioselective organocatalysis, which can utilize two hydrogen bonds via noncovalent interactions, has been shown to have catalyst tunability.<sup>39,41</sup> This bifunctionality has led to additional interest and synthesis of dual HBD catalysts through the modification of existing dual HBD catalysts or the creation of new dual HBD catalytic scaffolds.<sup>19,40,44</sup> Some considerations in the design of catalyst synthesis include a somewhat rigid structure, molecular recognition, catalytic activity in water, selectivity,

yield, and catalyst turnover.<sup>18,19,40</sup> However, Kozlowski has noted that the complex nature of catalyst design and hydrogen-bonding nature often relies on “trial and error” rather than generalization of types of catalytic design.<sup>41</sup> The use of dual HB donating interactions allow for increased strength and directionality in comparison to single HBD catalysts.<sup>40,42</sup>

The interest in dual HBD catalysts has initially focused on (thio)urea catalysts, which have notable activity and selectivity, which makes use of two hydrogen bonds for transformation.<sup>19,39,46,48,50,51,52</sup> (Thio)ureas are easily prepared and have tunability by varying the nitrogen substituents which allow the steric and electronic properties of these catalysts to be widely altered.<sup>17,39, 40</sup> Ureas, however are notoriously insoluble and therefore have limited use; therefore, thiourea catalytic research is more prevalent and used a comparison tool with other dual HBD catalysts.<sup>39,41,49</sup> In particular Schreiner’s thiourea catalyst is used for comparison due to the acknowledgment of it as the most active and versatile single HB donating catalyst.<sup>39,41,49</sup>

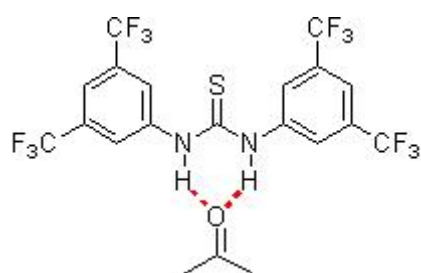


Figure 12: Schreiner’s catalyst

A variety of dual HBD thioureas have been synthesized since Schreiner’s catalyst was reported and their bonding functionality has enabled asymmetric orientation that can

interact with a variety of structurally diverse electrophiles.<sup>39,53</sup> The interest in exploring dual HB thioureas has opened the variety of synthetic possibilities of additional dual HB donating catalysts. Kozlowski et. al. reported on a library of HBD catalysts and of 33 catalysts reported only four showed cationic molecular structures.<sup>41</sup>

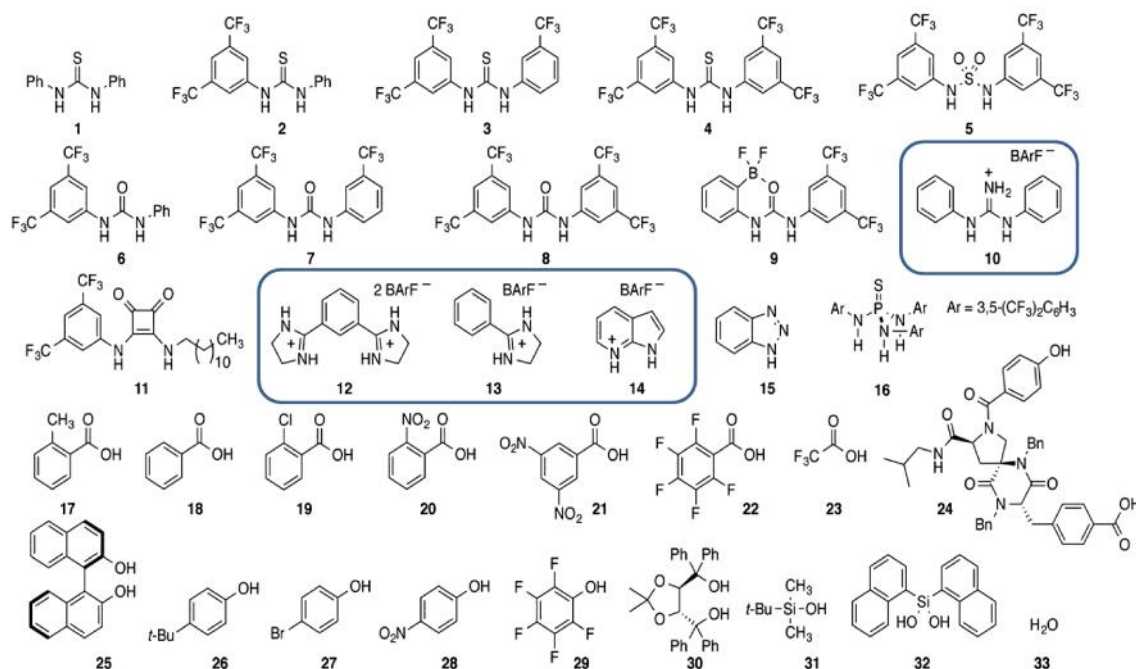


Figure 13: Kozlowski's catalysts examined as HBD catalysts<sup>41</sup>

Kozlowski reported the pseudo- first order kinetic rates of reaction for both the Diels-Alder and Michael Addition reactions.<sup>41</sup> A graph of the data suggests two significant conclusions. First, there appears to be strong correlation between effective Michael Addition catalysts and Diels-Alder catalysts. Second, the best catalysts in both reactions appear to be cationic catalysts.



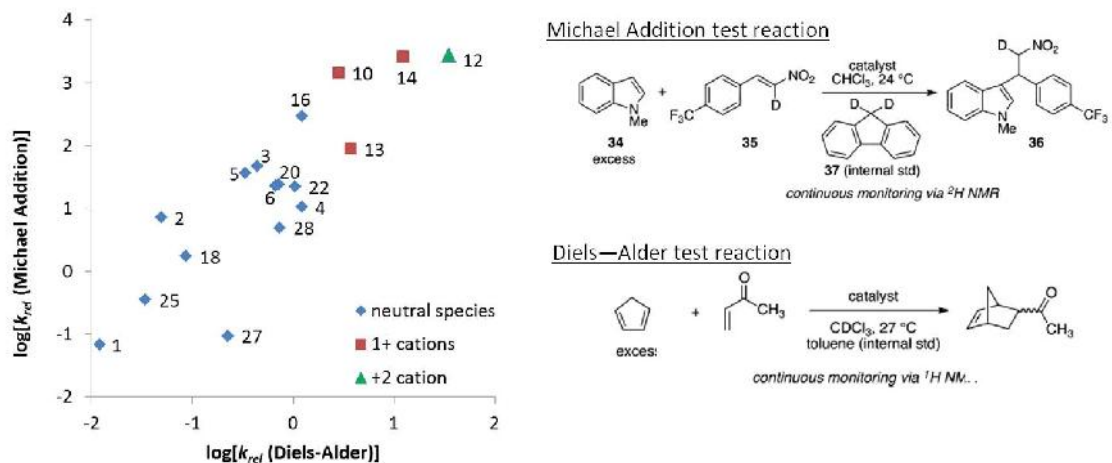


Figure 14: Data of catalytic tests done by Kozłowski<sup>41</sup>

### 3.2 Si diol chemistry

Expanding on the dual HBD catalyst design, synthesis of silanediol catalysts has been reported.<sup>19,47</sup> Kondo was the first to report the synthesis and catalytic application of a silanediol.<sup>16</sup> This BINOL-derived silanediol reported by Kondo showed anion recognition, indicating the possibility for application of other silanediol and tetracoordinated silicon diol complexes as HBD catalysts.<sup>16,20,45,54,55,56</sup>

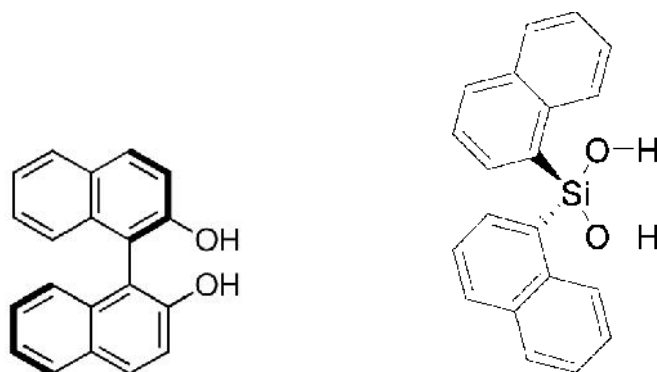


Figure 15: Image of BINOL (on left) and Kondo's di(1-naphthyl)silanediol (right)

Since then, Franz and Mattson groups have expanded the synthesis and application of silanediol catalysts which showed their ability for use in catalytic reactions.<sup>17,18,19,20,50,57</sup> Franz indicates the interest and appeal of silanols and silanediols as catalysts is due to the fact that “silanols (SiOH) make up the reactive hydroxyl groups on the surface of minerals, zeolites, and silica gel.”<sup>17</sup> Additional research groups have indicated the importance of this and the catalytic activity of the examples mentioned.<sup>45,55,56</sup> Both Franz and Mattson have investigated the intra- and inter-molecular properties of silanediol catalysts and their experimental results in hydrogen bonding catalysis.<sup>16,17,18,19,20</sup> Due to the Kozlowski’s published results of properties of HBD catalysts and the research of Mattson and Franz of silanediol HBD catalysts, the use of cationic hexacoordinated silicon(IV) complexes was chosen to study catalytic activity as hydrogen bond donors.<sup>17,18,19,37,41</sup>

### 3.3 Results and Discussion

#### 3.3.1 Self-recognition of diol catalysts

Franz et. al. has extensively reported the effect of self recognition and the effect of it on catalysis (Figure 16).<sup>17,18,57,58</sup> Self-association has been previously studied for other dual and bifunctional organocatalysts due the negative effects of the dimer formed which can block the hydrogen bonding positions, which can reduce catalytic conservation.<sup>17,47,55,57,58</sup> However, with silanediol catalysts, the molecular recognition can promote cooperative hydrogen bonding.<sup>19,47,57</sup>

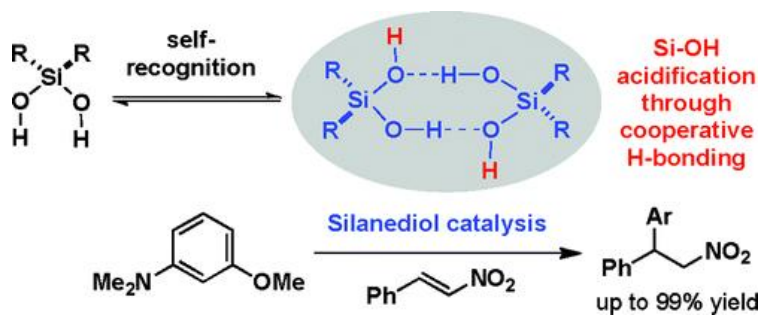


Figure 16: Franz's figure showing self-recognition by silanediol catalysts<sup>58</sup>

The preliminary crystal structure of  $[\text{Si}(\text{dmbpy})_2(\text{OH})_2](\text{PF}_6)_2$  (Figure 17) does not show any molecular recognition, which indicates that the hexacoordinated silicon complexes will not undergo dimerization or molecular recognition.<sup>58</sup>

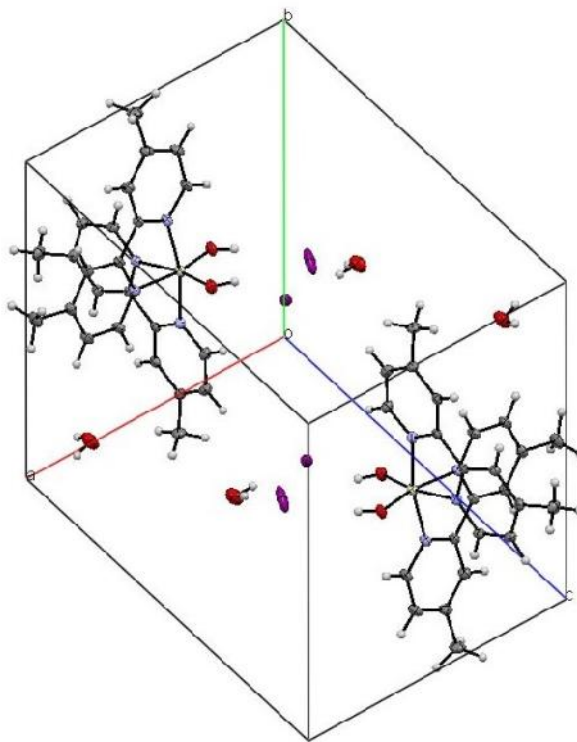


Figure 17: Preliminary crystal structure of  $[\text{Si}(\text{dmbpy})_2(\text{OH})_2](\text{PF}_6)_2$

### 3.3.2 Catalytic activity of a Michael Addition reaction

Synthesis and characterization of dual HBD catalysts have focused particularly on electrophile activation for the determination and comparison of catalytic ability.<sup>39</sup>

Michael Addition reactions have been used for primary catalytic reactivity tests due to the consideration of it as “one of the most important reactions for the construction of carbon-carbon bonds in organic reactions”.<sup>43,45,46,48,52,53,56,59,60</sup> The Michael Addition of indole is particularly appealing due to “the indole framework (that) is present in over 3,000 isolated natural products and 40 medicinal agents.”<sup>59,61</sup> For example, the synthesis of tryptophan and serotonin is the Michael Addition alkylation between indole and a nitroalkene.<sup>42,60,61</sup>

Initial studies to determine catalytic conversion were done using indole with trans- $\beta$ -nitrostyrene, using procedures set forth by Franz (Figure 18).<sup>58</sup> As specified by Franz, three equivalents of indole were used.<sup>58</sup>

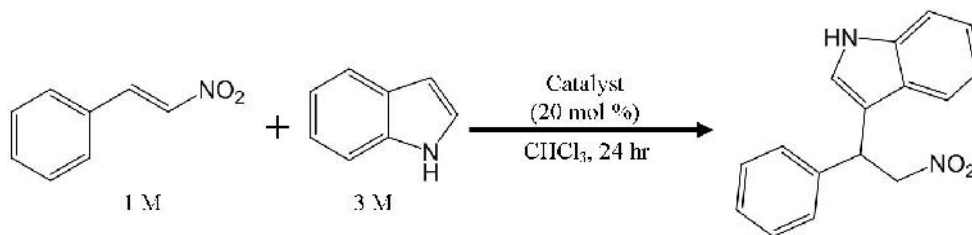


Figure 18: Catalytic reaction of indole with trans- $\beta$ -nitrostyrene

Early results of the silicon hexacoordinated diol,  $[\text{Si}(\text{bbbpy})_2(\text{OH})_2](\text{PF}_6)_2$ , showed catalytic conversion at even a 2% mol catalyzed reactions (Figure 19). This demonstrated the feasibility of the use of this complex for catalysis. However quantification was not achieved through GC-MS analysis.

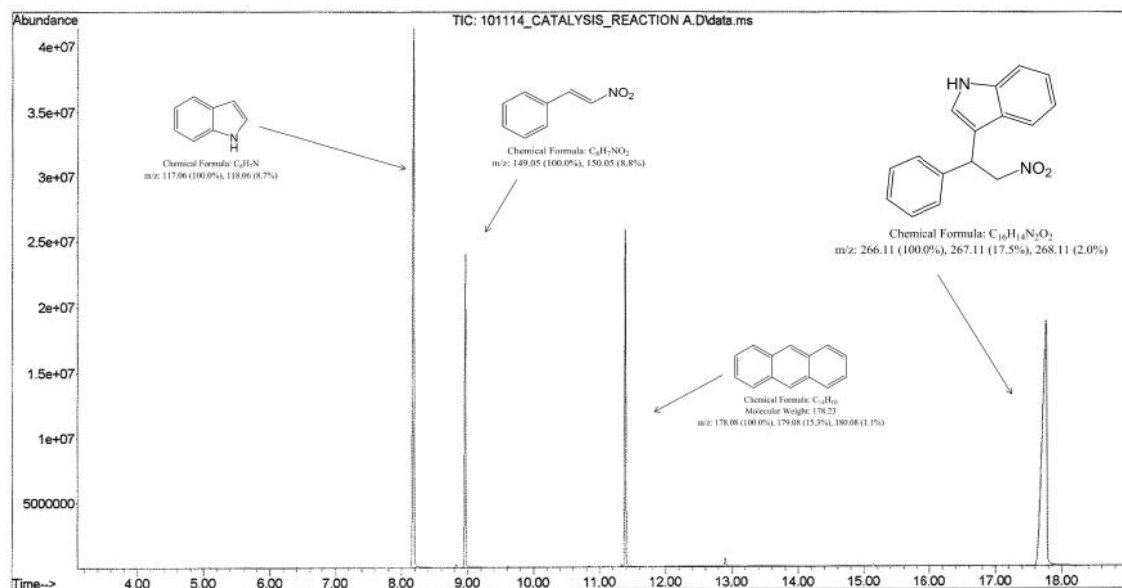


Figure 19: GCMS spectra of qualitative evidence of catalysis with 2%  $[\text{Si}(\text{bbbpy})_2(\text{OH})_2](\text{PF}_6)_2$  used. (Anthracene was used as an internal standard.)

NMR studies have been previously used for the quantification of kinetic rate data.<sup>20,41,43,51,54,58</sup> The pseudo-first order condition kinetic rates were the basis for our quantification of  $[\text{Si}(\text{bbbpy})_2(\text{OH})_2](\text{PF}_6)_2$  as a catalyst for the Michael Addition of n-methylindole and trans- -nitrostyrene.

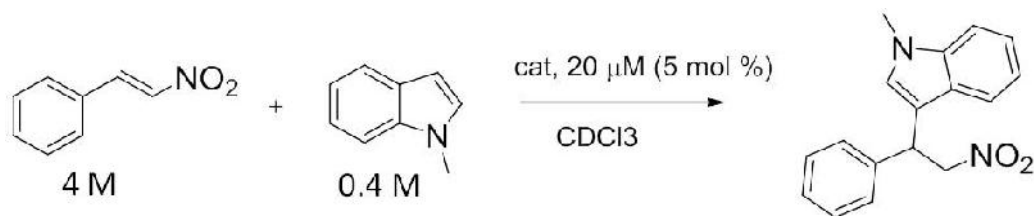


Figure 20: Reaction of n-methylindole with trans- -nitrostyrene

Preliminary results have shown that  $[\text{Si}(\text{bbbpy})_2(\text{OH})_2](\text{PF}_6)_2$  acts as a dual HBD catalyst with a 7 fold increase of reaction with 10% mol catalyst and a 3 fold increase of reaction with 5% mol catalyst (Figure 21), using Equation 1. These promising results suggest that further studies should be done to optimize this reaction.

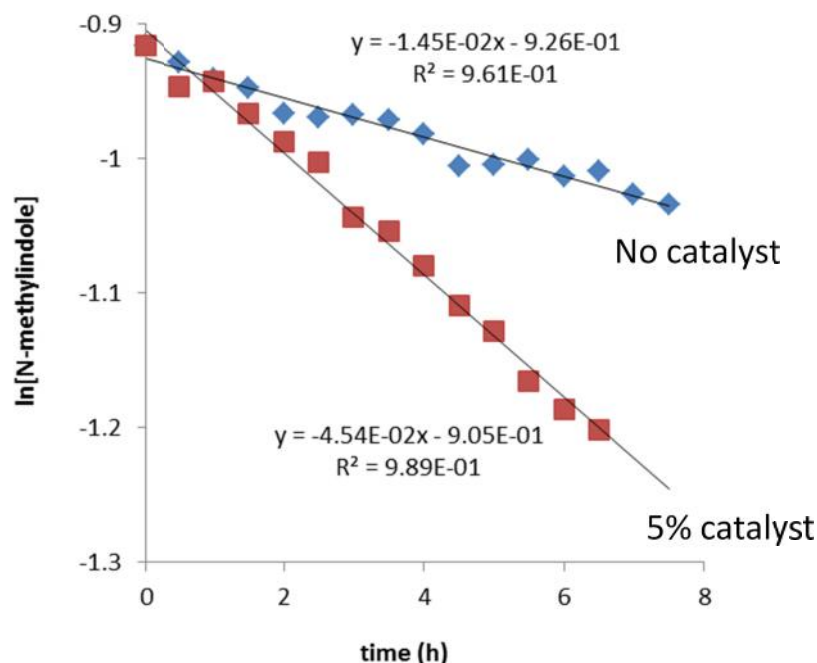


Figure 21: Initial Results showing a 3 fold increase of reaction (Figure 20) using 5% mol catalyst

$$k_{\text{cat}} / k_{\text{uncat}} = 3$$

$$(K_{\text{cat}} - k_{\text{uncat}}) / k_{\text{uncat}} = 2$$

Equation 1: Psuedo first order calculation of the reaction of n-methylindole with trans- -nitrostyrene

### 3.4 Experimental details

#### General Procedures

Silicon(IV) iodide (99% metals base) was used as provided from Alfa Aesar and handled under nitrogen in a glove box. NMR spectra were acquired using a JEOL 500 MHz NMR spectrometer. For the  $^{29}\text{Si}$  spectra, a  $60^\circ$  pulse width was used with a relaxation delay of 10 s, and a pre-transform blip routine was used to suppress the signal from the quartz NMR tube. Kinetic experiments were done.....Combustion analysis (C, H, and N)

was conducted by Atlantic Microlab, Inc. Crystals of suitable size of  $[\text{Si}(\text{dmbpy})_2(\text{OH})_2]$  were removed from the mother liquor, coated with a thin layer of paratone-N oil, mounted on the Agilent Gemini R Ultra diffractometer, and flash-cooled to 100° K in the cold stream of the Cryojet XL liquid nitrogen cooling device (Oxford Instruments) attached to the diffractometer. The Gemini R Ultra diffractometer was equipped with a sealed-tube long fine focus X-ray source with Mo target ( $\lambda = 0.71073 \text{ \AA}$ ) and Cu target ( $\lambda = 1.5418 \text{ \AA}$ ), four-circle kappa goniometer, and Ruby CCD detector. CrysAlis Pro software [15] was used to control the diffractometer and perform data reduction and analysis. The crystal structure was solved with ShelXS [16]. All non-hydrogen atoms appeared in the E-map of the correct solution. Alternate cycles of model-building in Olex2 [17] and refinement in ShelXL [16] followed. All non-hydrogen atoms were refined anisotropically. All hydrogen atom positions were calculated based on idealized geometry, and recalculated after each cycle of least squares. During refinement, hydrogen atom – parent atom vectors were held fixed (riding motion constraint). Crystallographic data is provided in Appendix 2.

## Experimental

$[\text{Si}(\text{dmbpy})_2(\text{OH})_2](\text{PF}_6)_2$ . Silicon(IV) iodide (1.15 g, 2.15 mmol), bipyridine (1.10 g, 5.97 mmol), and chloroform, were added to an ampoule inside a glove box, along with a stir bar. The sealed ampoule was then heated in an oil bath at 75° C for 12 hours. The resulting suspension was then filtered and rinsed with chloroform. The resulting orange powder was then rinsed with water, sonicated, and centrifuged. The resulting precipitate lightened to a yellow-orange color, was dried under vacuum. Once dry, the precipitate

was rinsed with ether 3 times and dried under vacuum. The crude product was converted to the hexafluorophosphate salt by dissolving in minimal amounts of water heated to 50°C. The precipitate did not dissolve entirely and was therefore vacuum filtered to remove any undissolved product. Once filtered,  $\text{NH}_4\text{PF}_6$  dissolved in water was added to the clear solution to obtain a white precipitate. The precipitate was rinsed with water and ether before drying in a vacuum. The yield was 88% (1.90 g, 1.36 mmol) based on  $\text{SiI}_4$ .  $^1\text{H}$  NMR ( $\text{CD}_3\text{CN}$ , 500 MHz) : 2.52 (3H, s), 2.81 (3H, s), 3.87 (1H, bs), 7.00 (1H, d,  $J = 5.8$  Hz), 7.4 (1H, dd,  $J = 7.0$  Hz), 8.05 (1H, dd,  $J = 7.0$  Hz), 8.44 (1H, s), 8.63 (1H, s), 9.47 (1H, d,  $J = 5.9$  Hz).  $^{13}\text{C}\{^1\text{H}\}$  NMR( $\text{CD}_3\text{CN}$ , 500 MHz) : 161.62, 159.05, 148.28, 144.52, 143.57, 142.90, 131.91, 130.81, 125.38, 125.33, 118.37, 22.43, 21.75 ppm.  $^{29}\text{Si}$  NMR( $\text{CD}_3\text{CN}$ , 500 MHz) : -156.49 ppm. Anal. Calc. For  $\text{C}_{24}\text{H}_{26}\text{N}_4\text{O}_2\text{SiP}_2\text{F}_{12}$  (720.50 g  $\text{mol}^{-1}$ ): C, 39.97; H, 3.60; N, 7.77%. Found: C, 39.79; H, 3.67; N, 7.79%. Crystals  $[\text{Si}(\text{dmbpy})_2(\text{OH})_2](\text{I})_2$  suitable for x-ray analysis were obtained by slow evaporation of the product from a saturated acetone solution.

$[\text{Si}(\text{bbbpy})_2(\text{OH})_2](\text{PF}_6)_2$  Silicon(IV) iodide (1.02 g, 1.90 mmol), bipyridine (1.41 g, 5.25 mmol), and chloroform, were added to an ampoule inside a glove box, along with a stir bar. The sealed ampoule was then heated in an oil bath at 75°C for 12 hours. The resulting suspension was then filtered and rinsed with chloroform. The resulting orange powder was then rinsed with water, sonicated, and centrifuged. The resulting precipitate lightened to a yellow-orange color, was dried under vacuum. Once dry, the precipitate was rinsed with ether 3 times and dried under vacuum. The crude product was converted to the hexafluorophosphate salt by dissolving in minimal amounts on water heated to



50°C. The precipitate did not dissolve entirely and was therefore vacuum suctioned through to remove any undissolved product. Once filtered,  $\text{NH}_4\text{PF}_6$  dissolved in water was added to the clear solution to obtain a white precipitate. The precipitate was rinsed with water and ether before drying in a vacuum. The yield was 91% (1.54 g, 1.90 mmol) based on  $\text{SiI}_4$ .  $^1\text{H}$  NMR ( $\text{CD}_3\text{CN}$ , 500 MHz) : 1.37 (9H, s), 1.60 (9H, s), 3.85 (1H, bs), 7.06 (1H, d,  $J = 6.4$  Hz), 7.54 (1H, dd,  $J = 6.4$  Hz), 8.23 (1H, dd,  $J = 6.4$  Hz), 8.61 (1H, s), 8.79 (1H, s), 9.51 (1H, d,  $J = 6.5$  Hz).  $^{13}\text{C}\{^1\text{H}\}$  NMR( $\text{CD}_3\text{CN}$ , 500 MHz) : 173.10, 170.64, 148.63, 145.06, 144.07, 143.36, 127.62, 127.17, 122.47, 122.40, 118.35, 37.77, 37.14, 30.37, 30.13 ppm.  $^{29}\text{Si}$  NMR( $\text{CD}_3\text{CN}$ , 500 MHz) : -157.15 ppm.

## CHAPTER 4: CONCLUSION

The emergence of hexacoordinate polypyridylsilicon complexes as substitutionally inert, structurally rigid scaffolds is a promising new direction for 3-dimensional molecular design, and has already proven successful in biological applications. The current study demonstrates that these complexes, particularly the bis(bipyridyl)(arene)dialato)silicon(IV) complexes (4 and 5), also exhibit reversible redox activity and could potentially serve as electron transfer or multi-electron transfer reagents. While the first reduction potential of the compounds does not appear to vary much, the stability of the reduced species depends on the nature of the ligand, with catecholates > biphenolate > phenolate > ethylene glycolate > methoxy.

Additionally, the bisbipyridylsilicon(IV) diol system has been demonstrated to be an effective catalyst for a Michael Addition reaction of an indole by trans- $\beta$ -nitrostyrene. While this catalyst has been proven to be effective, the catalytic enhancement has been modest. At this point, it warrants further experimentation.

First, it seems that dual HBD catalysts have a wide variety of chemistry that they can do. It would be interesting to explore addition reactions, like Diels-Alder, and might be particularly good at the reactions that involve coordination of an oxyanionic transition state or reactions that involve the coordination of an anion. The cationic nature of the catalyst provides these attractive areas to explore.

Furthermore, it has been shown with this thesis that ligand substitution or ligand modification has a significant effect of the solubility of the catalyst, which could be

further exploited to increase the overall catalytic efficiency. The solubility of the bisbipyridylsilicon(IV) diols is low in  $\text{CHCl}_3$ . It appears to be enhanced by coordination to the trans- $\beta$ -nitrostyrene. But increasing the solubility through ligand design or counterion design is an important direction for further research.

Finally, and most importantly, there is the possibility for doing chiral catalysis with bis-bipyridylsilicon(IV) diols. This thesis shows that the bis-bipyridylsilicon(IV) diols do not appear to dimerize or self-recognize in solution which suggests that the  $C_2$  symmetric monomers are an attractive potential chiral catalyst. Attempts to resolve the bis-bipyridylsilicon(IV) diols are currently underway in the group and chiral catalysis will be attempted soon.

## REFERENCES

- <sup>1</sup>Maguylo, C.; Chukwu, C.; Aun, M.; Monroe, T.; Ceccarelli, C.; Jones, D.; Merkert, J.; Donovan-Merkert, B.; Schmedake, T. *Polyhedron*, **2015**, 94, 52–58.
- <sup>2</sup>Suthar, B., Aldongarov, A.; Irgibaeva, I.; Moazzen, M.; Donovan-Merkert, B.; Merkert, J.; Schmedake, T. *Polyhedron*, **2012**, 31, 754-758.
- <sup>3</sup>Lee, D.; Moon, S.; Sizeland, A.; Gould, N.; Gbarbea, E.; Owusu, D.; Jones, D.; Schmedake, T. *Inorganic Chemistry Communications*. **2013**, 33, 125-128.
- <sup>4</sup>Chuit, C.; Corriu, R. J. P.; Reye, C.; Young, J. C. *Chemical Reviews*, **1993**, 93, 1371-1448.
- <sup>5</sup>Herzog, S.; Krebs, F. *Naturwissenschaften*, **1963**, 50, 330-331.
- <sup>6</sup>Herzog, S.; Zimmer, F. *Zeitschrift fuer Chemie*, **1967**, 7(10), 396.
- <sup>7</sup>Kummer, V.; Koster, H. *Zeitschrift fur Anorganische und allgemeine chemie (ZAAC)*, **1973**, 402, 297-304.
- <sup>8</sup>Kummer, V.; Koster, H. *Zeitschrift fur Anorganische und allgemeine chemie (ZAAC)*, **1973**, 398, 279-292.
- <sup>9</sup>Kummer, V.; Gaisser, K.; Seifert, J.; Wagner, R. *Zeitschrift fur Anorganische und allgemeine chemie (ZAAC)*, **1979**, 459, 145-156.
- <sup>10</sup>Morancho, P.; Pouvreau, P.; Constant, G. *Organometallic Chem.* **1979**, 166, 329-338.
- <sup>11</sup>Liu, Hong Ling, Ohmori, Y.; Kojima, M.; Yoshikawa, Y. *Journal of Coordination Chemistry*, **1998**, 44, 3, 257-268.
- <sup>12</sup>Suthar, B. Synthesis and Characterization of Hexacoordinate Polypyridal Silicon (IV) Complexes. M.S. Thesis, University of North Carolina at Charlotte, Charlotte, NC, 2010.
- <sup>13</sup>Kummer, D.; Gaiser, K. E.; Seshadri, T. *Chern. Ber.* **1977**, 100, 1950-1962.
- <sup>14</sup>Chukwu, C. Synthesis and Characterization of Hexacoordinate Polypyridyl and Catechol Silicon(IV) Complexes. M.S. Thesis, University of North Carolina at Charlotte, Charlotte, NC, 2011.
- <sup>15</sup>(a) Henker, J.; Gloeckner, S.; Meggers, E.; *Journal of Biological Inorganic Chemistry*, 2014, 19, S367-S367. (b) Fu, C.; Harms, K.; Zhang, L.; Meggers, E.; *Organometallics*, **2014**, 33, 3219-3222.

- <sup>16</sup>Kondo, S.; Harada, T.; Tanaka, R.; Unno, M. *Org. Lett.*, **2006**, 8, 20, 4621–4624.
- <sup>17</sup>Tran, N.; Min, T.; Franz, A. K. *Chem. Eur. J.* **2011**, 17, 9897–9900.
- <sup>18</sup>Liu, M.; Tran, N.; Franz, A. K.; Lee, J. K. *J. Org. Chem.* **2011**, 76, 7186–7194.
- <sup>19</sup>Auvil, T. J.; Schafer, A. G.; Mattson, A. E. *Eur. J. Org. Chem.* **2014**, 2633–2646.
- <sup>20</sup>Schafer, A. G.; Wieting, J. M.; Fisher, T. J.; Mattson, A. E. *Angew. Chem. Int. Ed.* **2013**, 52, 11321–11324.
- <sup>21</sup>For relevant reviews, see: (a) C. Chuit, R. J. P. Corriu, C. Reye and J. C. Young, *Chemical Reviews*, **1993**, 93, 1371–1448. (b) J. Y. Corey, *Chemical Reviews*, **2011**, 111, 863–1071. (c) M. Benaglia, S. Guizzetti and L. Pignataro, *Coordination Chemistry Reviews*, **2008**, 252, 492–512. (d) E. P. A. Couzijn, J. C. Slootweg, A. W. Ehlers and K. Lammertsma, *Zeitschrift Fur Anorganische Und Allgemeine Chemie*, **2009**, 635, 1273–1278. R. R. Holmes, *Chemical Reviews*, **1996**, 96, 927–950. (e) D. Kost and I. Kalikhman, *Accounts of Chemical Research*, **2009**, 42, 303–314.
- <sup>22</sup>England, J.; Wieghardt, K.; *Inorg. Chem.* **2013**, 52, 10067–10079.
- <sup>23</sup>Broudy, P. M.; Berry, A. D.; Wayland, B. B.; Macdiarmid, A. G., *J. Am. Chem. Soc.* **1972**, 94, 7577–7578.
- <sup>24</sup>Xiang, Y.; Fu, C.; Breiding, T.; Sasmal, P. K.; Liu, H.; Shen, Q.; Harms, K.; Zhang, L.; Meggers, E., *Chem. Comm.* **2012**, 48 (57), 7131–7133.
- <sup>25</sup>Fu, C.; Harms, K.; Zhang, L.; Meggers, E., *Organometallics*, **2014**, 33, 3219–3222.
- <sup>26</sup>Hensen, K.; Mayr-Stein, R.; Ruhl, S.; Bolte, M., *Acta Crystallographica Section C-Crystal Structure Communications* **2000**, 56, 607–609.
- <sup>27</sup>Sawitzki, G.; Schnering, H. G. V.; Kummer, D.; Seshadri, T., *Chemische Berichte-Recueil* **1978**, 111 (11), 3705–3710.
- <sup>28</sup>Kummer, D.; Gaisser, K. E.; Seshadri, T., *Chemische Berichte-Recueil* **1977**, 110 (5), 1950–1962.
- <sup>29</sup>Pierpont *INorg Chem* 1990 3797 and Haga. Dodsworth, Lever, *Inorg. Chem.* **1986**, 25, 447.
- <sup>30</sup>Masui, H.; Lever, A.; Auburn, P., *Inorganic Chemistry*. **1991**, 30, 2402–2410.
- <sup>31</sup>Connelly, N. G.; Geiger, W. E., *Chem. Rev.* **1996**, 96, 877–910.
- <sup>32</sup>Yamamoto, H.; Futatsugi, K. *Angew. Chem. Int. Ed.* **2005**, 44, 1924–1942.

- <sup>33</sup>Doyle, A. G.; Jacobsen, E. N. *Chem. Rev.*, **2007**, *107* (12), 5713–5743.
- <sup>34</sup>Akiyama, T. *Chem. Rev.* **2007**, *107*, 5744–5758.
- <sup>35</sup>McGuirk, C. M.; Katz, M. J.; Stern, C. L.; Sarjeant, A.; Hupp, J. T.; Farha, O. K.; Mirkin, C. A. *J. Am. Chem. Soc.* **2015**, *137*, 919–925.
- <sup>36</sup>Tang, W.; Johnston, S.; Li, C.; Iggo, J. A.; Bacsá, J.; Xiao, J. *Chem. Eur. J.* **2013**, *19*, 14187–14193.
- <sup>37</sup>Schafer, A. G.; Wieting, J. M.; Mattson, A. E. *Org. Lett.*, **2011**, *13*(19), 5228–5231.
- <sup>38</sup>Chen, Y.; Yekta, S.; Yudin, A. E. *Chem. Rev.* **2003**, *103*, 3155–3211.
- <sup>39</sup>Taylor, M. S.; Jacobsen, E. N. *Angew. Chem. Int. Ed.* **2006**, *45*, 1520–1543.
- <sup>40</sup>Schreiner, P. R. *Chem. Soc. Rev.*, **2003**, *32*, 289–296.
- <sup>41</sup>Walvoord, R. R.; Huynh, P.; Kozłowski, M. C. *J. Am. Chem. Soc.* **2014**, *136*, 16055–16065.
- <sup>42</sup>Hesticova, M.; Sebesta, R. *Tetrahedron*, **2014**, *70*, 901–905.
- <sup>43</sup>Scherer, A.; Mukherjee, T.; Hampel, F.; Gladysz, J. A. *Organometallics*, **2014**, *33*, 6709–6722.
- <sup>44</sup>Yamamoto, H. *Proc. Jpn. Acad., Ser. B.*, **2008**, *84*, 134–146.
- <sup>45</sup>Jeganathana, M.; Kanagaraja, K.; Dhakshinamoorthy, A.; Pitchumani, K. *Tetrahedron Letters*, **2014**, *55*, 2061–2064.
- <sup>46</sup>Akiyama, T.; Itoh, J.; Fuchibe, K. *Adv. Synth. Catal.* **2006**, *348*, 999–1010.
- <sup>47</sup>Tran, N. T.; Wilson, S. O.; Franz, A. K. *Chem. Commun.*, **2014**, *50*, 3738–3740.
- <sup>48</sup>Ganesh, M.; Seidel, D. *J. Am. Chem. Soc.*, **2008**, *130*, 16464–16465.
- <sup>49</sup>Rodriguez, A. A.; Yoo, H.; Ziller, J. M.; Shea, K. J. *Tetrahedron Letters*, **2009**, *50*, 6830–6833.
- <sup>50</sup>Wieting, J. M.; Fisher, T. J.; Schafer, A. G.; Visco, M. D.; Gallucci, J. C.; Mattson, A. E. *Eur. J. Org. Chem.* **2015**, 525–533.
- <sup>51</sup>Beletskiy, E. V.; Schmidt, J.; Wang, X.; Kass, S. R. *J. Am. Chem. Soc.* **2012**, *134*, 18534–18537.

- <sup>52</sup>Roca-López, D.; Marqués-López, E.; Alcaine, A.; Merino, P.; Herrera, R. P. *Org. Biomol. Chem.*, **2014**, *12*, 4503–4510.
- <sup>53</sup>Takenaka, N.; Chen, J.; Captain, B.; Sarangthem, R. S.; Chandrakumar, A. *J. Am. Chem. Soc.* **2010**, *132*, 4536–4537.
- <sup>54</sup>Kim, J. K.; Sieburth, S. M. *J. Org. Chem.* **2012**, *77*, 2901–2906.
- <sup>55</sup>Beemelmans, C.; Husmann, R.; Whelligan, D. K.; Özçubukçu, S.; Bolm, C. *Eur. J. Org. Chem.* **2012**, 3373–3376.
- <sup>56</sup>Shumaila, A.; Kusurkar, R. S. *Synthetic Communications*, **2010**, *40*, 2935–2940.
- <sup>57</sup>Wilson, S. O.; Tran, N. T.; Franz, A. K. *Organometallics*, **2012**, *31*, 6715–6718.
- <sup>58</sup>Tran, N. T.; Wilson, S. O.; Franz, A. K. *Org. Lett.*, **2012**, *14*(1), 186–189.
- <sup>59</sup>Dessole, G.; Herrera, R. P.; Ricci, A. *SYNLEIT*, **2004**, *13*, 2374–2378.
- <sup>60</sup>Herrera, R. P.; Sgarzani, V.; Bernardi, L.; Ricci, A. *Angew. Chem. Int. Ed.*, **2005**, *44*, 6576–6579.
- <sup>61</sup>Lin, C.; Hsu, J.; Sastry, M. N. V.; Fang, H.; Tu, Z.; Liu, J.; Ching-Fa, Y. *Tetrahedron*, **2005**, *61*, 11751–11757.

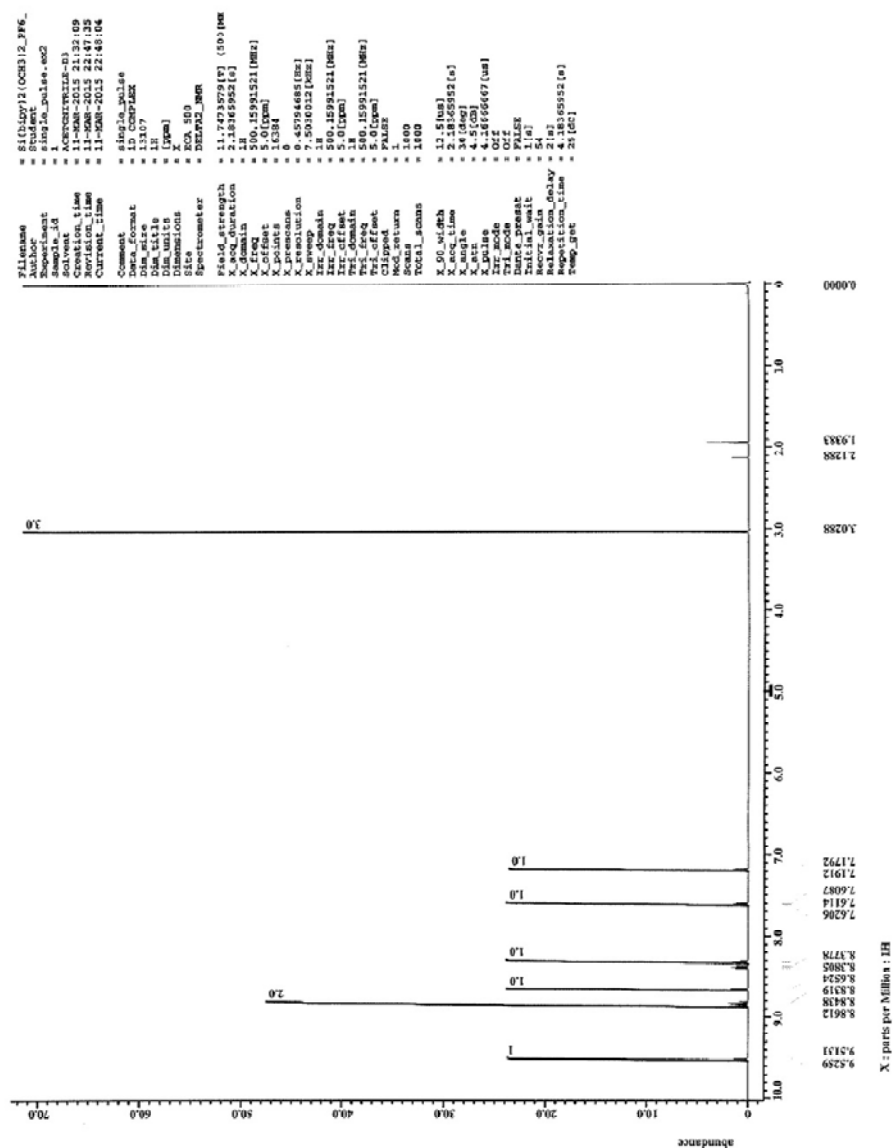
APPENDIX A: CHARACTERIZATION OF HEXACOORDINATE  
BIS(BIPYRIDYL)SILICON(IV) COMPLEXES<sup>1</sup>

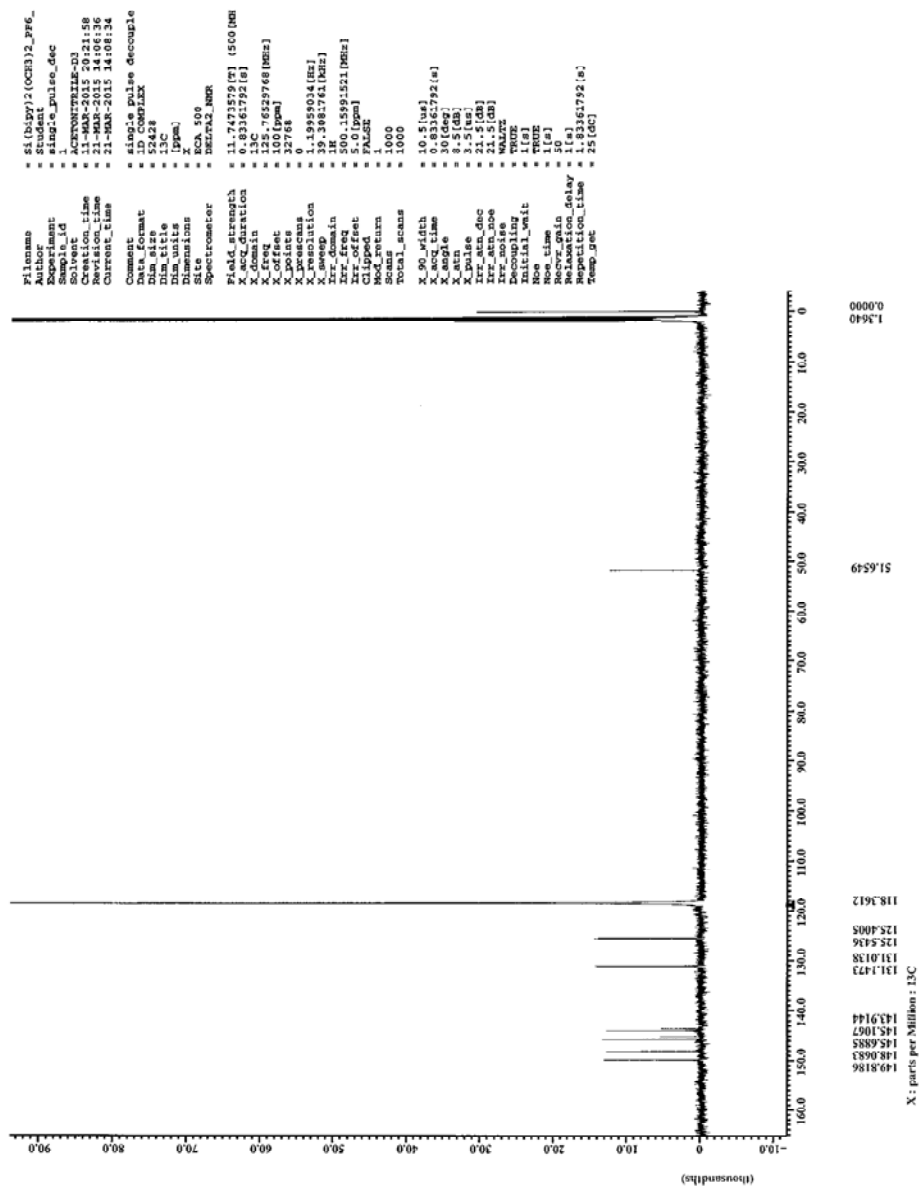
Compounds:  $[\text{Si}(\text{bpy})_2(\text{OMe})_2](\text{I})(\text{I}_3)$  (**1**),  $[\text{Si}(\text{bpy})_2(-\text{OCH}_2\text{CH}_2\text{O}-)]\text{I}_2$  (**2**),  
 $[\text{Si}(\text{bpy})_2(\text{OPh})_2](\text{I}_3)_2$  (**3**),  $[\text{Si}(\text{bpy})_2(\text{bph})](\text{PF}_6)_2$  (**4**), and  $[\text{Si}(\text{bpy})_2(\text{cat})](\text{PF}_6)_2$  (**5**),

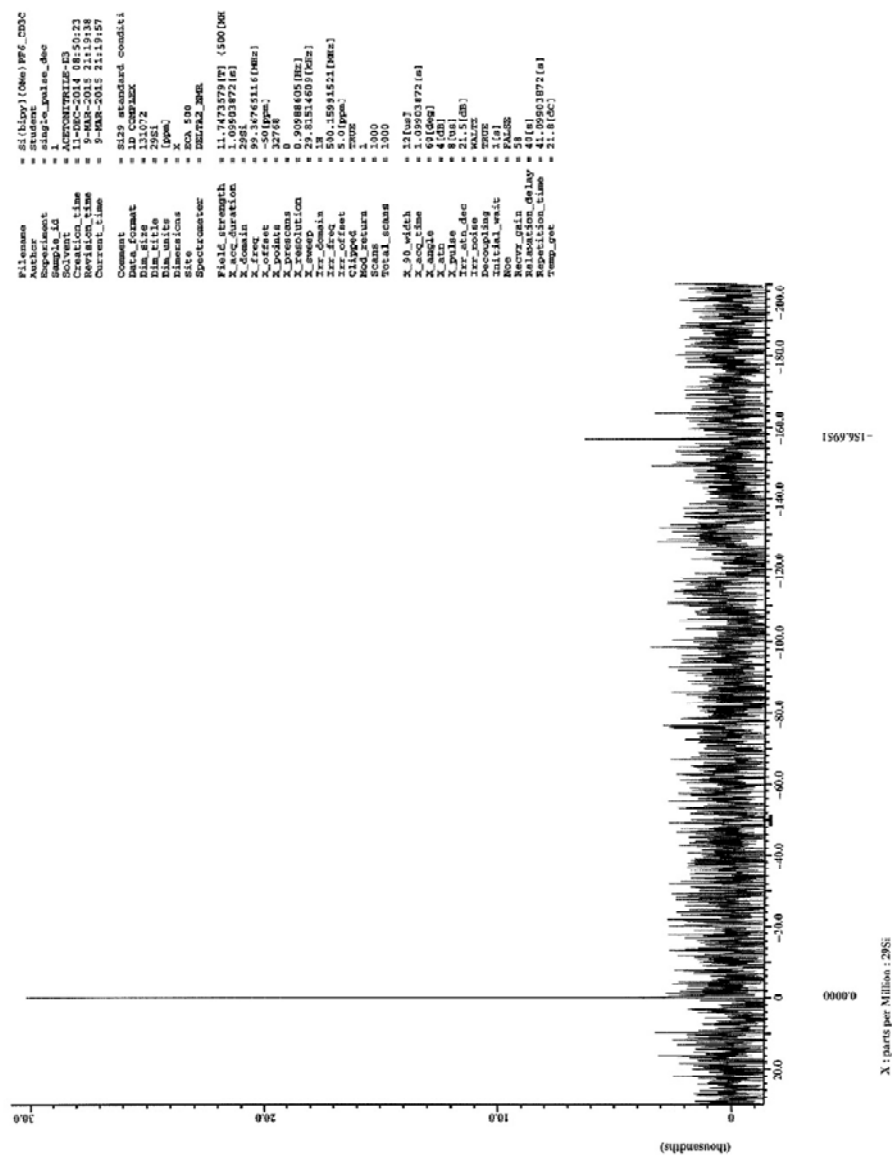
<sup>1</sup>H, <sup>13</sup>C, and <sup>29</sup>Si NMR spectra; IR spectra; and ESI-MS spectra of compounds **1-5**  
(hexafluorophosphate salts).

Cyclic Voltammetry scans of compounds **1-5** (hexafluorophosphate salts).

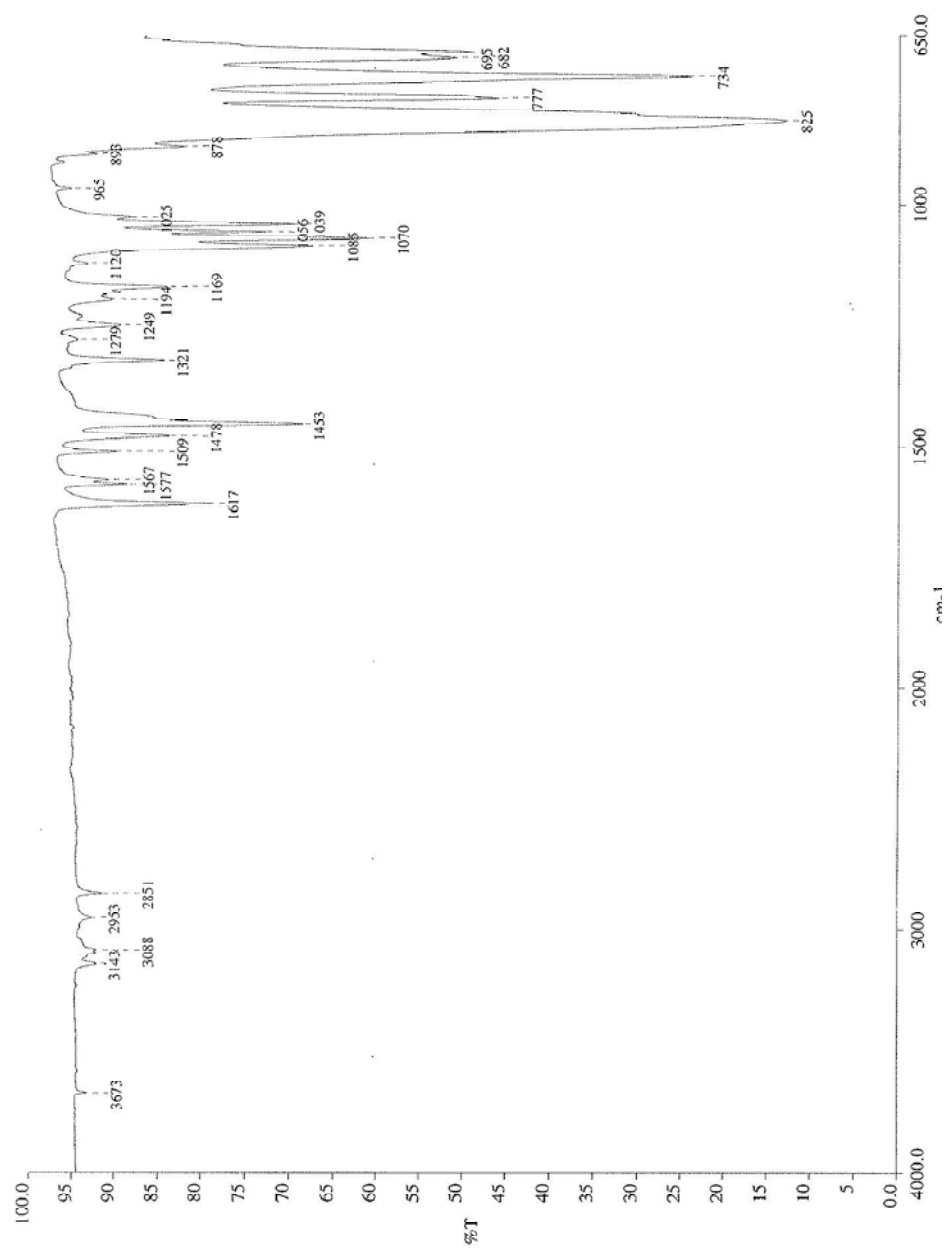




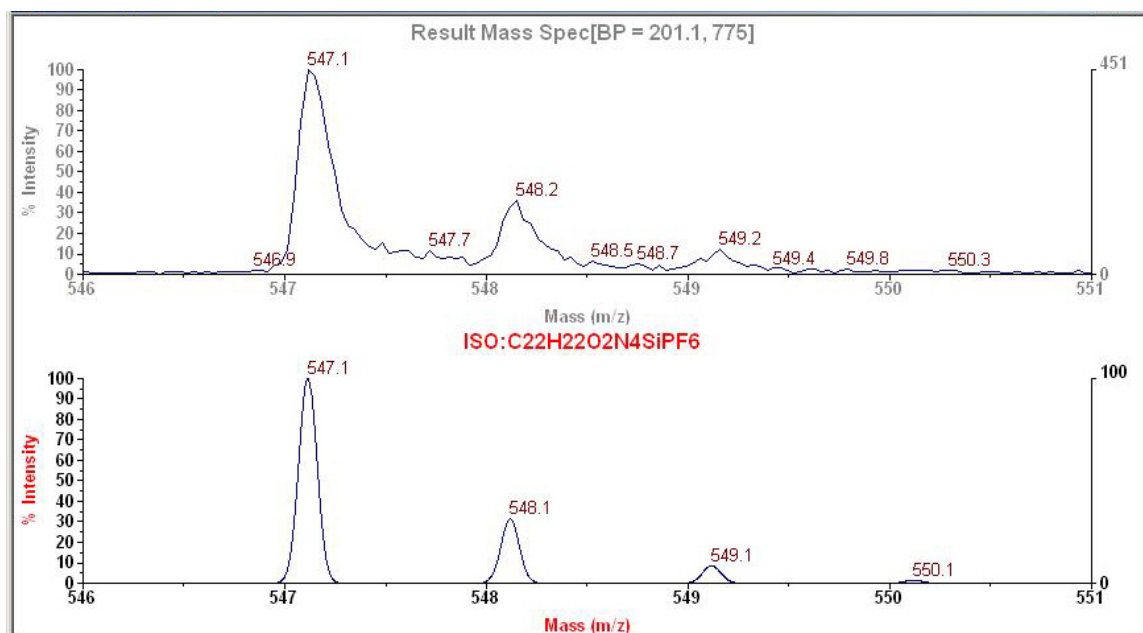




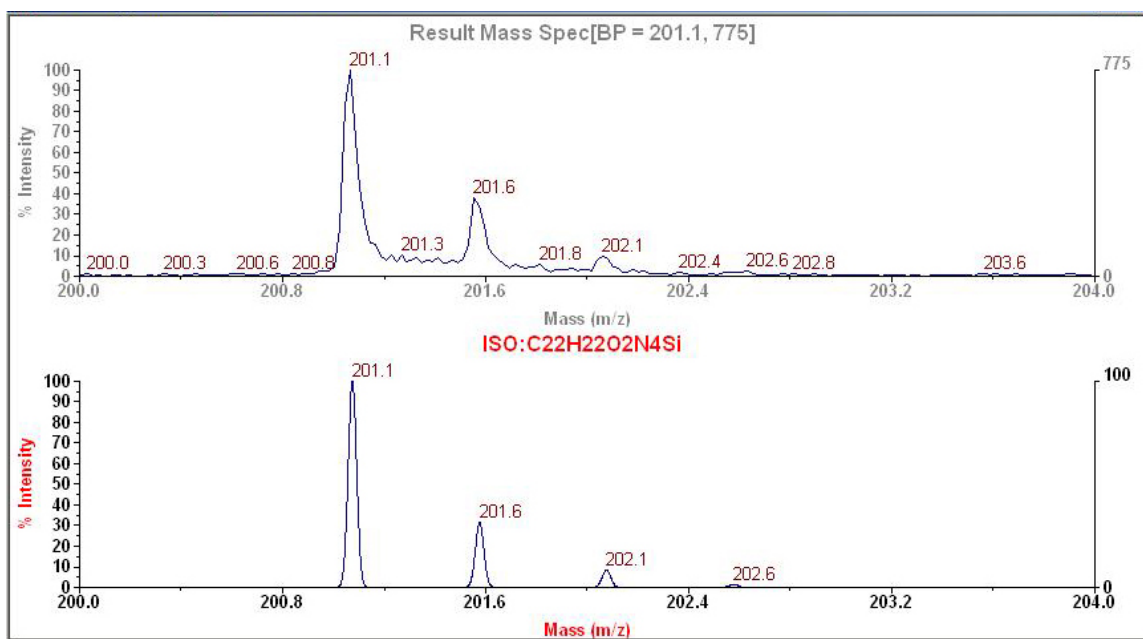
IR of [1](PF<sub>6</sub>)<sub>2</sub>.

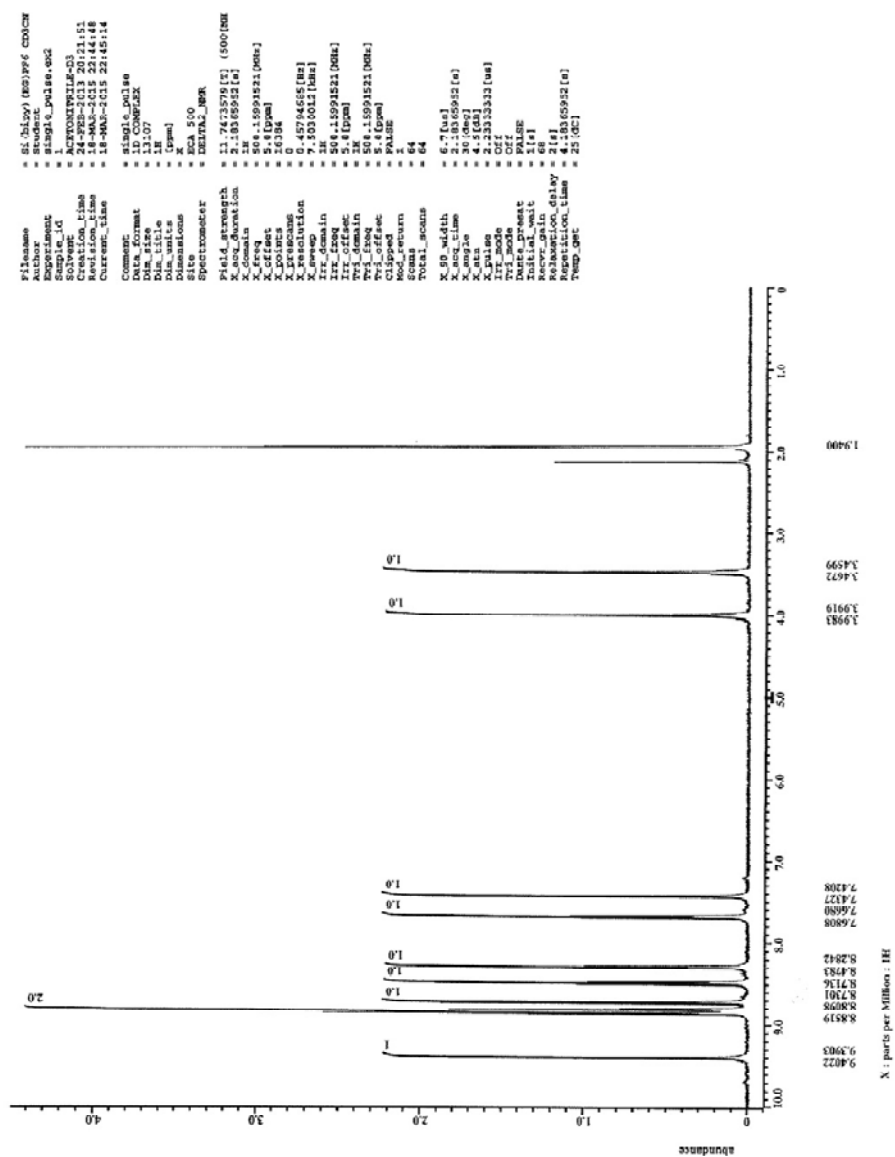


ESI-MS of  $[1](PF_6)^{+1}$ .

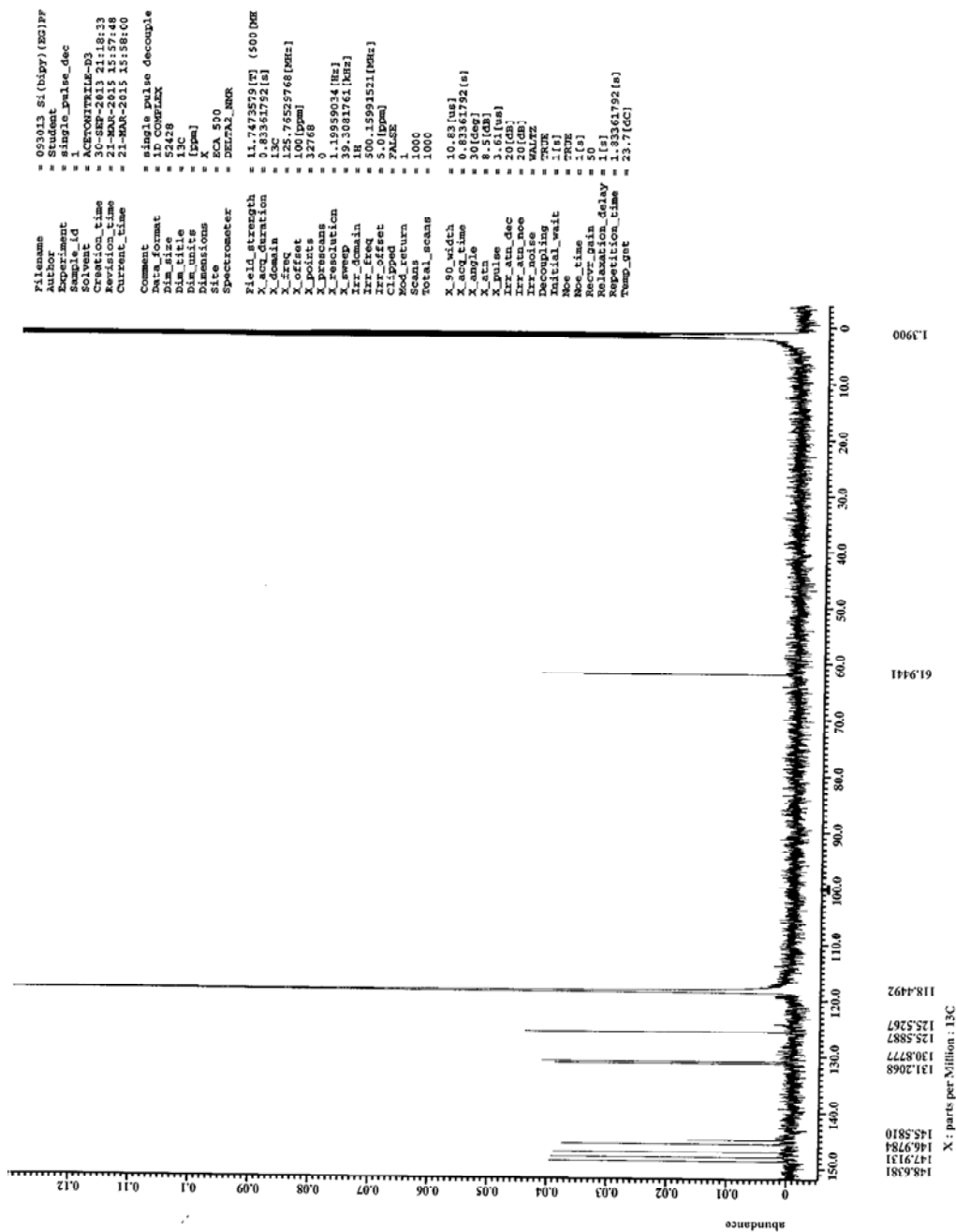


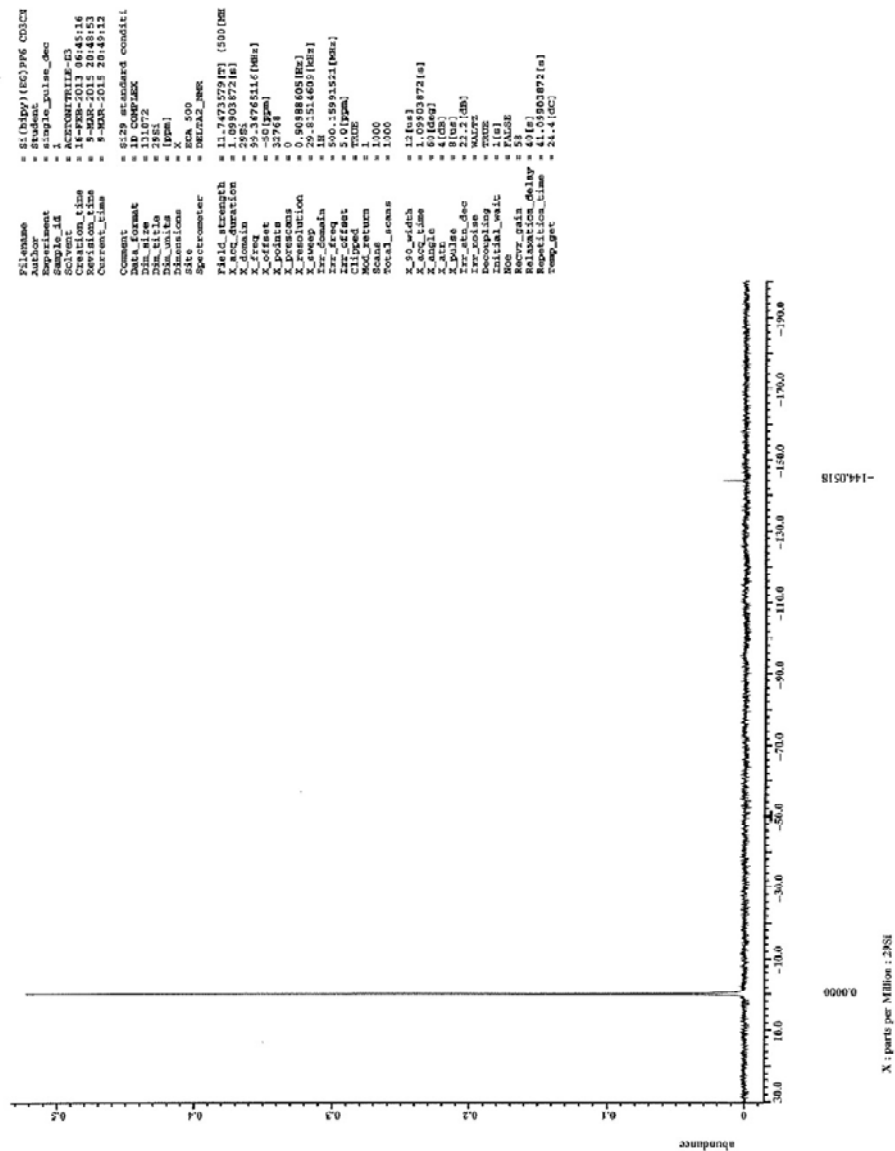
ESI-MS of  $[1]^{+2}$ .





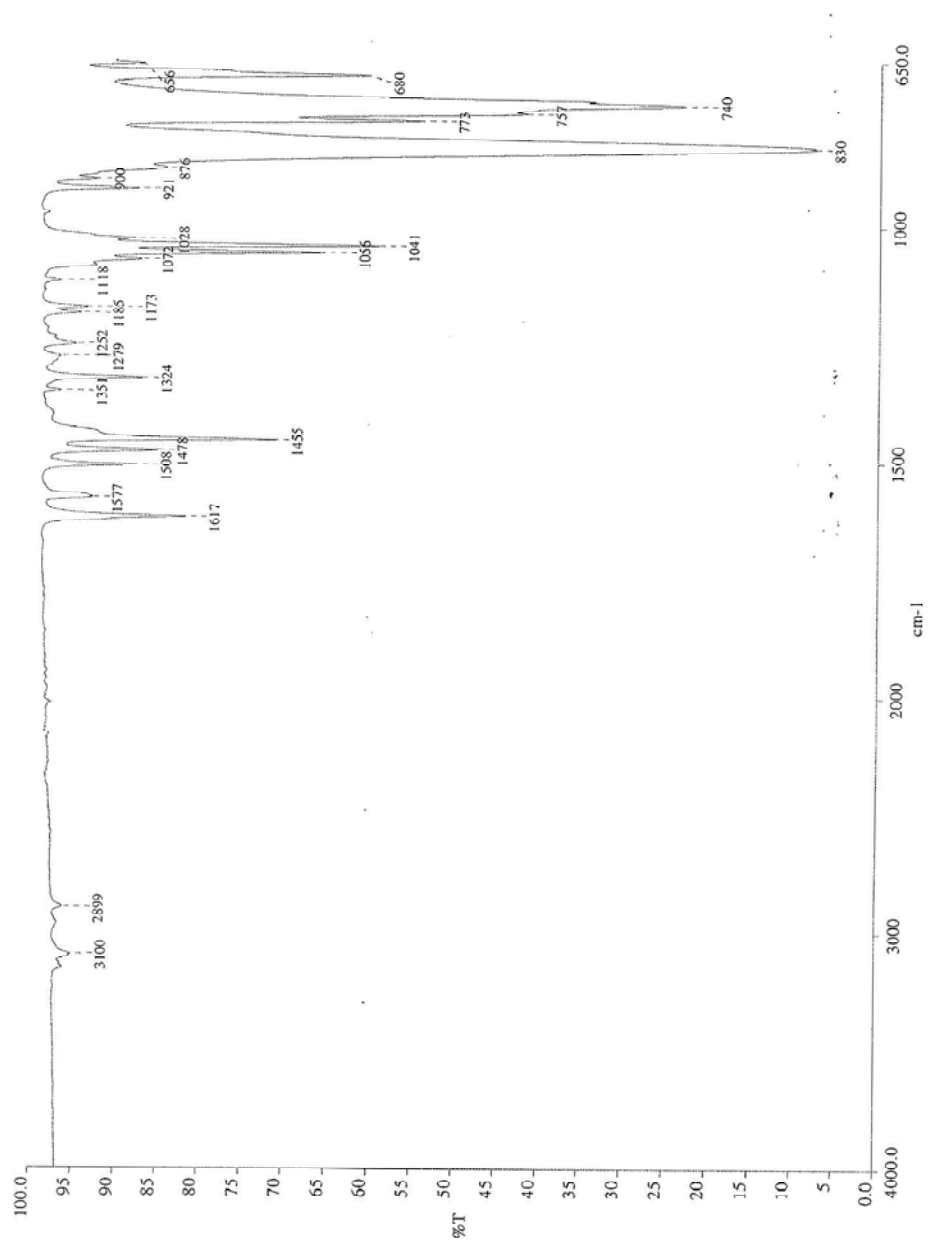
$^{13}\text{C}$  NMR of  $[\mathbf{2}](\text{PF}_6)_2$  in  $\text{CD}_3\text{CN}$ .



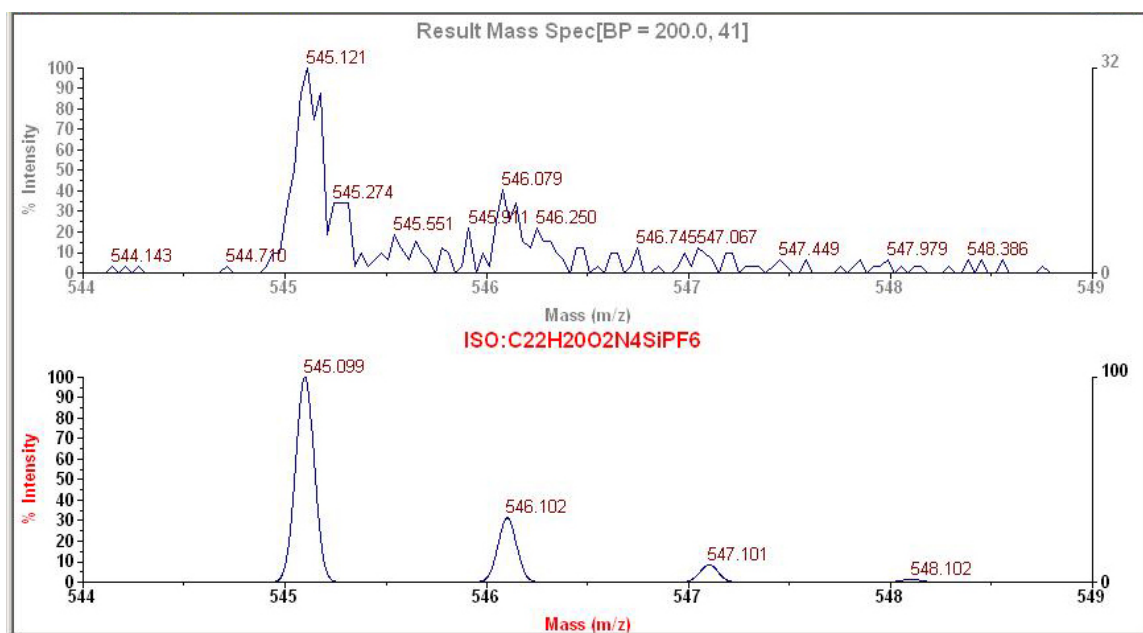




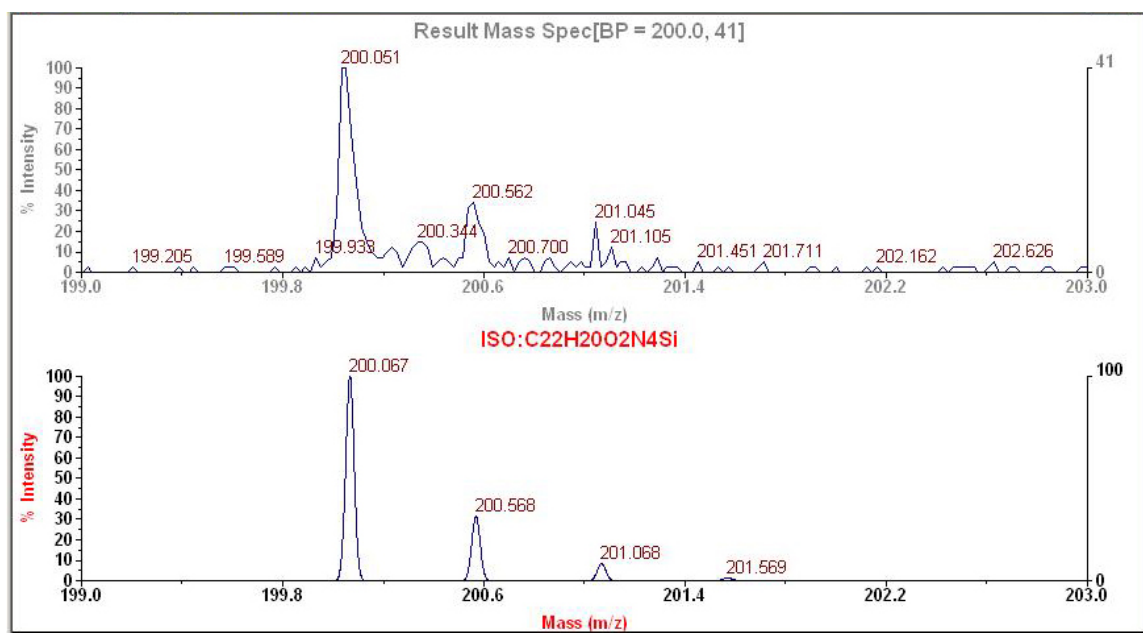
IR of **[2]**(PF<sub>6</sub>)<sub>2</sub>.

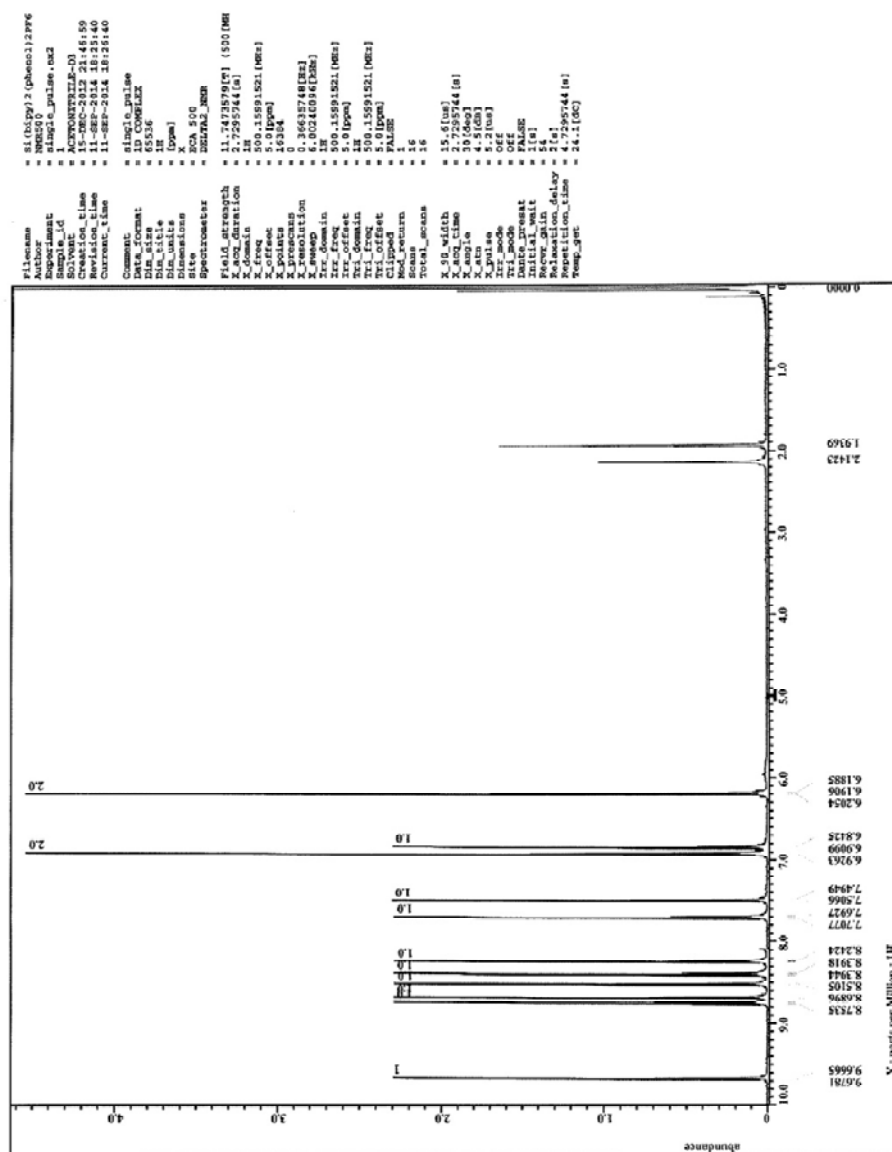


ESI-MS of  $[2](PF_6)^{+1}$

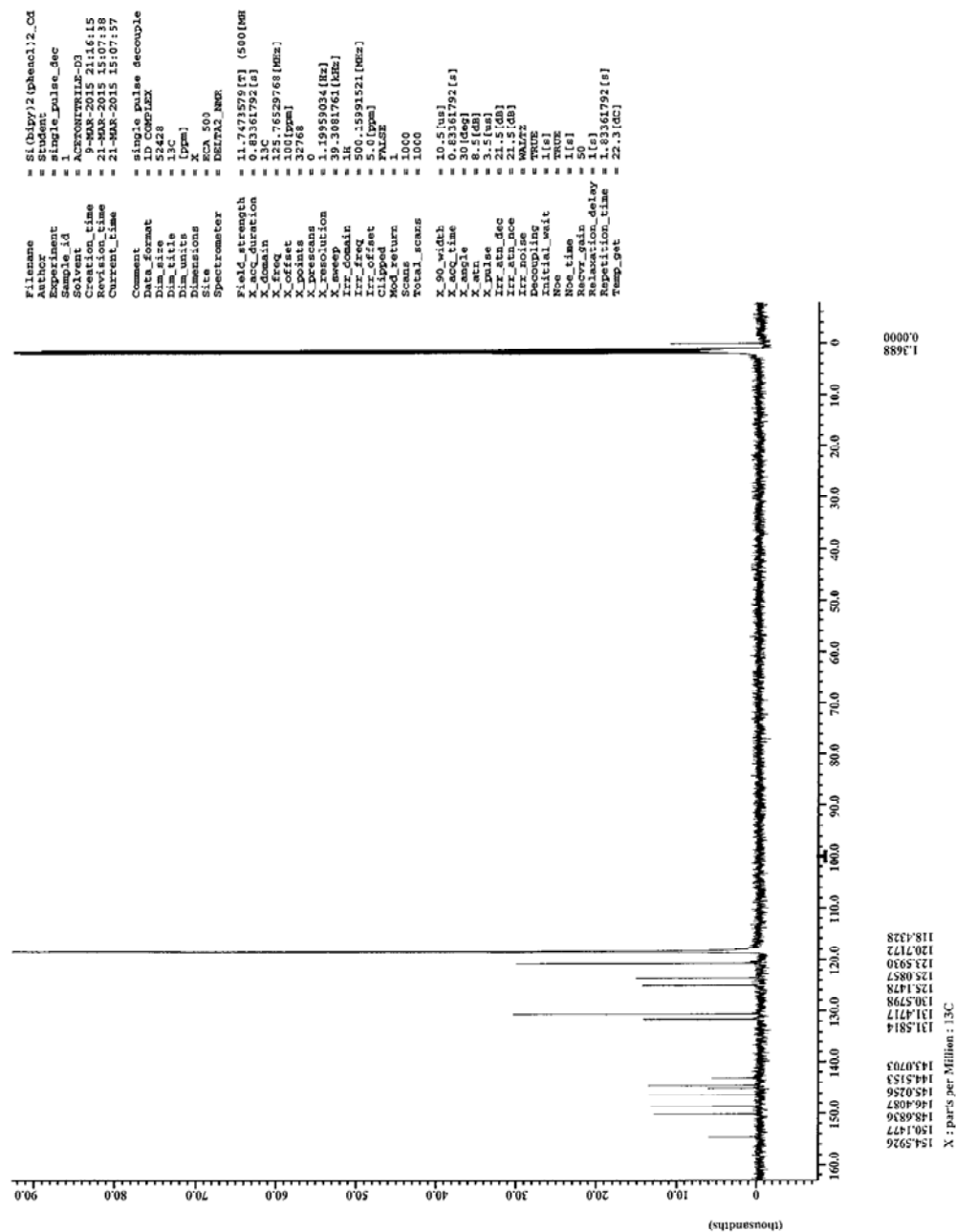


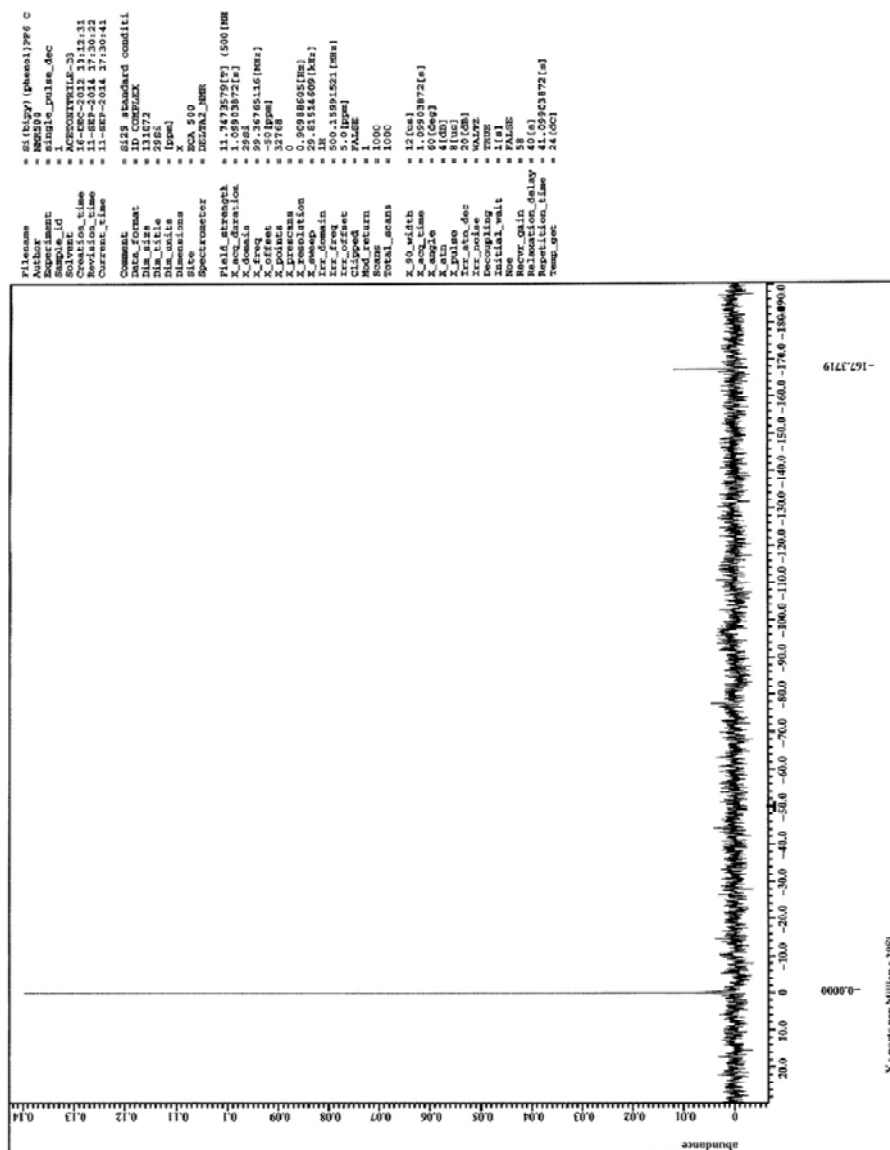
ESI-MS of  $[2]^{+2}$ .



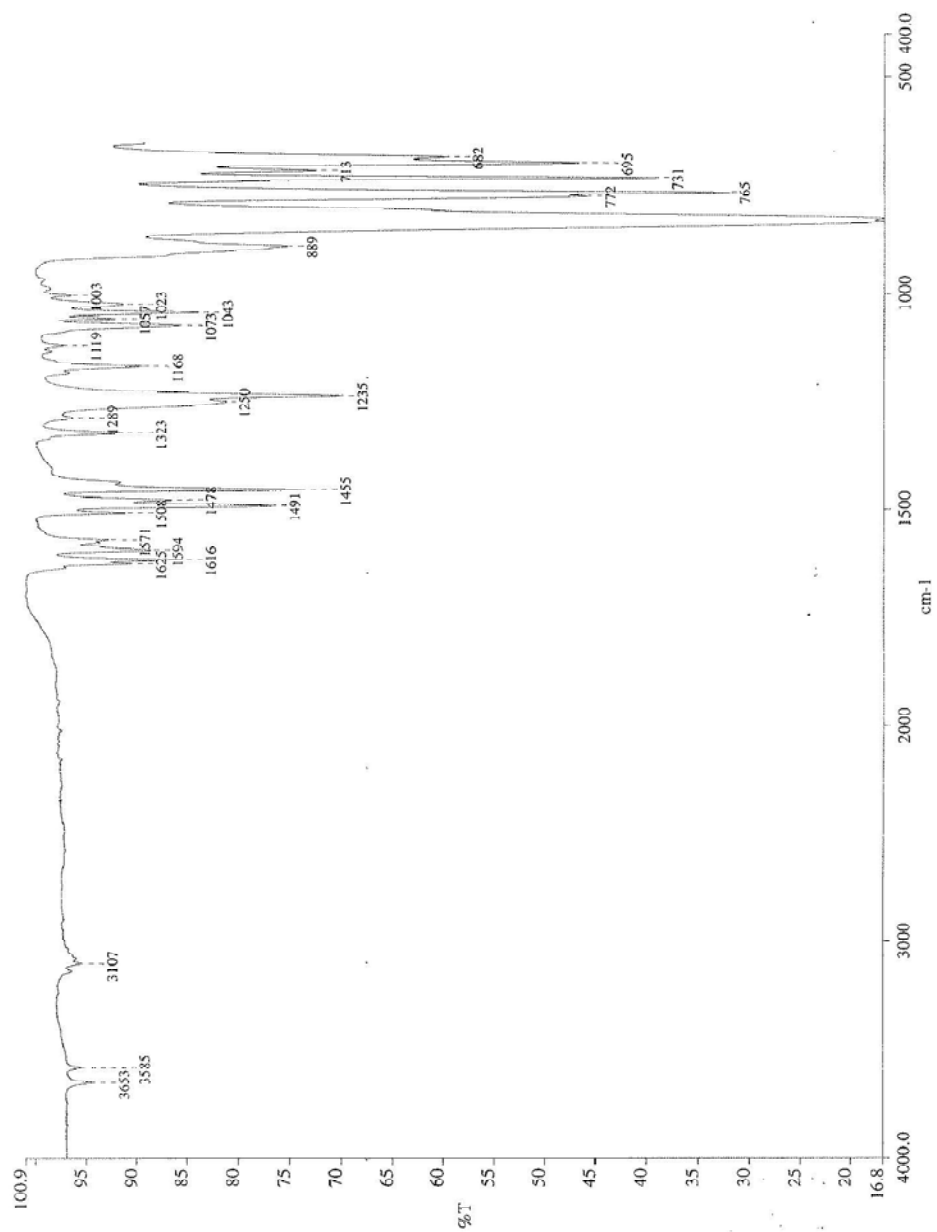


$^{13}\text{C}$  NMR of **[3]**(PF<sub>6</sub>)<sub>2</sub> in CD<sub>3</sub>CN.

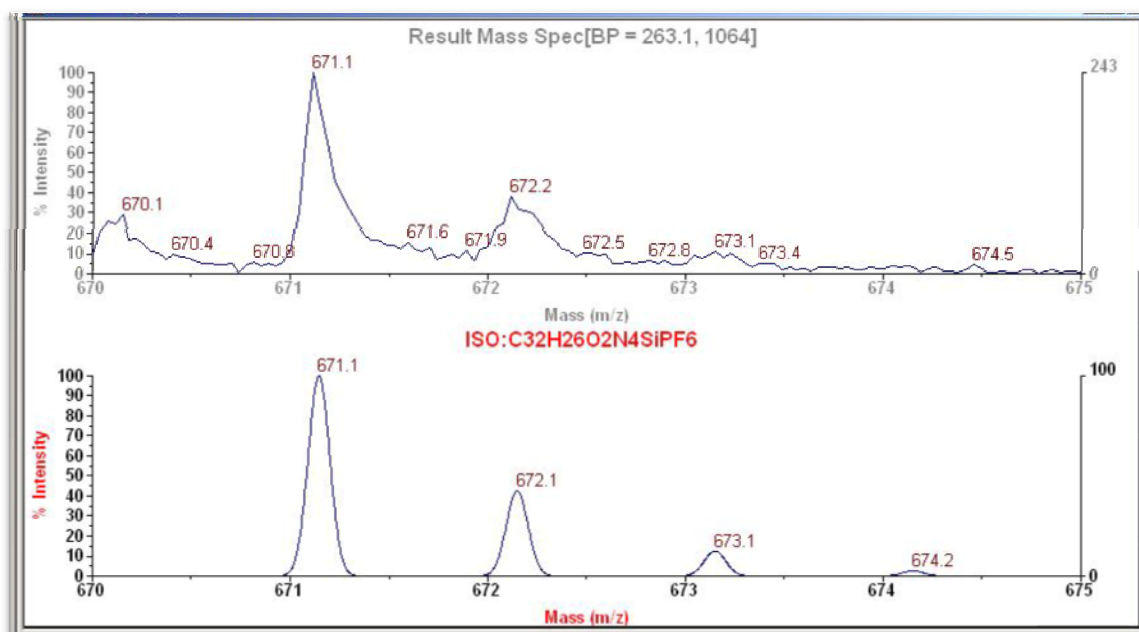




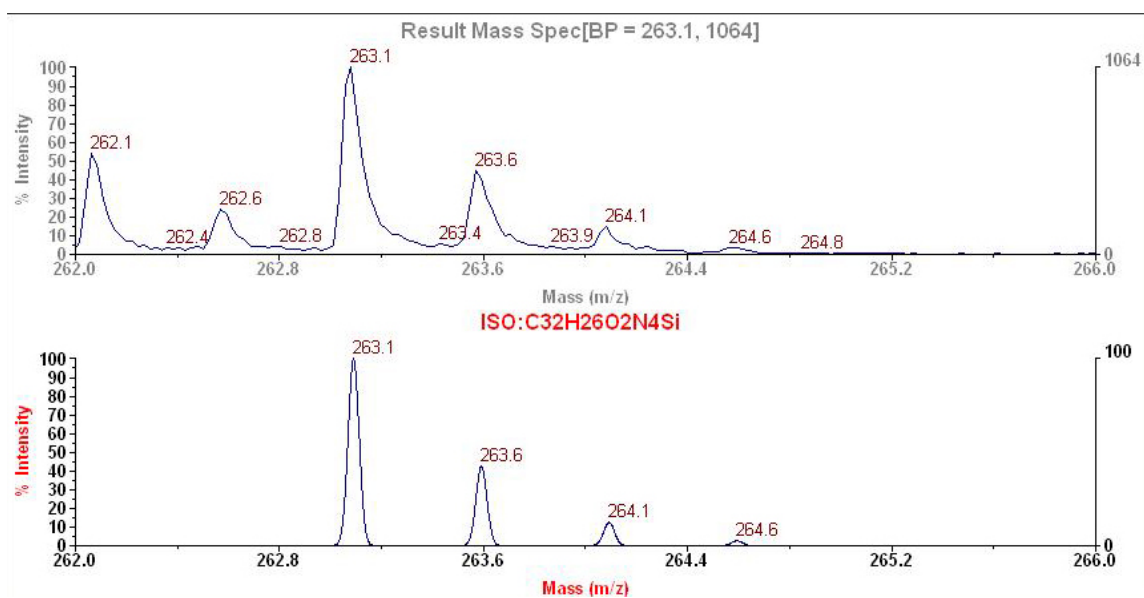
IR of **[3]**(PF<sub>6</sub>)<sub>2</sub>.

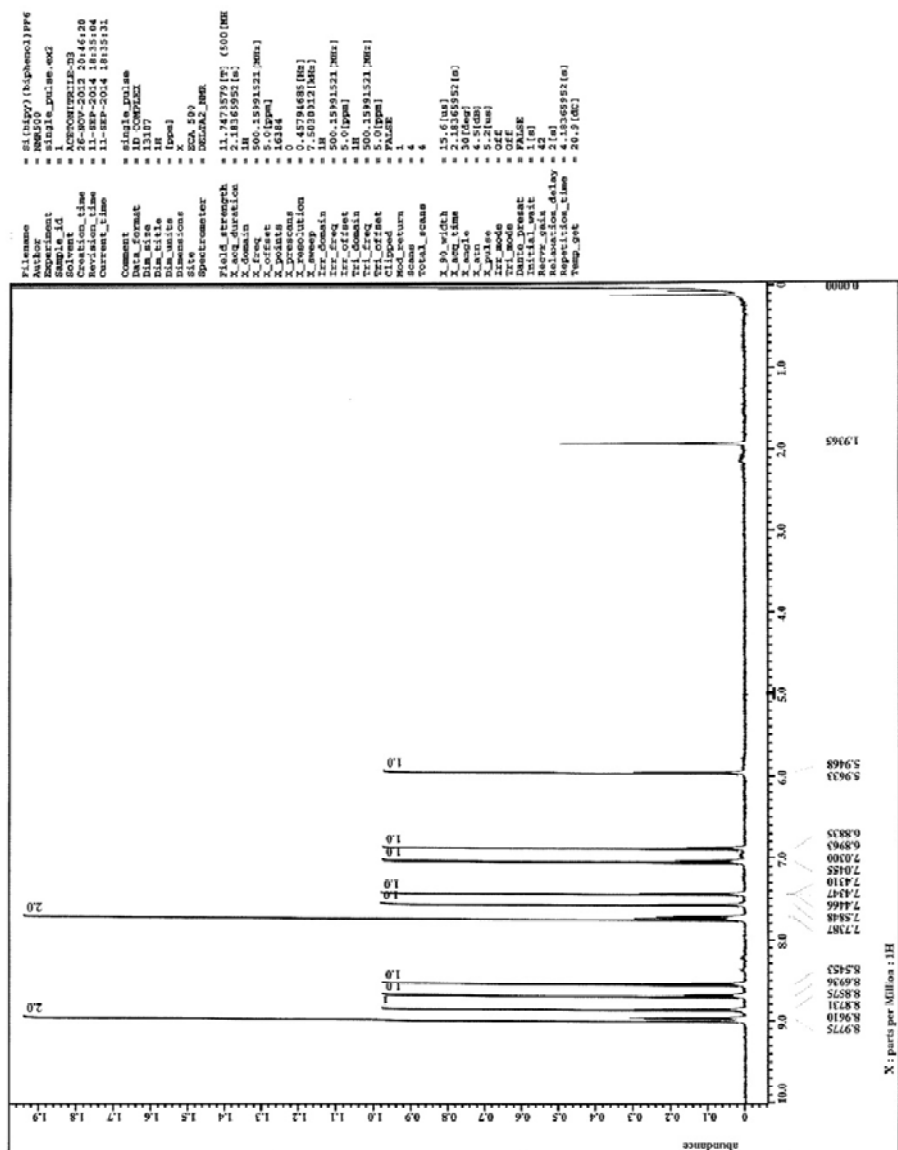


ESI-MS of  $[3](PF_6)^{+1}$ .

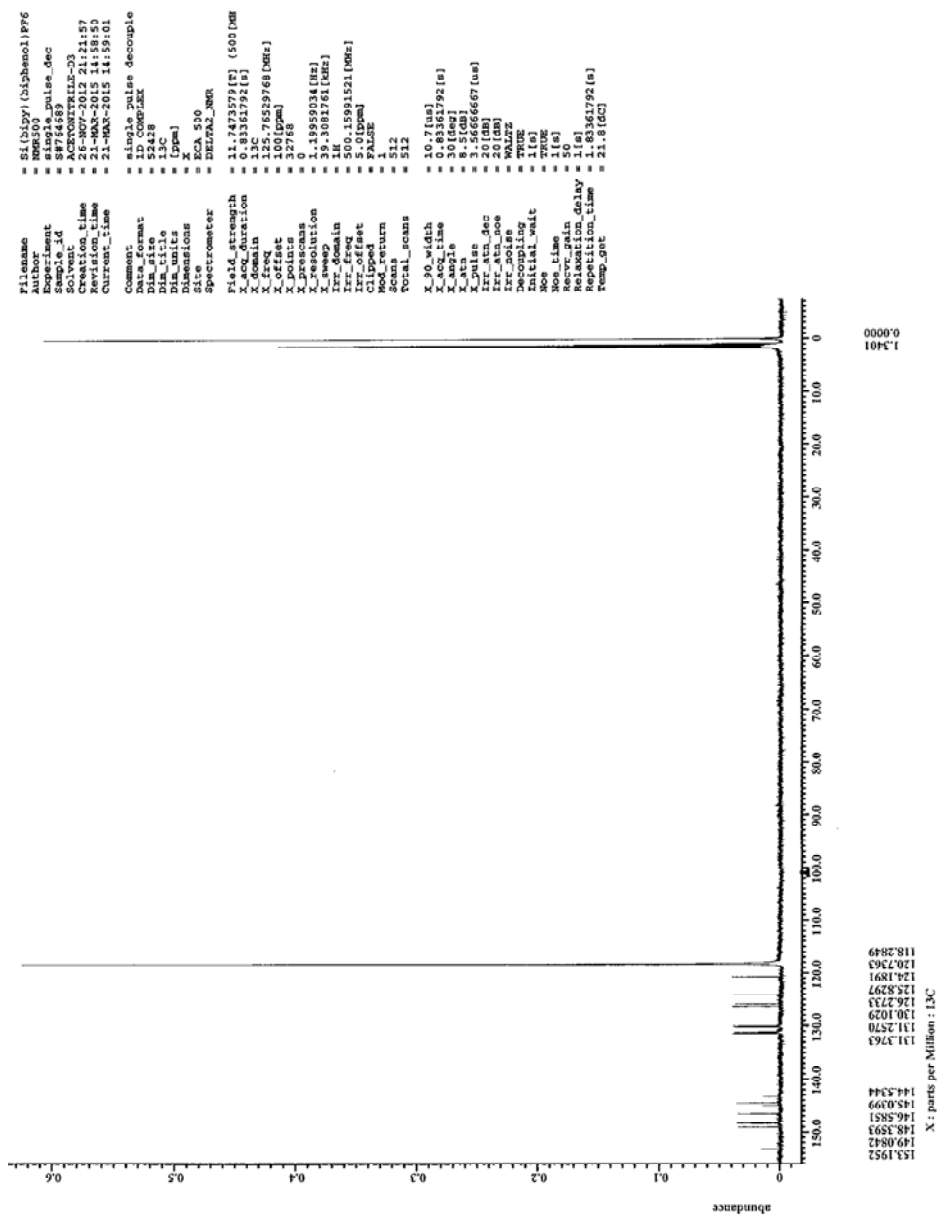


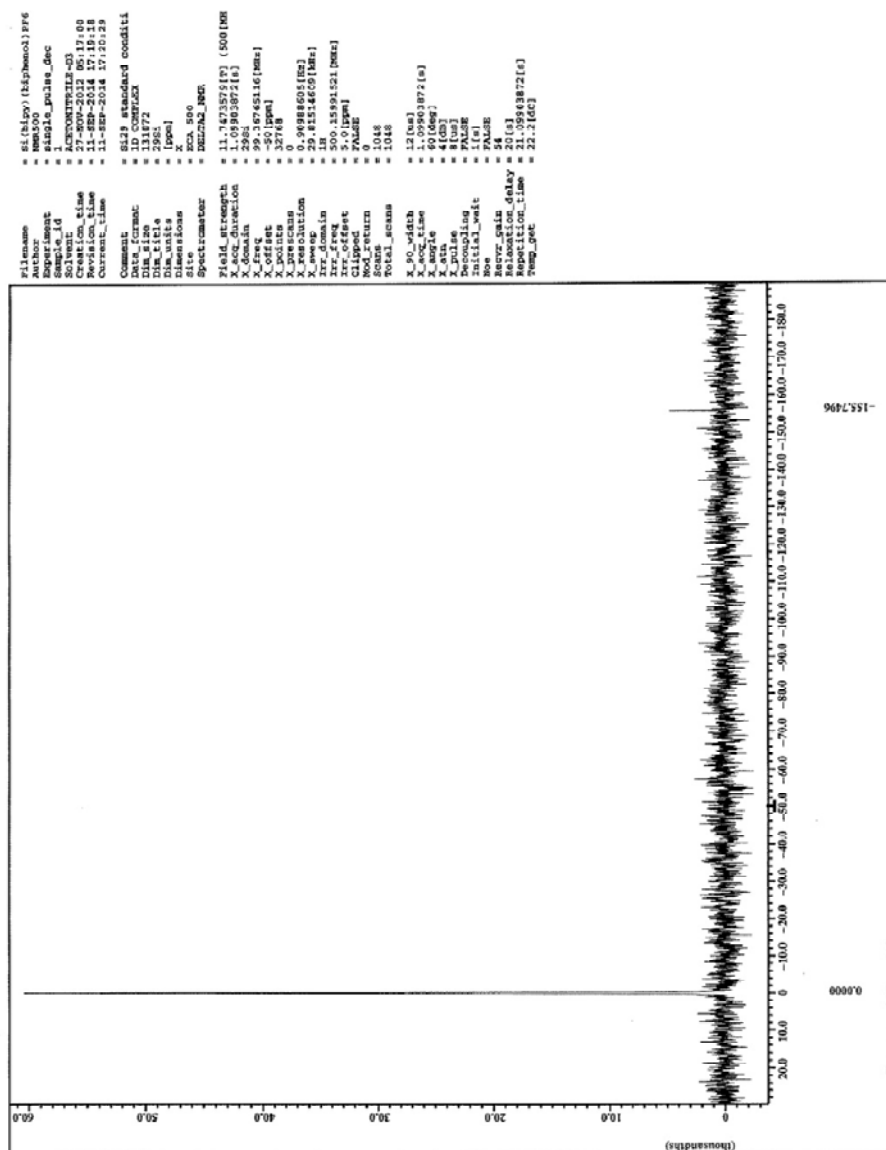
ESI-MS of  $[3]^{+2}$



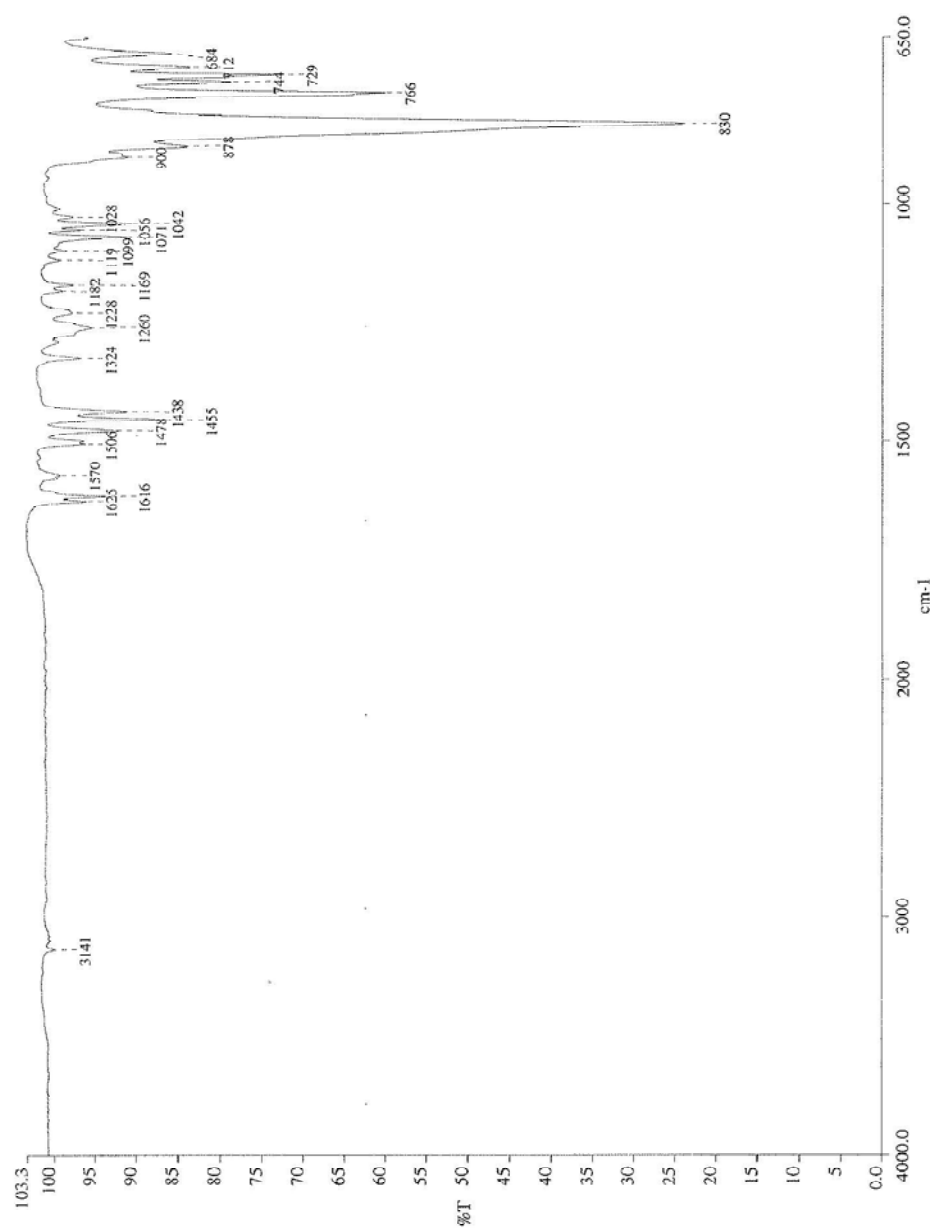




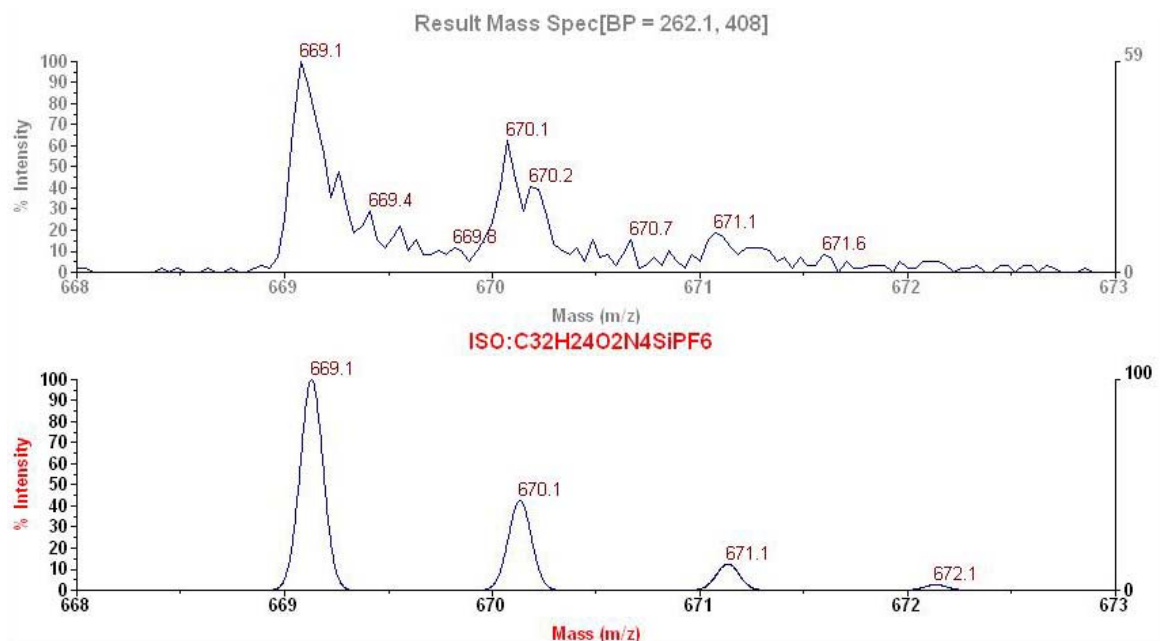




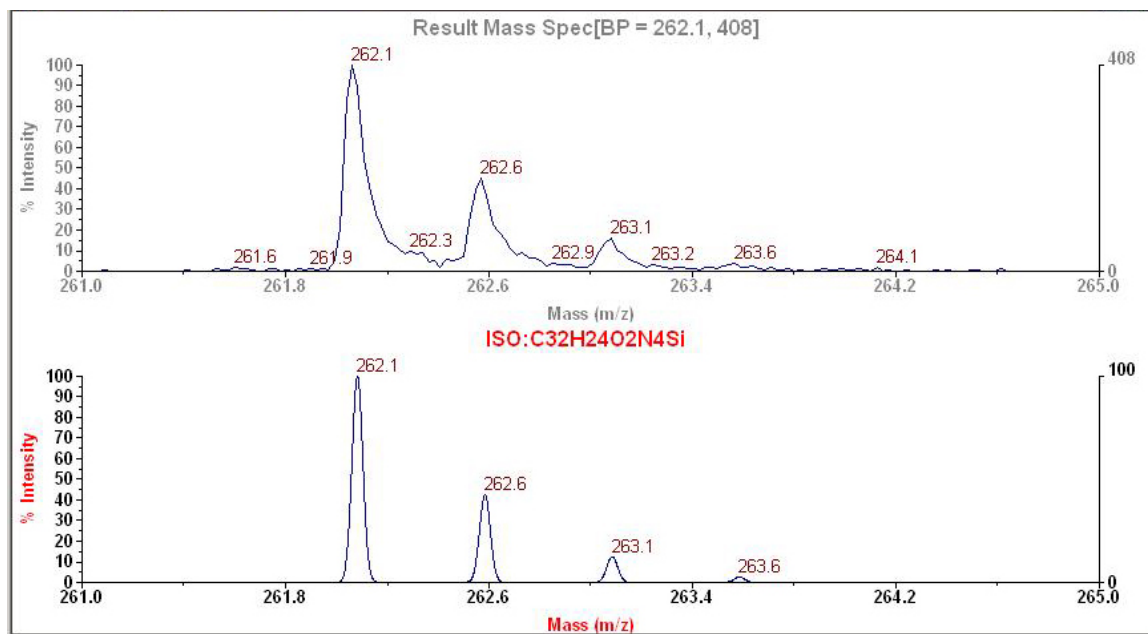
IR of [4](PF<sub>6</sub>)<sub>2</sub>.

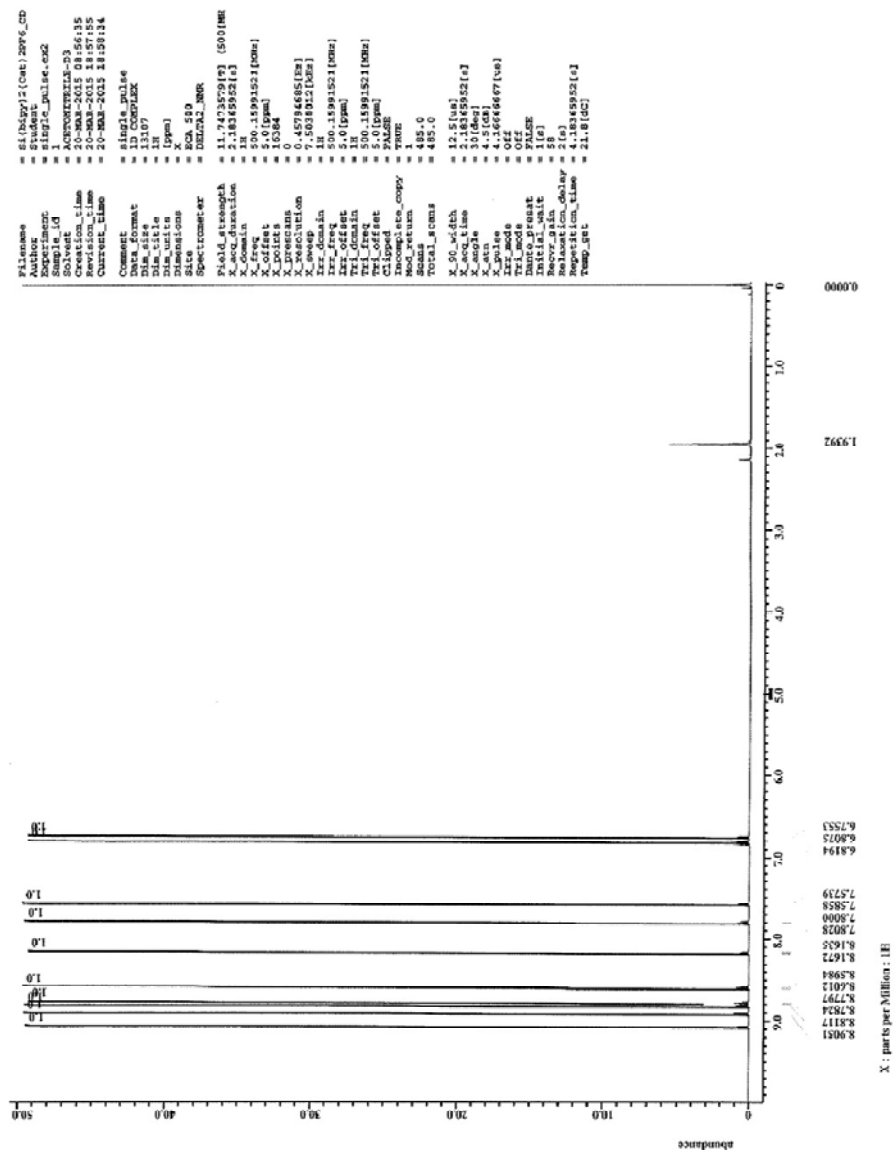


ESI-MS of  $[4](PF_6)^{+1}$ .

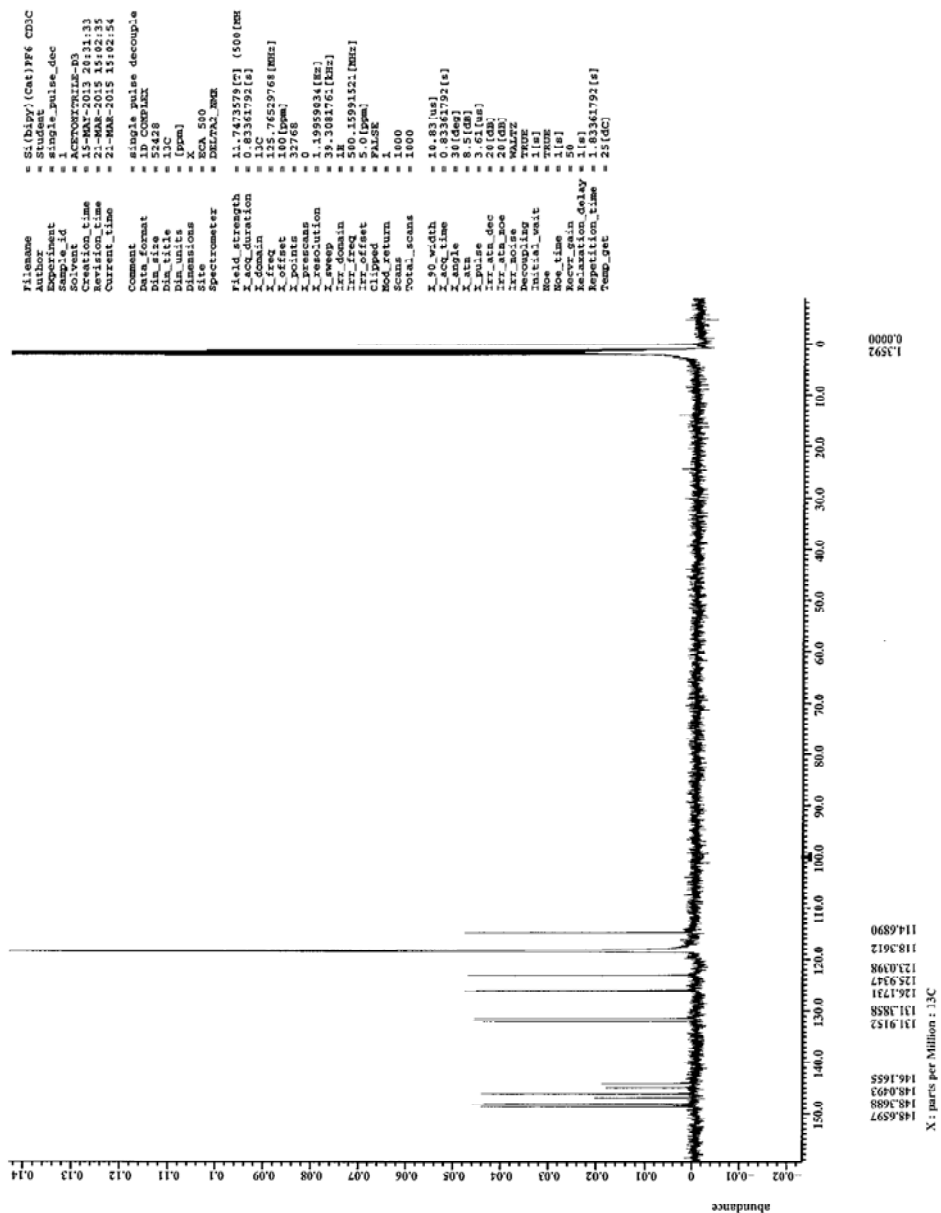


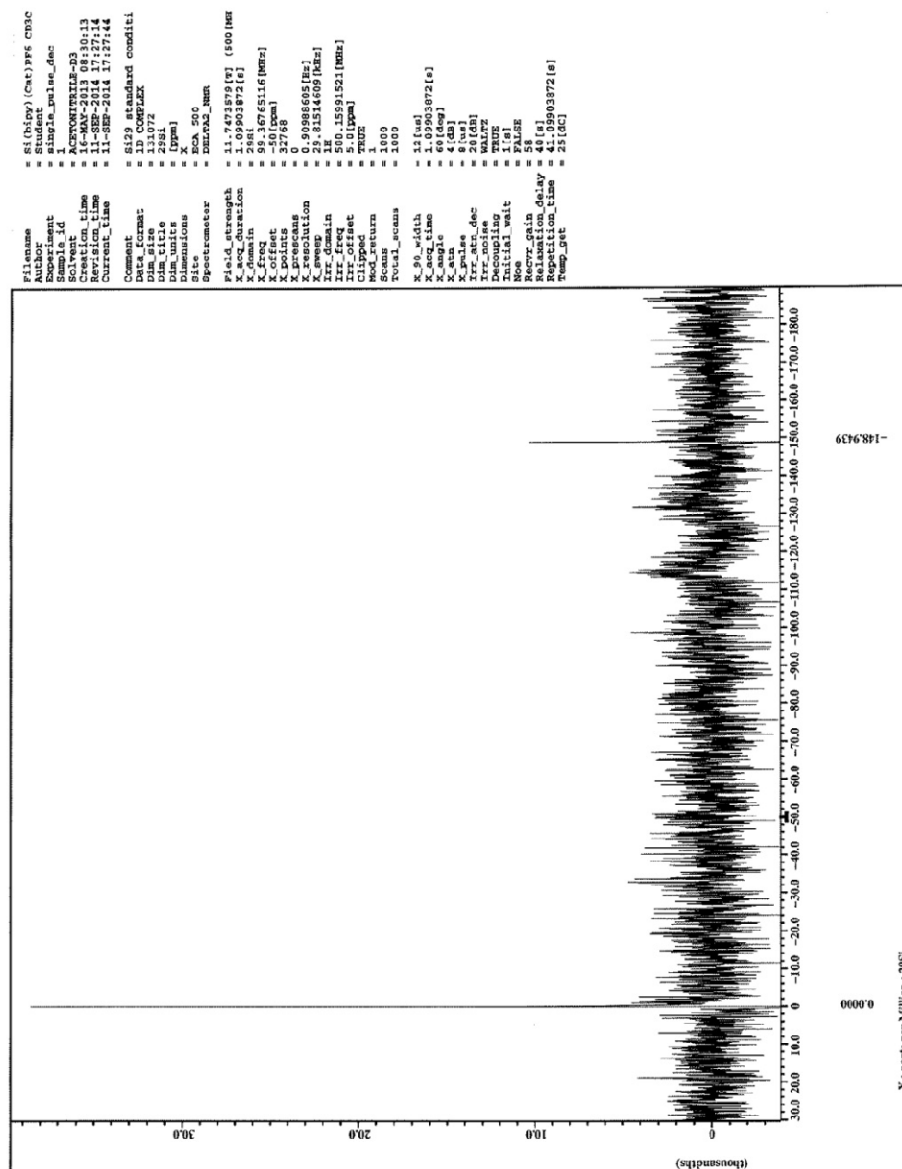
ESI-MS of  $4^{+2}$ .



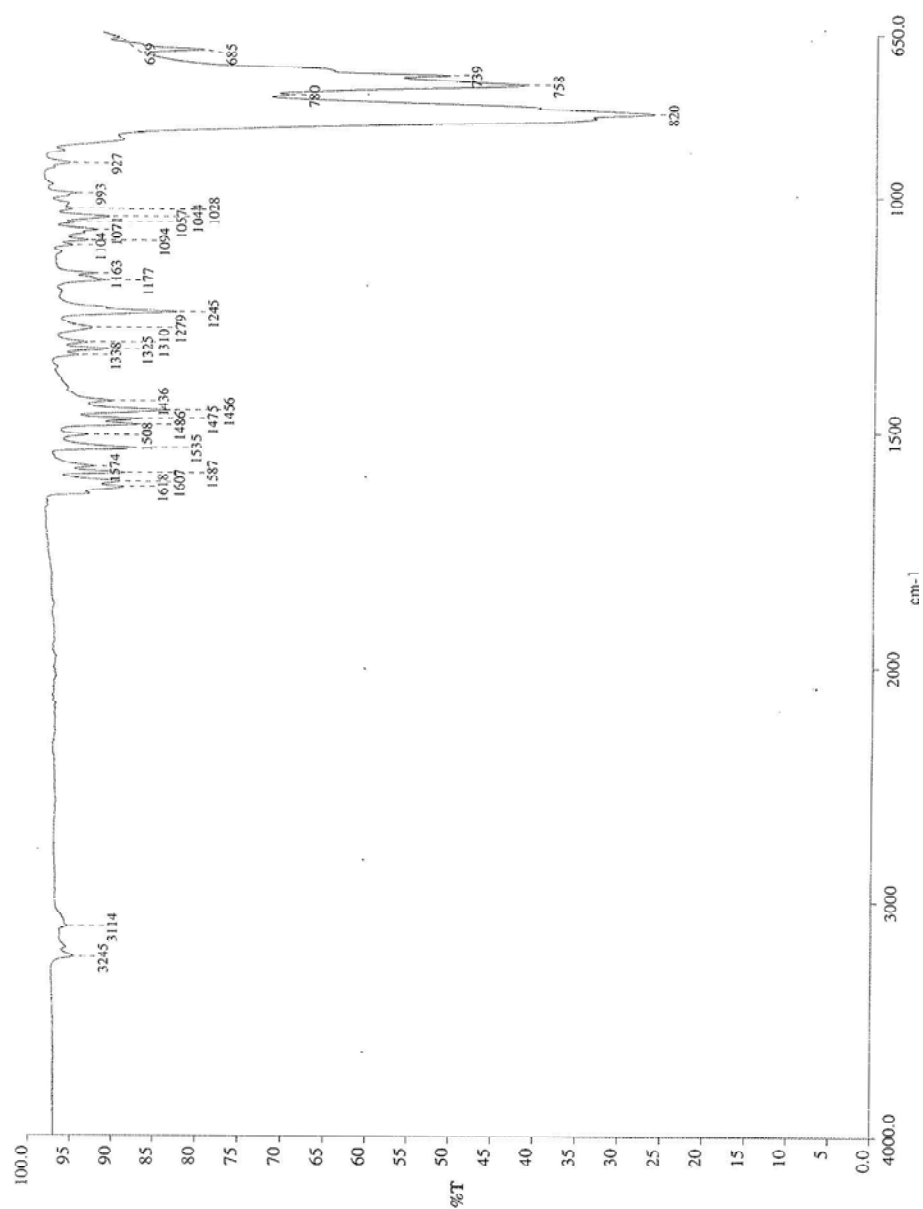


$^{13}\text{C}$  NMR of  $[\mathbf{5}](\text{PF}_6)_2$  in  $\text{CD}_3\text{CN}$ .



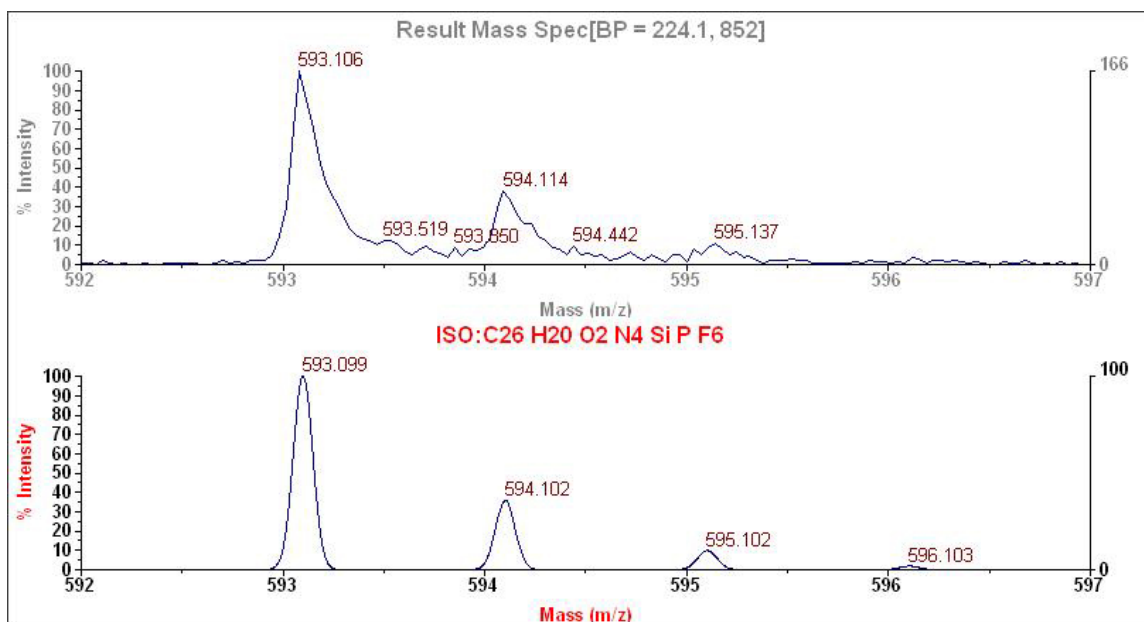


IR of [5](PF<sub>6</sub>)<sub>2</sub>.

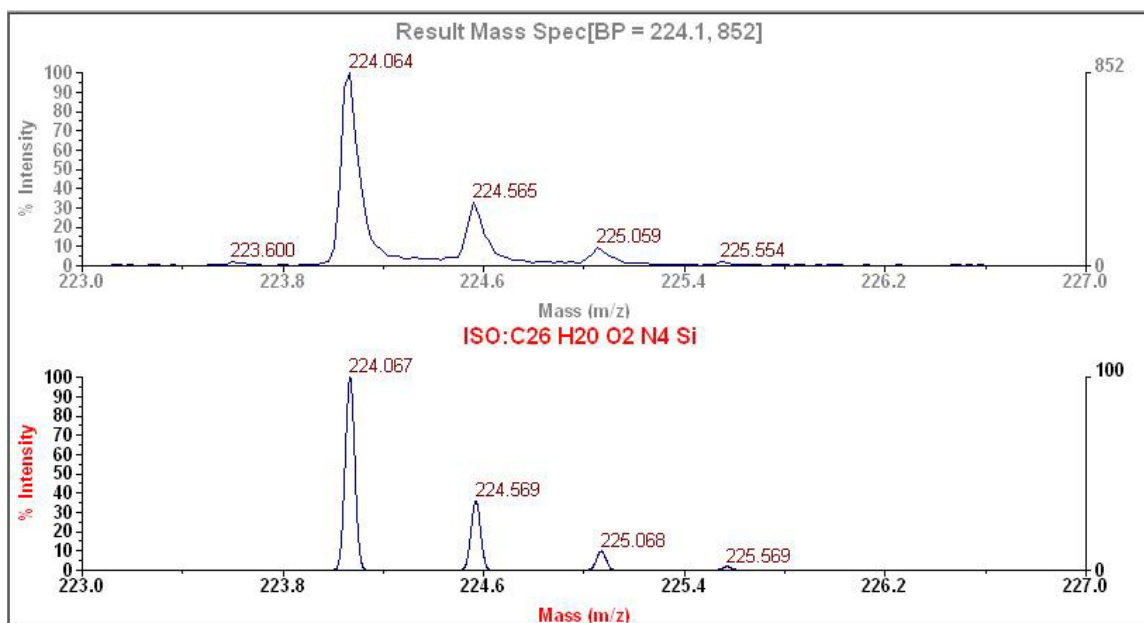




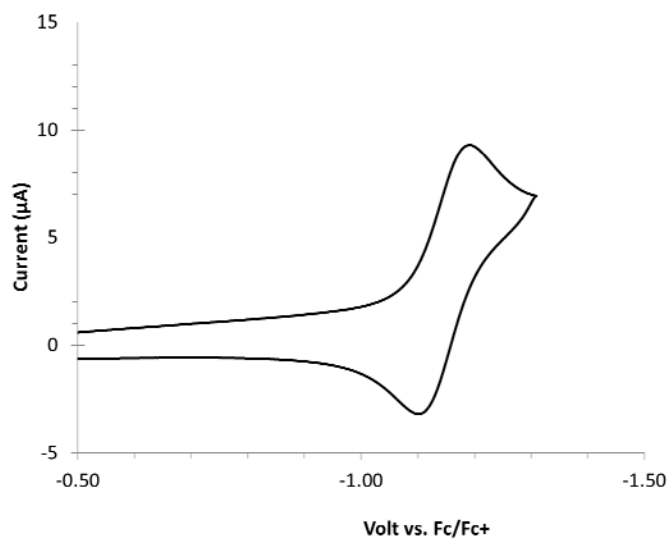
ESI-MS of  $[5](PF_6)^{+1}$ .



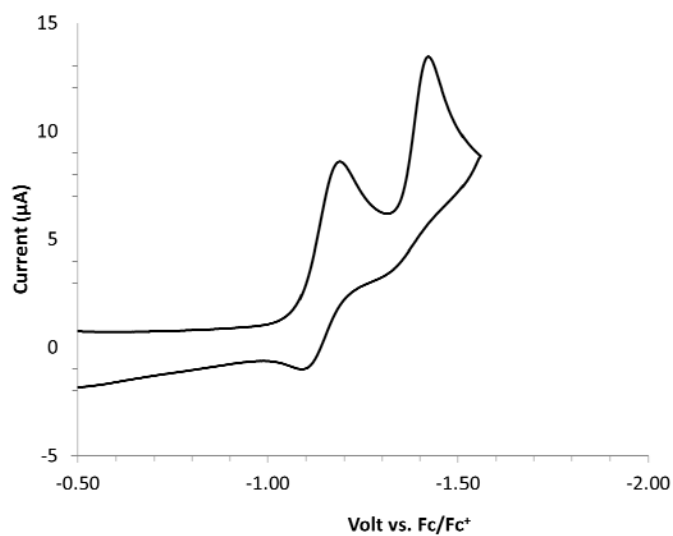
ESI-MS of  $5^{+2}$ .



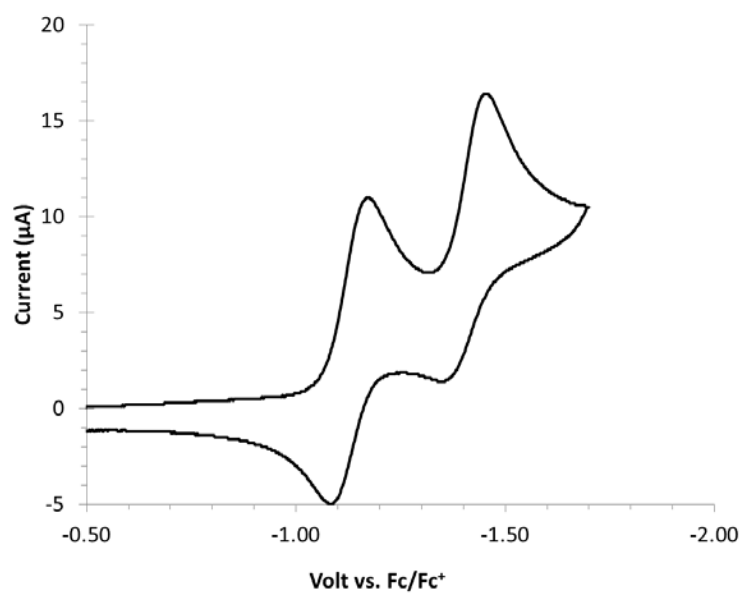
Cyclic voltammogram of  $[1](PF_6)_2$  in  $CH_3CN / 0.1\text{ M TBAPF}_6$  solution  $\square \square = 200\text{ mV/s}$ , platinum disk working electrode.



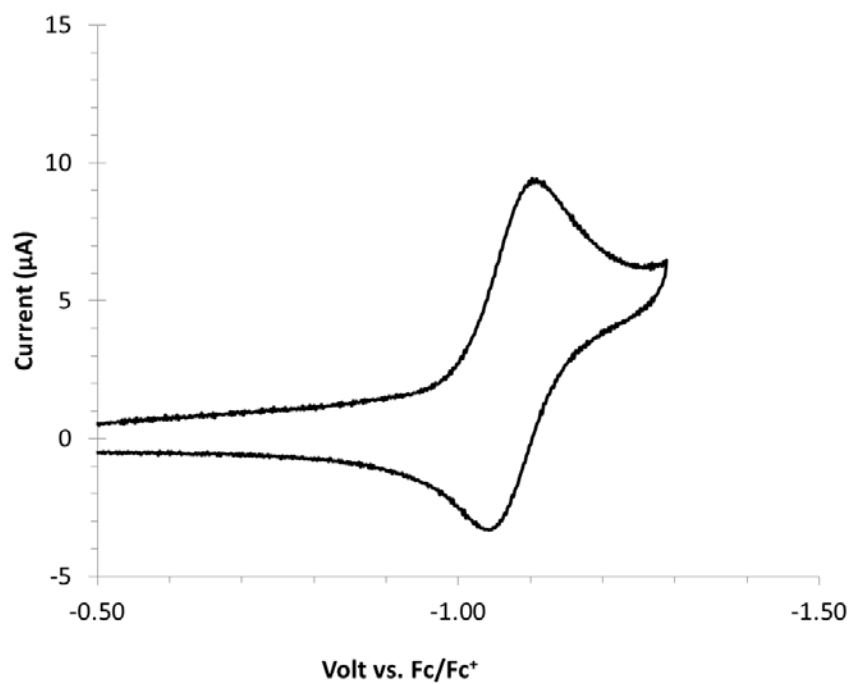
Cyclic voltammogram of  $[1](PF_6)_2$  in  $CH_3CN / 0.1\text{ M TBAPF}_6$  solution  $\square \square = 200\text{ mV/s}$ , platinum disk working electrode.



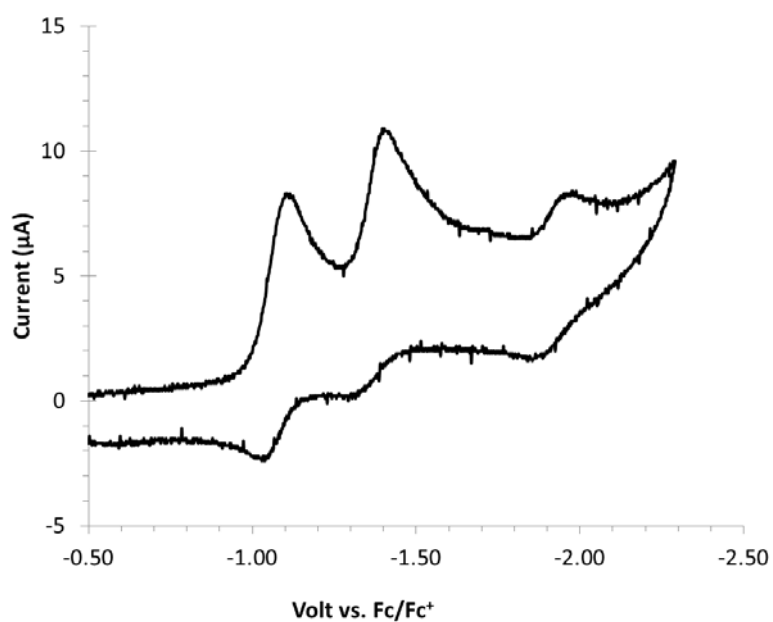
Cyclic voltammogram of  $[2](PF_6)_2$  in  $CH_3CN / 0.1\text{ M TBAPF}_6$  solution  $\square \square = 200\text{ mV/s}$ , platinum disk working electrode.



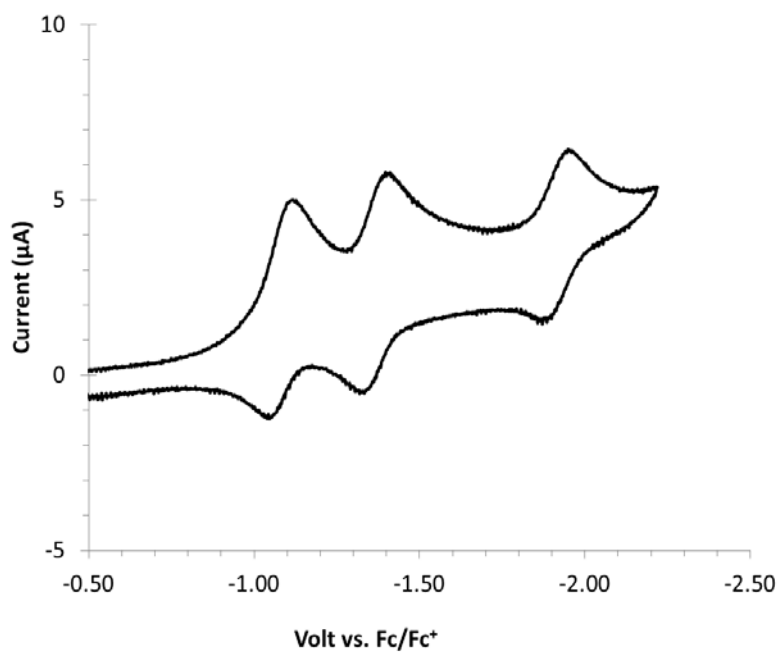
Cyclic voltammogram of  $[3](PF_6)_2$  in  $CH_3CN / 0.1\text{ M TBAPF}_6$  solution  $\square \square = 200\text{ mV/s}$ , platinum disk working electrode.



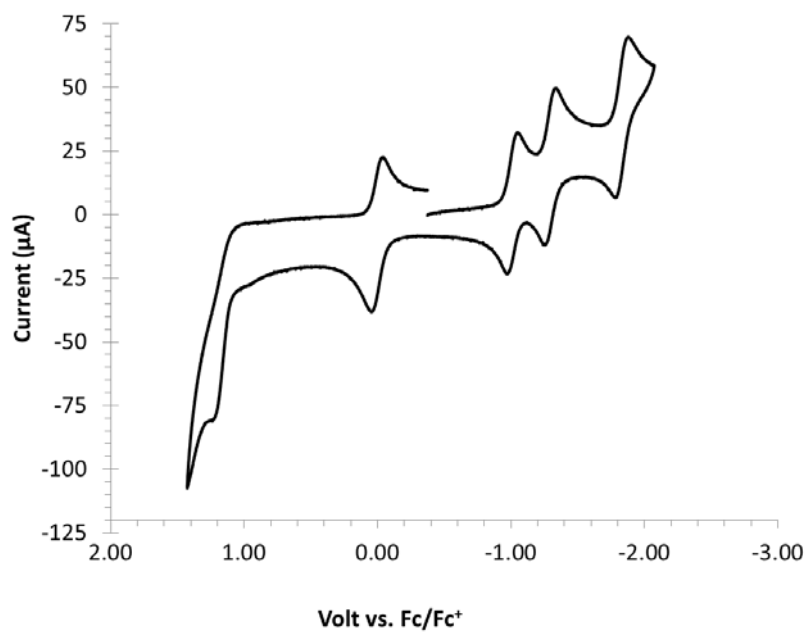
Cyclic voltammogram of  $[3](PF_6)_2$  in  $CH_3CN / 0.1\text{ M TBAPF}_6$  solution  $\square \square = 200$  mV/s, platinum disk working electrode.



Cyclic voltammogram of  $[4](PF_6)_2$  in  $CH_3CN / 0.1\text{ M TBAPF}_6$  solution  $\square \square = 200$  mV/s, platinum disk working electrode.



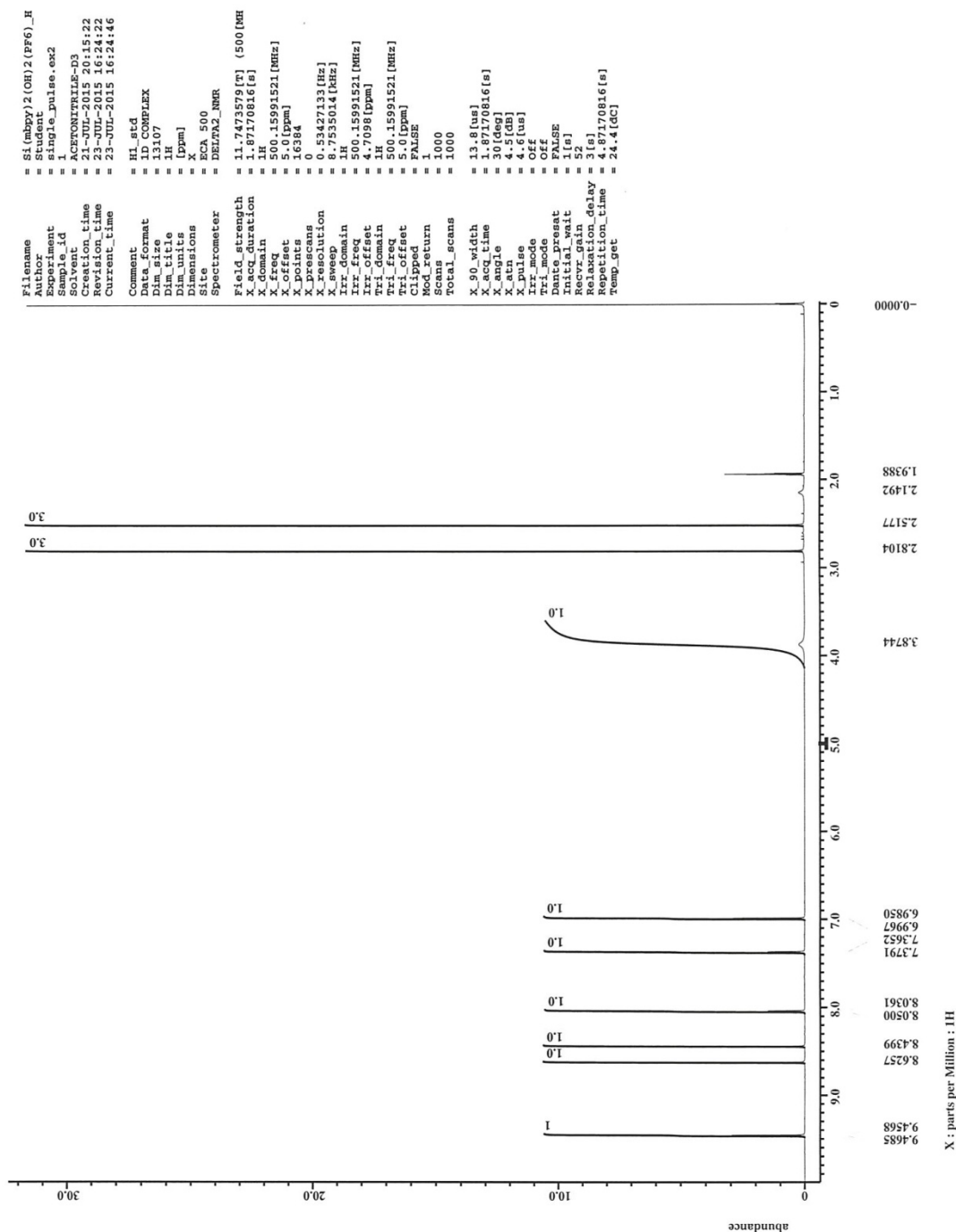
Cyclic voltammogram of  $[5](PF_6)_2$  in  $CH_3CN / 0.1\text{ M TBAPF}_6$  solution.  $\square = 200\text{ mV/s}$ , at  $200\text{ mV/s}$ , glassy carbon working electrode. Ferrocene ( $E_{1/2} = 0\text{ V}$ ) was added as an internal standard.



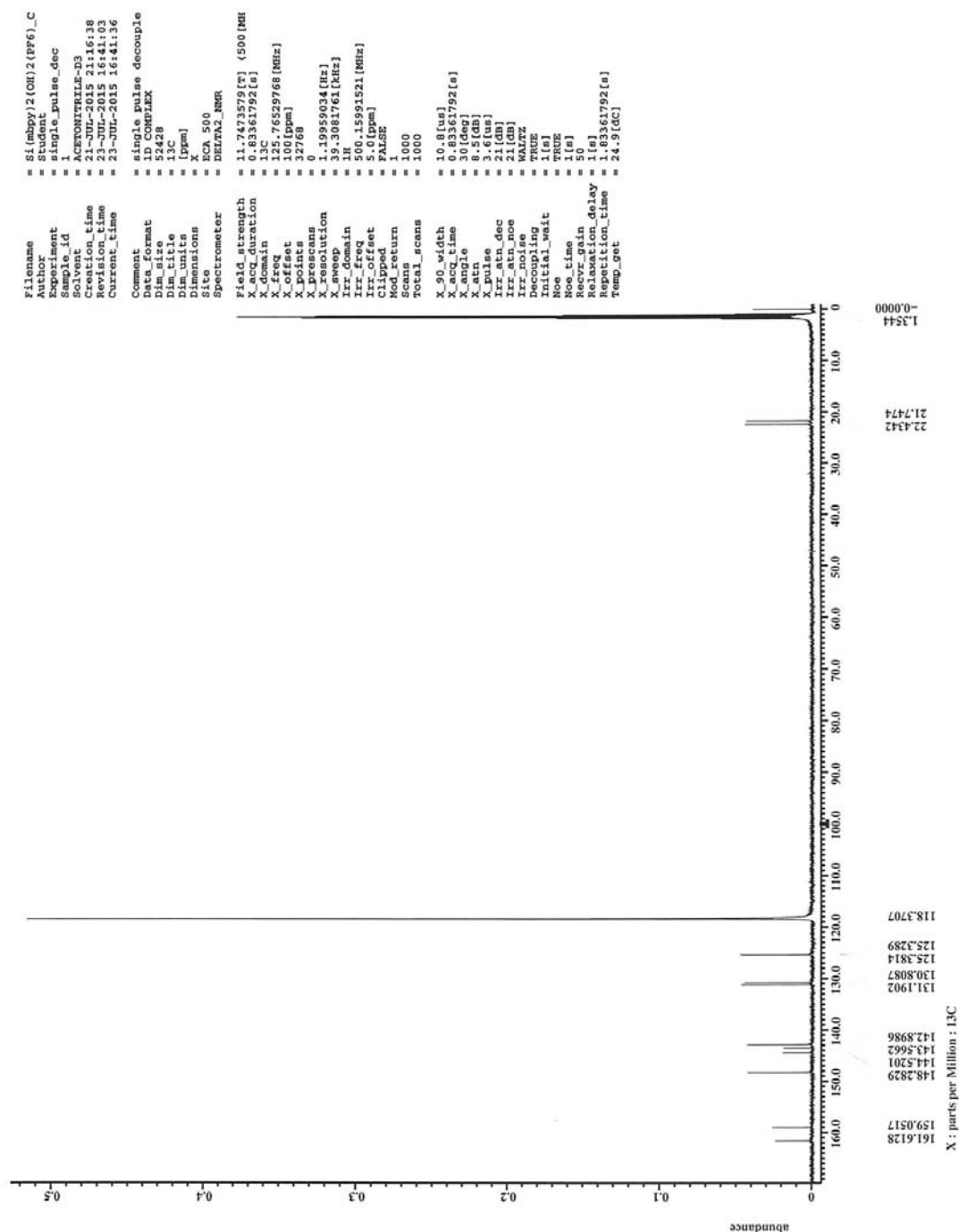
## APPENDIX B: CHARACTERIZATION OF HEXACOORDINATE DIOL COMPLEXES

Compounds:  $[\text{Si}(\text{dmbpy})_2(\text{OH})_2] (\text{PF}_6)$  (**6**),  $[\text{Si}(\text{bbbpy})_2(\text{OH})_2](\text{PF}_6)_2$  (**7**),

$^1\text{H}$ ,  $^{13}\text{C}$ , and  $^{29}\text{Si}$  NMR spectra; compounds **6-7** (hexafluorophosphate salts).

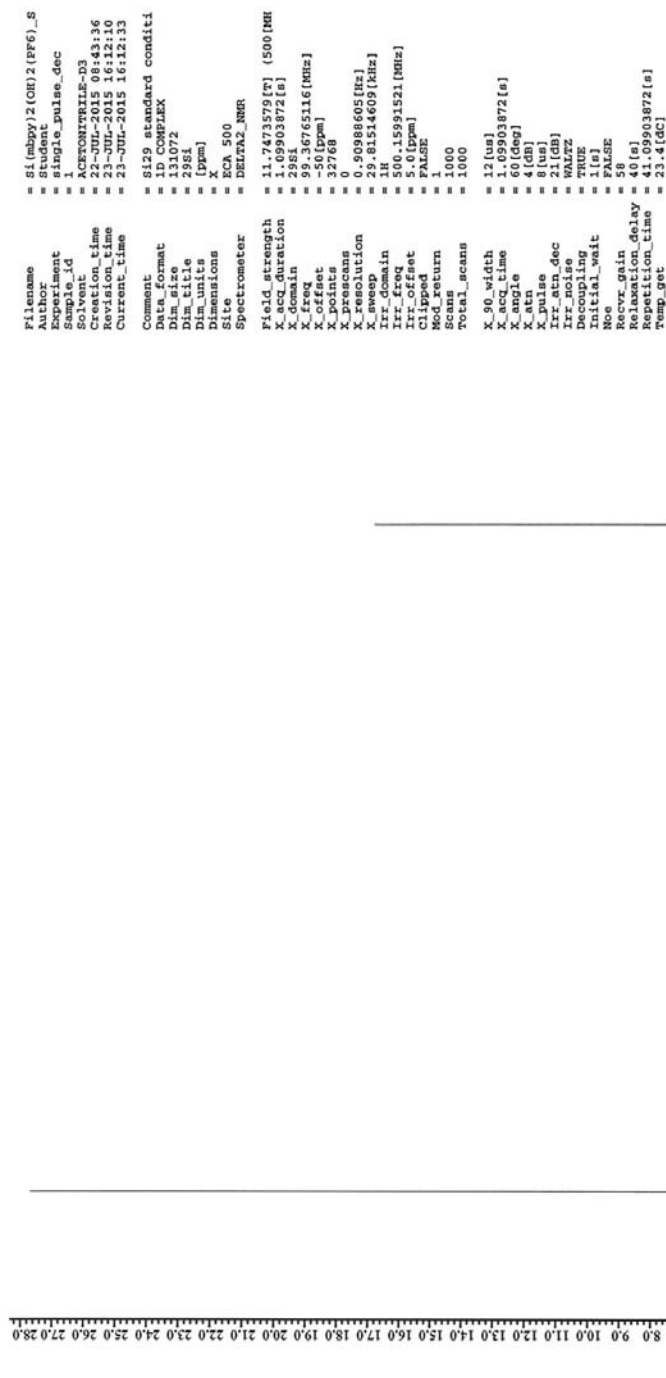


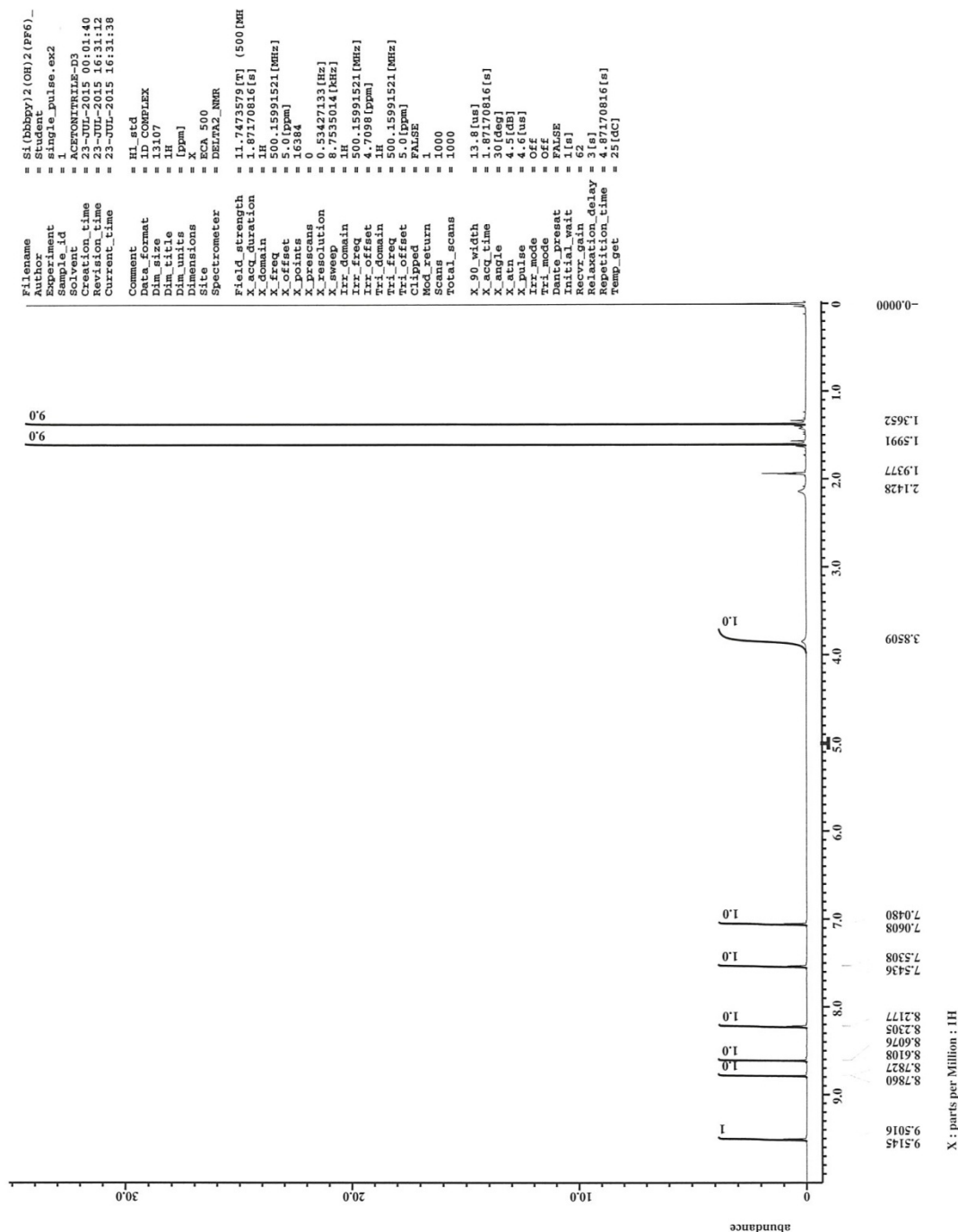
$^{13}\text{C}$  NMR of  $[\text{6}](\text{PF}_6)_2$  in  $\text{CD}_3\text{CN}$ .

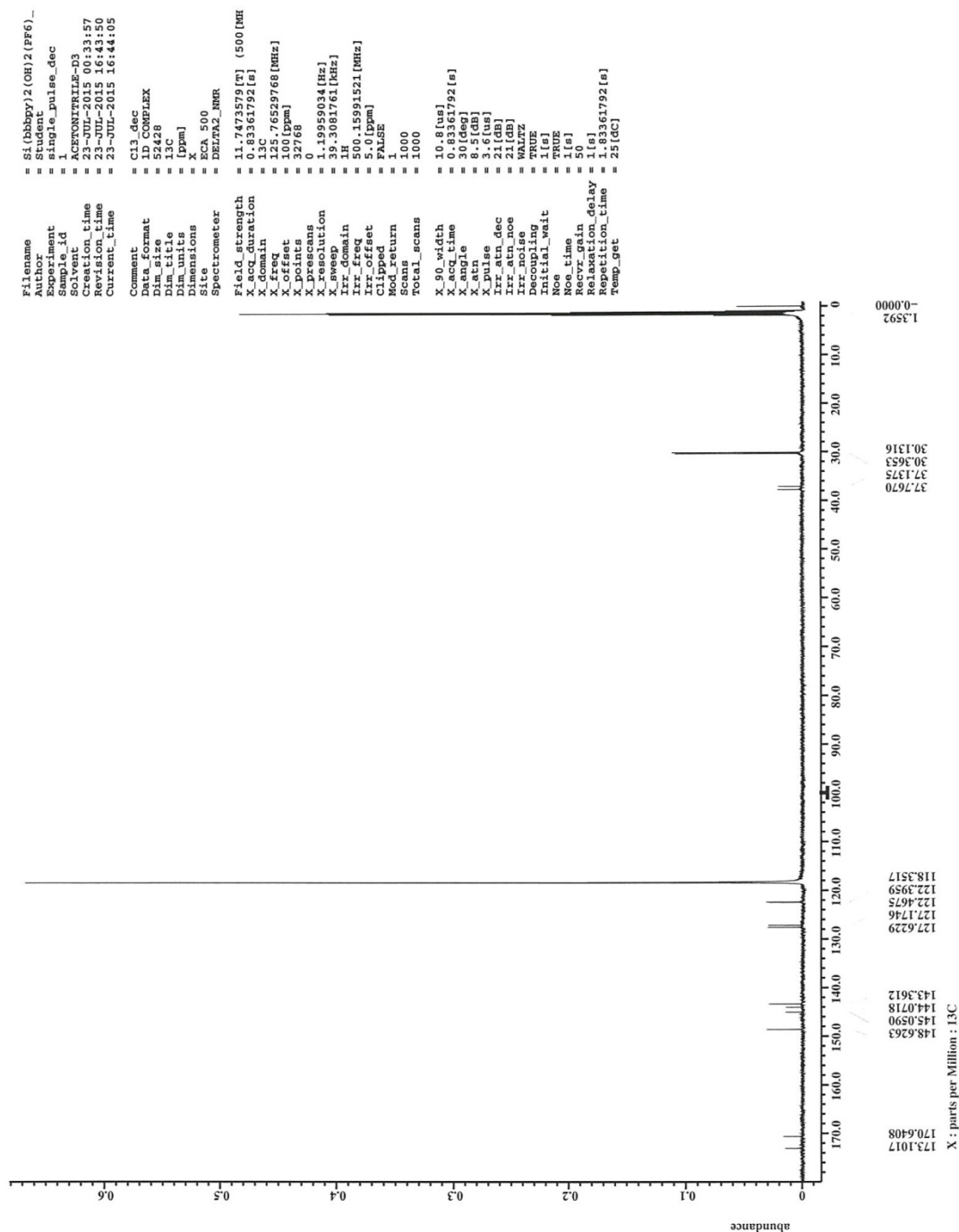




$^{29}\text{Si}$  NMR of  $[\mathbf{6}](\text{PF}_6)_2$  in  $\text{CD}_3\text{CN}$ .



$^1\text{H}$  NMR of  $[\text{7}](\text{PF}_6)_2$  in  $\text{CD}_3\text{CN}$ .

$^{13}\text{C}$  NMR of [7](PF<sub>6</sub>)<sub>2</sub> in CD<sub>3</sub>CN.

$^{29}\text{Si}$  NMR of [7](PF<sub>6</sub>)<sub>2</sub> in CD<sub>3</sub>CN.

